Improving Performance Assessment for Technologies of Energy Transition: Emissions, Economics, and Policy Implications

A DISSERTATION
SUBMITTED TO THE FACULTY OF THE GRADUATE SCHOOL OF THE
UNIVERSITY OF MINNESOTA
BY

Mo Li

IN PARTIAL FULFILLMENT OF THE REQUIREMENTS
FOR THE DEGREE OF
DOCTOR OF PHILOSOPHY

Timothy M. Smith, Advisor
Elizabeth J. Wilson, Co-Advisor

August, 2018

Acknowledgement

I would like to express my deepest gratitude and appreciation to my advisor, Dr. Timothy Smith, for the impeccable guidance and encouragement he provided me throughout my graduate school career. I am very fortunate to have had the freedom to find my own research path and work with him in pursuit of exploring and addressing energy related topics.

I would also like to thank my co-advisor, Dr. Elizabeth Wilson, for her socio-technical policy perspective that always gave inspiring feedbacks to my work. Similarly, I would like to thank my committee members, Dr. Anu Ramaswami and Prof. Patrick Huelman for their friendly guidance, stimulating questions and helpful suggestions provided to me in the development of this dissertation. Working with such talented scholars is truly a privilege and has made me a better researcher.

I am grateful to my research group as well as Dr. Yi Yang, and Dr. Stephen Rose at the Institute on the Environment. The energizing work environment I shared with and the thoughtful perspectives I heard from them have contributed to my intellectual growth over my years at the University of Minnesota. I am also grateful to my best friend, Mo Sun, for her patience when I needed to talk, her company when I needed to eat, and her help when I needed to debug.

Finally, I am blessed to have a wonderful family. My parents have tireless supported my academic and extracurricular endeavors ever since an early age. It was their eternal love and support that helped me overcome many difficult situations throughout my life and academic career in a foreign country. This dissertation would not be possible without you.

Abstract

Global climate change requires immediate actions to mitigate emissions from energy related sectors. Specifically, the electricity system plays a pivotal role in achieving the global emission reduction goals that many countries have publicly committed to. In the United States (U.S.), energy policies have focused on increasing electricity production from renewables, decreasing electricity consumption by improving energy efficiency, and shifting demand by using energy storage technology. This dissertation explores the specific challenges and information gaps that confront practitioners in three separate case studies, consequently contributing to electricity system and energy policy literature. It is the hope of the author that information provided helps to inform policy makers, electricity system operators, and private investors toward critical transition and transformation of the U.S. energy system.

The studies, taking the form of independent chapters, are summarized as follows. The first study presents an improved methodology for estimating the marginal emission factors (MEFs) of electricity generation in the Midcontinent Independent System Operator (MISO) system. Findings highlight the importance of including emitting and nonemitting resources in MEFs calculation in regions with high and growing renewables penetration and compare this approach to competing conventional approaches within the context of energy storage technologies. The second study demonstrates a multi-regional energy and emissions assessment of the ground source heat pump (GSHP) technology in comparison to the conventional heating and cooling technologies in residential houses. Findings indicate that applying EFs with higher spatial and temporal resolutions and using MEFs instead of average emission factors (AEFs) both give more accurate emission estimates. The third study assesses economics and emissions of grid-scale battery storage that arbitrages as a price taker in the MISO wholesale electricity market. Findings demonstrate specific locations where battery storage might initially be most profitable under historical pricing dynamics and reveal the heterogeneity in storage's economics and emissions throughout the MISO grid.

Contents

List of Tables

List of Figures

Chapter 1

Introduction

The damaging climate change resulted from human activities such as excessive resource exploitation and intensive industrialization have, in turn, crucially impacted our society and challenged the unprecedentedly growing global economy in a broad variety of ways. Increasing demand of energy due to population growth in recent decades have caused resource scarcity, ecosystem deterioration, and environmental pollution (Pachauri, Mayer, & IPCC, 2015). As the world's largest economy and richest nation, the United States (U.S.) has one of the highest per-capita energy consumption in the world (World Bank, 2014). Within the country, the electric power system has been recognized as one of the most carbon-intensive economic sectors, as it emits roughly 40% of all domestic greenhouse gases (U.S. EPA, 2016). Hence, transforming and decarbonizing the U.S. electricity system is one of the grand challenges for pursuing sustainability. Policies have been motivated to promote system efficiency and use of renewable resources. Advanced technologies and innovative strategies such as energy storage and electrification have also become priority in many areas (Navigant, 2016). The U.S. Midwest is at the heart of this transition. Within the Midcontinent Independent System Operator (MISO) footprint, state renewable portfolio standards (RPS) and the EPA's Clean Power Plan (CPP) have driven the deployment of over 16,000 MW of installed wind capacity, with additional megawatts planned to fill vacancies due to coal plants retirement, and new state laws promoting solar energy (MISO, 2016a). Therefore, the MISO region provides rich opportunities for reducing economic and environmental impacts of the electricity system, facilitating demand-side and behind-the-metering strategies, and improving public health and broader societal benefits as it serves 42 million customers (MISO, 2016b).

In practice, serious challenges remain in the processing of pursuing sustainable energy systems, including existing technological "lock in", lack of timely information and appropriate market structure, and inefficient communication infrastructure (Foxon, 2013; Williams et al., 2012). These challenges exist at both generation and demand sides, as well as in transmission and distribution systems. For instance, consumption decisions can be disconnected from environmental impacts due to consumers' invisibility into the

power generation. In fact, the embedded emission impacts of dispatched electricity can be highly variable based on specific location, season, and even time of day. Meanwhile, demand-side consumption behaviors are not informed well enough to effectively respond to the variations and reduce the impacts accordingly. Changes in regional climate and weather can also affect all major aspects of the electric power system: higher temperature may lower generation efficiency in thermal power plants, changing climate may cause issues in production from renewable sources such as wind turbines and solar panels; and high demand levels lead to increased energy cost and associated emissions.

This dissertation demonstrates three separate case studies to address sustainability challenges in the MISO electricity system. New approaches are made to break down and tackle the challenges in three aspects, including measuring emissions from electricity generation and demand, assessing economics of advanced technologies, and discussing policy implications of different strategies. These aspects account for the entire scope of the electricity system and are significant for understanding the current MISO system and analyzing various interventions. Proper measurement of emissions from electricity generation have substantial influences over policy and technology interventions aiming to reduce emissions. Investigation of electricity consumption strategies can address the impacts associated with direct operation of different technologies at demand side. Detailed economic estimation is critically important for rationalizing advancement in power grid modernization. The methodological design in this dissertation incorporates materiality, comparability and multi-metric dimensionality to address the sustainability challenges for MISO system; the findings can be integrated with policy- and decision-making criteria to effectively inform and guide practices towards decarbonized and modernized electricity systems. The research in this dissertation is organized in three separate studies and contributes to the electricity system and energy policy literature via the advancement of mixed methods and utilization of unique, spatiotemporal data.

Chapter 2 presents an improved methodology for estimating the marginal emission factors (MEFs) of electricity generation in the MISO system. Findings highlight the importance of including both emitting and nonemitting resources in MEFs calculations, as neglecting nonemitting resources can overestimate MEFs for carbon dioxide (CO_2), sulfur dioxide (SO_2) and nitrogen oxides (NO_x) by about 30% in regions with high and

growing renewables penetration. This expanded approach of calculating MEFs is further compared to the conventional approach within the context of energy storage technologies. Results of the application reveals heightened emission increases associated with load shifting of storage technologies. This study enables appropriate assessment of policy and technology interventions in terms of their environmental impacts and aims to stimulate effective policy and investment decisions toward electricity system transformation.

Chapter 3 demonstrates a multi-regional energy and emissions assessment of the ground source heat pump (GSHP) technology in comparison to the conventional natural gas furnace and air conditioner systems in residential houses. Twelve system-in-house scenarios are analyzed across three climatic regions and using various emission factors (EFs) of the MISO grid. GSHPs are found consuming less energy than the conventional systems but not necessarily reducing CO_2 emissions in all scenarios due to the grid fuel mix's spatiotemporal variability across locations. Findings reveal that applying EFs with higher spatial and temporal resolutions and using MEFs instead of AEFs both give more accurate and appropriate emission estimates. This study emphasizes the importance of applying accurate EFs to emissions performance assessment and recommends policymaking to properly incentivize the technologies that meet today's grid realities and renewable-integrated grid of tomorrow.

Chapter 4 utilizes spatiotemporal, real-time locational marginal prices (LMP) of electricity and MEFs of generation to estimate net operating revenues and emissions of grid-scale battery storage that arbitrages as a price taker in the MISO wholesale electricity market. Findings demonstrate specific locations where battery storage might initially be most profitable under historical pricing dynamics and reveal the heterogeneity in storage's economics and emissions throughout the MISO grid: storage installed in the North and Central subregions are more profitable but cause increase in emissions, while those in the South subregion are less profitable but lead to reduction in emissions. This study illustrates where one might expect energy storage to emerge in the MISO grid and discusses the importance of policy framework for future adoption of storage technologies serving under mechanisms like integrating renewables and maintaining grid reliability.

Chapter 5 offers a synthesized discussion of the studies presented in the dissertation.

Chapter 2

Marginal Emission Factors Considering Renewables: A Case Study of the U.S. Midcontinent Independent System Operator (MISO) System

With permission by my co-authors, this chapter is adapted from: Li, M., Smith, T. M., Yang, Y., & Wilson, E. J. (2017). Marginal Emission Factors Considering Renewables: A Case Study of the US Midcontinent Independent System Operator (MISO) System. *Environmental science & technology*, *51*(19), 11215-11223. DOI: 10.1021/acs.est.7b00034

Estimates of marginal emission factors (MEFs) for the electricity sector have focused on emitting sources only, assuming nonemitting renewables rarely contribute to marginal generation. However, with increased penetration and improved dispatch of renewables, this assumption may be outdated. Here, we improve the methodology to incorporate renewables in MEF estimates and demonstrate a case study for the Midcontinent Independent System Operator (MISO) system where wind has been commonly dispatched on the margin. We also illustrate spatiotemporal variations of MEFs and explore implications for energy storage technologies. Results show that because the share of renewables in MISO is still relatively low (6.34%), conventional MEFs focused on emitting sources can provide a good estimate in MISO overall, as well as in the Central and South subregions. However, in the MISO North subregion where wind provides 22.5% of grid generation, neglecting nonemitting sources can overestimate MEFs for CO_2, SO_2, and NO_x by about 30%. The application of expanded MEFs in this case also reveals heightened emission increases associated with load shifting of storage technologies. Our study highlights the importance of expanded MEFs in regions with high and growing renewables penetration, particularly as renewable energy policy seeks to incorporate demand-side technologies.

2.1 Introduction

Electricity generation is one of the most emission-intensive economic sectors in the United States (U.S.) and across the globe (Pachauri et al., 2015). Regional air pollution and its consequential damage to human health are largely attributable to air pollutant emissions from fossil fuel combustion in electricity generation (Smith et al., 2010; S. Wang & Hao, 2012). Climate, air pollution, and energy policies aim to create more sustainable energy systems and reduce emissions from electricity generation. Commonly suggested policy interventions include increasing electricity production from renewable energy sources like wind and solar, decreasing consumption by improving energy efficiency, and shifting demand by using bulk energy storage and demand response (E. S. Hittinger & Azevedo, 2015a; Lutsey & Sperling, 2008). Effective implementation of these policies depends on understanding how they change and affect the electricity generation system and contribute to reducing emissions.

The potential of an electricity generation system to reduce emissions has been measured by both marginal emission factors (MEFs) and average emission factors (AEFs) (Doucette & McCulloch, 2011; Hawkes, 2010; Siler-Evans, Azevedo, & Morgan, 2012). However, the use of AEFs, which reflect grid-average situations, to estimate the effect of an intervention may be problematic, because not all generating technologies would respond to changes in demand proportionally (Hawkes, 2010). In studying the electricity generation in the United States, for example, Siler-Evans et al. found that AEFs could significantly misestimate the amount of emissions avoided by an intervention (Siler-Evans et al., 2012). By contrast, MEFs estimate the emission intensity of marginal power generation that responds to a change in demand, and are a more appropriate metric to assess emission implications of policy and technology interventions, such as electric vehicle tax credits and energy storage, among others (Doucette & McCulloch, 2011; Hawkes, 2010; Siler-Evans et al., 2012).

Short-term MEFs reflect the dynamics of electric generation and consumption given relatively fixed and long-lived system capacity; these are affected by factors including the legacy technology mix, fuel type, operation cost, dispatchability, and timing (Hawkes, 2014). Long-term—which in the electric power system can be decades—MEFs reflect capacity addition or reduction and structural changes in the electricity system, and

are affected by factors such as resource constraints, capital cost and return rate, and policy incentives (Hawkes, 2014).

Short-term MEFs have been intensively studied, mainly via two approaches: 1) statistical models based on empirical data and 2) economic dispatch models (Ryan, Johnson, & Keoleian, 2016). Both methods have strengths and limitations (Ryan et al., 2016). The statistical approach reduces model complexity and calculation time by avoiding operational constraints and dispatch orders, but it relies heavily on empirical data (Hawkes, 2010; Ryan et al., 2016; Siler-Evans et al., 2012). When important data are missing, the accuracy of this approach is compromised (Siler-Evans et al., 2012). The economic dispatch approach estimates MEFs based on numerous data and sophisticated models (McCarthy & Yang, 2010; Peterson, Whitacre, & Apt, 2011; Ryan et al., 2016). However, its increased complexity and strict assumptions confine broader use (Axsen, Kurani, McCarthy, & Yang, 2011; Blumsack, Samaras, & Hines, 2008; Kintner-Meyer, Schneider, Pratt, & Pacific Northwest National Laboratory, 2007).

Regressions on historical data have been used as a simple and effective statistical method of estimating MEFs. Siler-Evans et al. (2012) developed a linear regression model to calculate MEFs for eight North American Electric Reliability Corporation (NERC) regions using hourly, generator-level emissions and generation data from the U.S. Environmental Protection Agency (EPA) Continuous Emissions Monitoring System (CEMS) (Siler-Evans et al., 2012). Holland and Mansur (2008) determined real-time pricing's effect on emissions in the NERC regions (Holland & Mansur, 2008). In Europe, Hawkes (2010) regressed and estimated marginal CO_2 rates for the United Kingdom (UK) national grid from 2002 through 2009 (Hawkes, 2010). The MEFs mentioned above have been further refined considering spatial and temporal variations, and have been broadly used to evaluate emissions associated with plug-in hybrid electric vehicles (PHEVs) (Archsmith, Kendall, & Rapson, 2015; Graff Zivin, Kotchen, & Mansur, 2014; Holland, Mansur, Muller, & Yates, 2015, 2016; Jansen, Brown, & Samuelsen, 2010; Stephan & Sullivan, 2008; Tamayao, Michalek, Hendrickson, & Azevedo, 2015; Yuksel, Tamayao, Hendrickson, Azevedo, & Michalek, 2016). The U.S. EPA also provides non-baseload MEFs in the Emissions & Generation Resource Integrated Database (eGRID) (Diem & Quiroz, 2012a); the method and results have been widely used in governmental

policies and tools such as EPA's Clean Power Plan (CPP) and Power Profiler application (U.S. EPA, 2012).

Economic dispatch models have been used to estimate MEFs in different regional grids in the US: California Independent System Operator (CAISO) (Marnay et al., 2002), Electric Reliability Council of Texas (ERCOT) (Newcomer, Blumsack, Apt, Lave, & Morgan, 2008; Raichur, Callaway, & Skerlos, 2016), Midcontinent Independent System Operator (MISO) (Bettle, Pout, & Hitchin, 2006), New York Independent System Operator (NYISO) (Raichur et al., 2016), and Pennsylvania-New Jersey-Maryland Interconnection (PJM) (Newcomer et al., 2008); and Europe: the power system of England and Wales (Bettle et al., 2006) and the Belgian electricity generation system (Voorspools & D D'haeseleer, 2000). MEFs implications have been intensively examined in various generation- and demand-side applications, including PHEVs (Axsen et al., 2011; Blumsack et al., 2008; Choi, Kreikebaum, Thomas, & Divan, 2013; Kim & Rahimi, 2014; Kintner-Meyer et al., 2007; H. Lund & Kempton, 2008; McCarthy & Yang, 2010; Peterson et al., 2011; van Vliet, Brouwer, Kuramochi, van den Broek, & Faaij, 2011; Yuksel & Michalek, 2015), integration of renewable energy (Keith, Biewald, Sommer, Henn, & Breceda, 2003; McConnell, Hadley, & Xu, 2011), distributed generation (Hadley & Van Dyke, 2003), energy efficiency (Du & Mao, 2015; K. Wang & Wei, 2014), energy storage (Anderson & Leach, 2004; Carson & Novan, 2013; E. S. Hittinger & Azevedo, 2015a; Kanoria, Montanari, Tse, & Zhang, 2011; Stadler, Siddiqui, Marnay, Aki, & Lai, 2011), and a ban on new coal-fired power plants (Newcomer & Apt, 2009).

One critical commonality of the existing studies is the exclusion of non-emitting generation from the calculation of MEFs, specifically renewable and nuclear sources. This is partly because of the lack of data (Siler-Evans et al., 2012), but largely because of the assumption that non-emitting sources, particularly renewable resources, do not serve as marginal generation given their near-zero operational cost and non-dispatchability (Graff Zivin et al., 2014; Hawkes, 2010; Siler-Evans et al., 2012). However, in the U.S., significant deployment of renewables (over 75,000 MW in 2016) and parallel developments, including transmission system expansion, dispatching mechanism improvement, and electricity market development, in regional electricity systems, such as

MISO and PJM, have shown that renewable resources like wind can be and have been deployed frequently on the margin (Figure 2.1) (MISO, 2014d; PJM, 2014). In 2014, for example, MISO's monthly average percentage of time that wind was on the margin exceeded 60% in seven out of the twelve months (MISO, 2014d). The remarkable presence of wind generation on the margin is due to technological and policy innovations affecting dispatch of MISO's 16,000 MW of wind, in particular, the Dispatchable Intermittent Resources (DIRs) program launched in 2011 (MISO, 2011; Stafford & Wilson, 2016). The program relies on advanced wind forecasting accuracy in MISO and enables automatic wind dispatchment and curtailment in real-time, with the aim of improving market efficiency and system reliability and reducing curtailments (MISO, 2011). In 2014, MISO's 5-min interval forecast was developed and improved; MISO's Day-Ahead and 4-Hour-Ahead hourly wind forecasting accuracy exceeded 95% (MISO, 2015e); and monthly DIR participation in MISO accounted for 79%-83% of the total wind generation, a significant increase from 9.8% in June, 2011 (MISO, 2011). Thanks to the DIRs program, wind participated in MISO's real-time market like fossil fuels with a fairly low monthly curtailment rate ranging from 4.2% to 8.3% in 2014 (MISO, 2015d). This significantly improves wind's dispatchability that indicates wind generation's responsiveness to the request of power system operator (i.e. MISO) or power plant owner. Also, to better capture power system dynamics, the Independent System Operator New England (ISO-NE) has revised their estimates of MEFs (ISO New England, 2016). Their early MEFs covered only natural gas- and oil-fired generators, but from 2011 they have used a new method to estimate MEFs based on the locational marginal units, including non-emitting generators, identified by locational marginal prices.

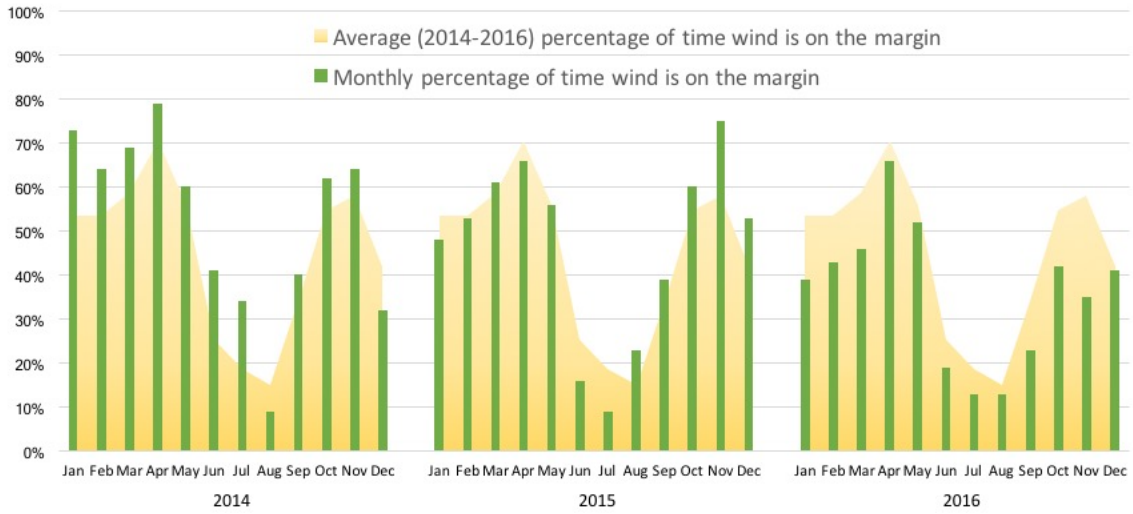

Figure 2. 1. Monthly percentage of time that wind is on the margin in 2014, 2015, and 2016 in MISO. Data are from MISO's 5-min real-time fuel on the margin data (MISO, 2014a, 2015a, 2016a). Note that more than one fuel type may be on the margin, hence the percentage of each fuel type may sum to more than 100%.

Recognizing the recent developments in renewable penetration and policy innovations, here we apply the broadly-used linear regression approach (Graff Zivin et al., 2014; Hawkes, 2010; Siler-Evans et al., 2012) to estimate MEFs for MISO, taking into account both emitting and non-emitting sources. We term our estimates "expanded MEFs" to differentiate from previous MEFs, which we term "conventional MEFs". Because of MISO's largest geographic footprint in the U.S (MISO, 2015b) (900,000 square miles or 2.3 million square kilometers) and the substantial heterogeneity in fuel mix across its regions (MISO, 2014c), we estimate MEFs for its North, Central, and South subregions, as well as MISO as a whole. We compare the differences between the expanded MEFs and the conventional MEFs to assess the impact of non-emitting sources such as renewables on MEFs. We also demonstrate spatiotemporal variations of the expanded MEFs and explore the implications for bulk energy storage technologies and demand side management (DSM) programs that are based on load shifting techniques such as demand response (DR), smart metering, and other emerging technologies. In addition, we inspect the fuel mix in marginal generation with respect to system load. We conclude with discussion of the broad policy and technology implications of MEFs considering non-emitting sources.

2.2 Methods

We estimate MEFs using the linear regression approach(Hawkes, 2010; Siler-Evans et al., 2012) with 2014 hourly emissions and generation data. Based on this approach, changes in emissions (ΔE_h) are a function of changes in generation (ΔG_h) within an hour (Equation 1):

$$\Delta E_h = \beta \Delta G_h + \varepsilon \quad (1)$$

$$\text{where } \Delta E_h = E_h - E_{h-1} \quad (2)$$

$$\text{and } \Delta G_h = G_h - G_{h-1} \quad (3)$$

The slope of the linear regression (β) gives us an estimate of MEFs. In the previous MEFs studies, ΔG_h covers only emitting sources (Equation 4):

$$\Delta G_h = G_{emitting,h} - G_{emitting,h-1} \quad (4)$$

When the penetration of renewables is low or they are undispatchable and thus accounting for emitting sources only may be adequate for the estimation of MEFs. However, when renewables penetration becomes high with substantially improved dispatchability, accounting for emitting sources only may significantly overestimate the MEFs. In our expanded MEFs (Equation 5), we include both emitting and non-emitting sources,

$$\Delta G_h = (G_{emitting,h} + G_{non-emitting,h}) - (G_{emitting,h-1} + G_{non-emitting,h-1}) \quad (5)$$

We use the approach to separately calculate MEFs of electricity generation in MISO's North, Central, and South subregions. With regard to geographical coverage, North includes Iowa, Minnesota, Montana, North Dakota, South Dakota, and Manitoba, Canada; Central includes Indiana, Illinois, Kentucky, Michigan, Missouri, and Wisconsin; and South includes Arkansas, Louisiana, Mississippi, and Texas (MISO, 2015b). Details of the MISO subregions are shown in the supporting information (section 1).

The approach can also be applied to subsets of the sample to derive MEFs with more granular temporal resolutions. For example, month-hour MEFs can be calculated by employing the regression on all observations within the same hourly interval in twelve months for 288 separate times. And daily MEFs can be calculated by employing the regression on all observations within the same hourly interval for 24 separate times.

2.2.1 Data Sources

The primary data sources for our expanded MEFs estimates are the EPA's Air Market Program Data (AMPD), which provides emissions and generation data for emitting sources, and hourly generation by fuel type data from MISO, which provides generation data for non-emitting sources. The AMPD is a web-based application that contains data collected as part of EPA's emissions trading programs (U.S. EPA, 2018). The AMPD data provide hourly generator-level CO_2, SO_2 and NO_X emissions as well as gross power production. We sort the data into the MISO subregions by cross-indexing power plant identification numbers with survey Form EIA-860, an independent database maintained by U.S. Energy Information Administration, and the MISO subregion map (EIA, 2018; MISO, 2015b). We then aggregate the hourly generator-level emissions and generation data to create the AMPD hourly subregional emissions and generation data.

The hourly generation data provided by MISO covers all fuel types, but we only use the information on non-emitting sources, i.e. hydro, nuclear and wind. To accurately estimate the contribution of non-emitting sources in MEFs, we use an identification index to help determine what fuel types are on the margin in a specific hourly interval for each MISO subregion. We collect the 5-minute real-time fuel on the margin data from MISO (MISO, 2014a). In the data, MISO defines the marginal fuel(s) as the type(s) of generating units that are dispatched to serve the next 1 MW of energy (MISO, 2014b) for each fuel type, not the actual generation volume. We aggregate the data from 5-minute to hourly level and obtain the total count of non-emitting generating units that operate on the margin within each hourly interval. The total count is then transformed into the identification index that indicates the presence or absence of particular non-emitting fuel types in marginal generation. Eventually, we use the index to filter the hourly non-emitting generation data, keeping the observations that are identified "on the margin",

and saving them as the MISO hourly non-emitting generation data for each MISO subregion. Note that there can be one or more on-the-margin fuel types within each hourly interval.

2.2.2 Marginal Fuel Type

We rely on the linear regression model and the MISO hourly generation by fuel type data to estimate each fuel type's share in marginal generation across various temporal scales and grid production levels. To constrain our analysis more precisely to the identified on-the-margin generation, we use the identification index created from MISO's 5-minute real-time fuel on the margin data to filter the hourly generation by fuel type data, then keep the observations that are identified "on the margin" as a subset. In this subset, we calculate change in generation for all fuel types within each hourly interval, then apply the similar linear regression model used for estimating MEFs to calculate the share of all possible fuel types in marginal generation. We also explore the share of fuel type in marginal generation with regard to system generation increase. We bin the hourly system generation by every fifth percentile and apply separate regressions on data within each bin. This allows us to intuitively observe the probability of each fuel type being on the margin at different levels of system generation, which is a proxy of system demand.

2.3 Results

2.3.1 Expanded and Conventional MEFs

Overall results of the expanded MEFs and the conventional MEFs for MISO and its subregions, as well as marginal fuel type under the two methods are presented Table 2.1. MEFs estimates for CO_2, SO_2, and NO_X are reported with ± two standard deviations of the estimates and R2 values (details of the linear regression are shown in Appendix A and Figure A.1). The difference between the two MEFs reflects the impact of non-emitting sources, primarily wind in this case. It also reflects the error of overestimation by using conventional MEFs when non-emitting sources contribute considerably to marginal electricity generation. Tables 2.1 reveals that the overall error is small for MISO, but it

can be as high as around 30% for the North due to the high wind penetration (22.5% of 2014 grid generation (MISO, 2014c)). The more wind is on the generation margin (North > Central > South), the greater the error of overestimation by using the conventional MEFs (e.g., 28.13% > 3.7% > 0.0% for CO_2). Because the share of renewables like wind and hydro in MISO is still fairly low (less than 10% (MISO, 2014c), also shown in Table A.1) and nuclear reactors rarely operate on the margin, estimates of the expanded and conventional MEFs do not show a difference in MISO overall, as well as in the Central and South subregions.

The expanded MEFs for CO_2 are found to be 0.76 tons/MWh for MISO in 2014, with a variation between 0.62 and 0.82 tons/MWh in different subregions. CO_2 emissions are lower in the North (0.67 tons/MWh) and South (0.62 tons/MWh) than in the Central region (0.82 tons/MWh). This is because wind contributes 30% to marginal electricity generation in North and natural gas contributes nearly 80% in South. Our model's R^2 value is large in MISO (0.95), Central (0.96) and South (0.93), indicating that CO_2 emissions respond strongly to changes in system generation. It also echoes the fact that coal and gas constitute the majority of marginal generation within these regions and subregions. The R^2 value in the North regression is lower in North (0.64), indicating that higher wind penetration in marginal generation (30.4%) weakens the corrolation between changes in system generation and changes in CO_2 emissions, because wind has zero emissions in operation.

SO_2 is a major emission from coal combustion, therefore its expanded MEFs are higher in MISO (2.59 lbs/MWh), North (1.99 lbs/MWh) and Central (3.34 lbs/MWh) where marginal generation is more coal-dependent, but lower in South (1.38 lbs/MWh) where coal only accounts for 21.3% of the marginal generation. The R^2 values are relatively high in MISO (0.74) and Central (0.73), which is consistent with the strong relationship between changes in coal-heavy generation and changes in SO_2 emissions in MISO and Central. The R^2 values are relatively low in the North (0.41) and South (0.42) subregions, this is because wind's and gas's significant contribution to marginal generation weakens the causal relationship between changes in generation and changes in SO_2 emissions in North and South, respectively.

The expanded MEFs for NO_X is higher in MISO (1.30 lbs/MWh), North (1.43 lbs/MWh) and South (1.51 lbs/MWh) than those in Central (1.09 lbs/MWh). Similar to other emissions, the R^2 value in the North (0.46), due to wind's frequent presence in marginal generation, is the lowest compared to that in MISO (0.79), Central (0.71) and South (0.59).

Table 2. 1. The Expanded and Conventional Marginal Emission Factors (MEFs) for Regional (MISO) and Subregional (North, Central and South) Electricity Generation in 2014.
There are significant differences in the average regional and subregional fuel mix: in MISO, the percentage of generation from coal, natural gas, nuclear, and wind is 57.7%, 15.5%, 16.2%, and 6.3%, respectively; in North, the percentage of generation from coal, natural gas, nuclear, and wind is 57.7%, 2.6%, 12.8%, and 22.5%, respectively; in Central, the percentage of generation from coal, natural gas, nuclear, and wind is 75.0%, 7.5%, 12.9%, and 2.4%, respectively; in South, the percentage of generation from coal, natural gas, and nuclear is 23.8%, 41.8%, and 26.1%, respectively.

	Region	CO_2 (tons/MWh) MEF ± 2σ	R^2	SO_2 (lbs/MWh) MEF ± 2σ	R^2	NO_X (lbs/MWh) MEF ± 2σ	R^2	Marginal Fuel (%) coal	gas	wind
Expanded MEFs	MISO	0.76 ± 0.004	0.95	2.59 ± 0.032	0.74	1.30 ± 0.014	0.79	59.2	36.8	0.3
	North	0.67 ± 0.010	0.64	1.99 ± 0.052	0.41	1.43 ± 0.034	0.46	66.8	3.8	28.9
	Central	0.82 ± 0.004	0.96	3.34 ± 0.044	0.73	1.09 ± 0.014	0.71	73.2	22.4	0.1
	South	0.62 ± 0.004	0.93	1.38 ± 0.034	0.42	1.51 ± 0.026	0.59	20.8	78.9	NA
Conventional MEFs	MISO	0.78 ± 0.002	0.98	2.67 ± 0.032	0.77	1.33 ± 0.014	0.82	61.4	37.2	NA
	North	0.86 ± 0.004	0.95	2.54 ± 0.044	0.61	1.87 ± 0.026	0.72	94.2	5.4	NA
	Central	0.85 ± 0.002	0.99	3.47 ± 0.044	0.75	1.12 ± 0.014	0.73	76.6	22.8	NA
	South	0.62 ± 0.004	0.93	1.38 ± 0.034	0.42	1.51 ± 0.026	0.59	20.8	79.0	NA
Expanded MEFs ~ Conventional MEFs diff.%	MISO	2.8		3.1		2.6				
	North	28.1		28.4		31.8				
	Central	3.7		3.9		3.5				
	South	0.0		0.0		0.0				

Expanded MEFs ~ Conventional MEFs diff. % = (Conventional MEFs – Expanded MEFs)/Expanded MEFs × 100

2.3.2 Spatiotemporal Variations and Trends of Expanded MEFs

We observe significant trends of the expanded MEFs across hours depending on the month. Figure 2.2 shows the seasonal and diurnal time variations of the expanded MEFs for CO_2. In MISO, the expanded MEFs are higher, overall, at night than during the day. We attribute this to carbon-intensive coal generation that is often the primary contributor to meet the marginal demand in low-demand hours (see Figure 2.3), such as

11pm-2am next day. Moreover, coal-fired generators are less efficient during low-demand hours than average, because they have to operate at lower capacity factors (Ryan et al., 2016). The expanded MEFs in the North subregion are found to be lower in colder months, which is thought to be the result of greater availability of wind resources and consequently more wind generation on the margin. August has the highest expanded MEFs than any other month in the North when wind resources are scarcest and the marginal demand for air conditioning is primarily fueled by coal. The expanded MEFs in Central do not have extreme contrasts across months and hours, but a few trends are still noticeable. For example, the expanded MEFs for CO_2 during 10am-8pm in August and in the hour ending at 2pm in months from June to October are found to have lower MEFs for CO_2 than neighboring hours. This difference is likely caused by marginal generation's dependence on natural gas to meet peak demand for air conditioning during these time periods in this subregion (see Figure 2.3). The expanded MEFs in South are relatively higher in the early morning than in the rest of the day particularly in the summer months because marginal generation during low-demand hours is satisfied by coal- and gas-fired units (see Figure 2.3) and the coal-fired units' ramp-up emission rates are usually high. The moderate expanded MEFs for CO_2 in most hours and months reflect a largely constant level of gas-fired marginal generation in South, due to strong presence of natural gas in the system fuel mix.

We also notice obvious differences of the expanded MEFs across MISO and its subregions (see Appendix A and Figure A.2). Overall, they vary the most in North and relatively less in Central and South. The outstanding low MEFs in North echo the fact that North has the greatest wind penetration in marginal generation compared to the other two subregions (see Table 2.1), while the relatively high MEFs in early-morning and late-night hours indicate the yet heavy reliance on coal in North. Central and South depend intensively on coal and natural gas for marginal generation, respectively, so the MEFs are higher in Central and relatively moderate in South.

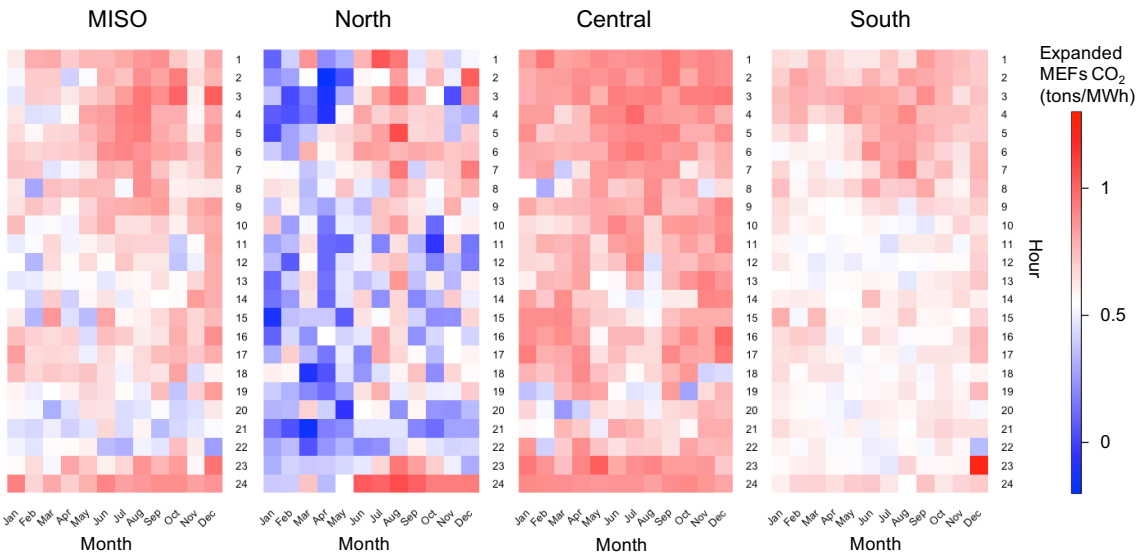

Figure 2. 2. Monthly and Hourly Expanded MEFs for CO_2 for Regional (MISO) and Subregional (North, Central and South) Electricity Generation in 2014

2.3.3 Marginal Fuel Type and MEFs

Inspired by Figure 3 in Siler-Evans et al. (2012) (Siler-Evans et al., 2012), we created Figure 2.3 to show the share of marginal generation by fuel type (top) and the expanded MEFs for CO_2, SO_2 and NO_X (bottom) in correspondence to the level of system generation, which is a proxy for system demand. North and Central are both quite coal-heavy in generation. When system demand is low, coal is the dominant marginal fuel in both subregions, resulting in relatively high MEFs for CO_2 (left axis) and SO_2 (right axis). However, as demand increases, share of coal slightly decreases in North, but dramatically drops in Central. The share gap is gradually picked up by wind in North and quickly picked up by gas and hydro in Central. Such substitution of coal by wind and gas leads to the reduced MEFs for CO_2 (left axis) and SO_2 (right axis) in North and Central, respectively, but it has little effect on the MEFs for NO_X level in both subregions. South is the most gas-heavy subregion. At the lowest demand level, coal accounts for roughly 55% of marginal generation, but declines to less than 2% at peak demand, while gas takes up the other 45% at low demand and almost all marginal generation at peak demand. The replacement of coal by gas in marginal demand causes the decline of MEFs for CO_2 (left axis) and SO_2 (right axis). The expanded MEFs for NO_X rapidly increase with system demand and gas generation.

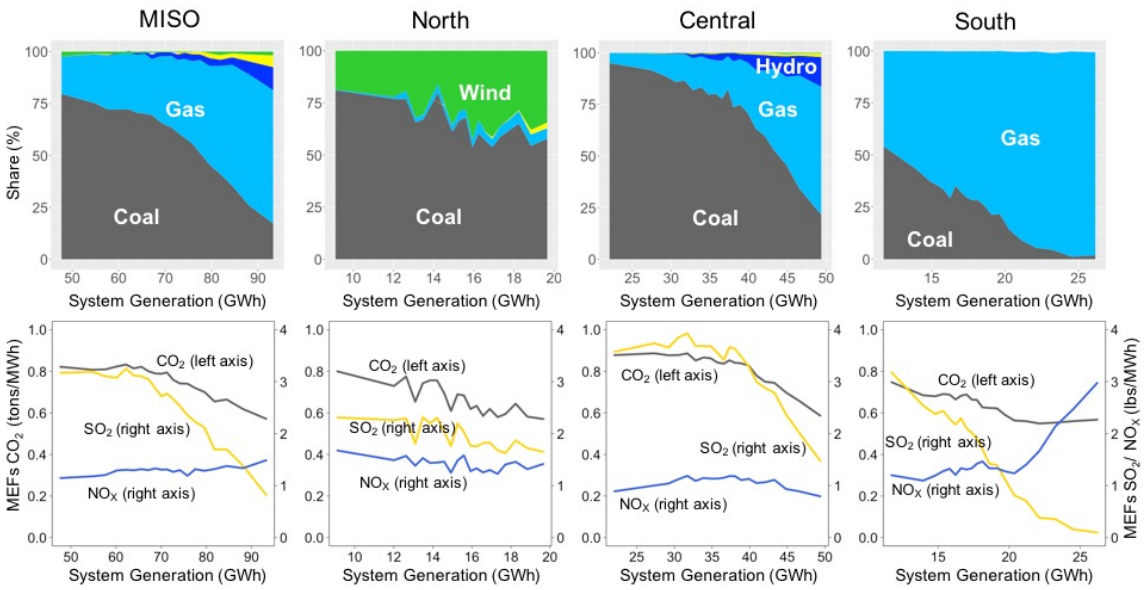

Figure 2. 3. Share of Marginal Fuel Type (top) and Expanded MEFs for CO_2, SO_2 and NO_X (bottom) as a Function of System Generation.
Following from Siler-Evans et al. (2012) (Siler-Evans et al., 2012): X axes are binned by fifth percentile of system generation (GWh) in each region and subregion in 2014. Only coal (grey), gas (light blue), hydro (dark blue), other (yellow), and wind (green) are shown here because nuclear is rarely on the margin of generation. The expanded MEFs (bottom) have two Y axes: the left axis applies to CO_2 (tons/MWh) and right axis applies to NO_X and SO_2 (lbs/MWh).

2.3.4 Application of MEFs

We demonstrate several applications of the expanded MEFs for CO_2 in this section. We examine bulk energy storage technologies that charge during low-demand hours (bottom 15%) and discharge during high-demand hours (top 15%) as well as demand side management (DSM) programs that are based on load shifting techniques and are designed to move demand load from high-demand hours to low-demand hours. These technologies are capable of shaving peak demand, maintaining grid reliability, and improving system efficiency (Moura & de Almeida, 2010; P. Wang, Huang, Ding, Loh, & Goel, 2011). The bulk energy storage technologies are particularly useful in hedging against the variability of intermittent generation from renewable resources like wind and solar (Anderson & Leach, 2004; Kanoria et al., 2011).

Existing studies reveal that the operation of energy storage can cause emission increases (Carson & Novan, 2013; Denholm & Kulcinski, 2004; E. S. Hittinger & Azevedo, 2015a; E. Hittinger, Whitacre, & Apt, 2010; Lueken & Apt, 2014). Hittinger and Azevedo (2015), for example, investigated and compared such increased effects across U.S. NERC regions. However, they used the conventional MEFs and neglected

possible contribution of renewables like wind to marginal generation, which may overestimate the emission increases resulting from the operation of energy storage (E. S. Hittinger & Azevedo, 2015a).

In Table 2.2, we compare the expanded and conventional MEFs for CO_2 during high-demand and low-demand hours for MISO and its subregions. The comparison illuminates that the conventional MEFs in general underestimate the potential emission increase (column "H ~ L diff. at 100% efficiency") as compared with the expanded MEFs, even if the bulk energy storage technologies operate at a round-trip efficiency of 100%. This is especially true for the North subregion (0.168 *versus* 0.037). Although the expanded MEFs are lower compared to the conventional MEFs during both high-demand and low-demand hours in North, the increase of expanded MEFs from high-demand hours to low-demand hours is enlarged. This is because wind contributes to marginal generation more frequently during high-demand hours than during low-demand hours (Figure 2.3). This consequently helps reduce the expanded MEFs CO_2 more during high-demand hours than during low-demand hours.

We also look at bulk energy storage technologies operating at a round-trip efficiency of 75%, which was indicated as the base-case in Hittinger and Azevedo (2015) (E. S. Hittinger & Azevedo, 2015a). The results show that the potential emission increase caused by operation of the storage technologies at 75% efficiency (column "H ~ L diff. at 75% efficiency" in Table 2.2) is significantly enlarged compared to that caused by the 100% efficient technologies.

The comparison also reveals significant regional differences in the avoided CO_2 emissions resulting from the same load-shifting intervention. The level of renewable penetration and the dependence on coal are the key factors that cause the differences across the regions.

Table 2. 2. Potential Emissions Increase Resulting from Bulk Energy Storage Technologies Charging during Low-demand Hours and Discharging during High-demand Hours.
The difference between MEFs in low-demand and high-demand hours is calculated using (Low-demand hours – High-demand hours). Values in parentheses are the percentage difference between MEFs in low-demand and high-demand hours, which is calculated using (Low-demand hours – High-demand hours)/High-demand hours × 100.

	Region	High-demand hours	Low-demand hours	H ~ L diff. at 100% efficiency	H ~ L diff. at 75% efficiency
Expanded MEFs CO_2 (tons/MWh)	MISO	0.622	0.811	0.189 (30.3%)	0.459 (73.8%)
	North	0.601	0.769	0.168 (28.0%)	0.435 (70.7%)
	Central	0.649	0.881	0.232 (35.7%)	0.525 (81.0%)
	South	0.559	0.700	0.141 (25.2%)	0.375 (67.0%)
Conventional MEFs CO_2 (tons/MWh)	MISO	0.673	0.826	0.153 (22.7%)	0.428 (63.6%)
	North	0.857	0.894	0.037 (4.4%)	0.336 (39.2%)
	Central	0.735	0.884	0.148 (20.2%)	0.443 (60.2%)
	South	0.559	0.700	0.141 (25.2%)	0.374 (66.9%)

2.4 Discussion

It has been broadly acknowledged that marginal emission factors (MEFs) are more appropriate, than average emission factors, in evaluating the avoided emissions of interventions in the electricity system (Doucette & McCulloch, 2011; Farhat & Ugursal, 2010; Hawkes, 2010; Marnay et al., 2002; Siler-Evans et al., 2012). The conventional MEFs focused on emitting sources such as coal and natural gas. This approach may suffice to assess the avoided emissions from interventions that aim to displace fossil-fueled generators (Graff Zivin et al., 2014; E. S. Hittinger & Azevedo, 2015a; Siler-Evans et al., 2012) when there is low penetration and dispatchability of non-emitting sources such as wind. With renewables playing an increasingly important role and gaining improved dispatchability, however, the conventional MEFs may significantly overestimate the magnitude of avoided emissions and underestimate the role of renewables in shaping MEFs. Our expanded MEFs considering both emitting and non-emitting sources on the margin provides more accurate estimates of the avoided emissions from interventions including bulk energy storage, PHEVs, and demand response (DR).

Our results have important implications for regional electricity system policy making. Although the MISO overall has a low level of renewable penetration and renewables make a small contribution to marginal generation, there is significant heterogeneity at the subregional level. Wind penetration in the North is high and so is its

contribution to marginal generation. Due to transmission congestions and renewables curtailment, further deployment of wind power in the North may not be as effective at reducing emissions as in other subregions of MISO that also have abundant wind resources. Energy policies using MEFs would benefit from specified consideration of subregional differences in fuel mix.

We find significant hour-to-hour differences of the expanded MEFs for CO_2 in North, but modest hour-to-hour differences in Central and South. In North, the MEFs for CO_2 tend to be lower in winter and nighttime when system demand is low and the wind resource is abundant and more often on the margin; whereas in Central and South, the MEFs for CO_2 tend to be higher during night hours, when system demand is low and coal and gas are more often on the margin. The spatiotemporal heterogeneity of MEFs provide valuable guidance for policy makers and practitioners to evaluate the environmental impacts of emerging technologies with respect to their operational characteristics. For example, PHEVs that are scheduled to charge overnight will end up having quite low emission impacts if their owners reside in North, but relatively high emission impacts if their owners live in Central and South.

We note that deploying bulk energy storage technologies and demand-side management programs in MISO to shift 1 MWh of electricity generation from high- to low-demand hours can result in a CO_2 emission increase of 0.189 tons or 30%, if the technologies have a round-trip efficiency of 100%, and 0.459 tons or 73.8%, if the technologies have a more realistic round-trip efficiency of 75%. The emission shortcoming of storage technologies has been recognized in previous studies and may jeopardize many valuable services provide by the storage technologies, including reliability, responsiveness, and integration of intermittent renewable resources (Carson & Novan, 2013; E. S. Hittinger & Azevedo, 2015a; Lueken & Apt, 2014). However, the studies underestimate the potential emission increases due to neglecting the marginal generation from renewables (Carson & Novan, 2013; E. S. Hittinger & Azevedo, 2015a; Lueken & Apt, 2014). We find that, in the North subregion where wind accounts for almost one third of the marginal generation, the negligence leads to underestimating the marginal emission increase from storage technologies by 4.5 times, if the technologies have a round-trip efficiency of 100%, and 1.3 times, if the technologies have a more

realistic round-trip efficiency of 75%. Therefore, policy makers and technology investors ought to be cognizant of the issues when assessing the value of additional bulk energy storage.

Our expanded MEFs have accounted for MISO system-wide generation profile changes in recent years and comprehensively estimate the avoided emissions of interventions in the current MISO electricity system. We recommend other markets of Independent System Operators (ISO) and Regional Transmissions Operators (RTO) to consider the impact of renewables when calculating MEFs. Our method and estimates may be further improved if MISO discloses the locational marginal generators (LMG) that are dispatched to meet the next increment of system load and balance the system. Future improvement in MEFs methods will enable proper assessment of policy and technology interventions in terms of their societal impacts and will stimulate effective investment and policy decisions.

A limitation of our study is the omission of electricity trade in estimation of MEFs. Detailed data on how electricity flows between MISO subregions or between MISO and other regions are not readily available. Electricity import rate in different eGRID subregions ranges from 0 to 30%, although 30% would be an extreme case and 15% is already an upper bound for many regions (Diem & Quiroz, 2012b); monthly electricity net interchange rate between MISO and other balancing authority regions ranges from 2 to 12% (EIA, 2016). Assuming an unlikely net interchange rate of 30% between MISO subregions, the expanded MEFs would be lower than the conventional MEFs by about 10% in the wind-rich North subregion (Table A.2 and Figure A.3). And assuming a more reasonable 15%, the expanded MEFs would be lower by 14-18%. The results indicate that considering electricity interchange would not affect our main message that it is important to incorporate renewables in MEFs estimation in high renewable penetration regions so as to provide more accurate estimates of avoided emissions by policy interventions. This is especially true given the trend of continuous renewables expansion around the world.

Chapter 3

Multi-Regional Energy and Emissions Assessment on Electrification of Residential for Space Conditioning

Ground source heat pumps (GSHP) have been examined globally as an efficient electrification technology that provides energy savings and emission reductions when deployed in residential houses. However, existing studies have largely focused on GSHPs in a particular climatic region and used average emission factors (AEFs) of the power grid to assess GSHPs' emissions performance. Here, we demonstrate a multi-regional study to compare several modeled GSHP systems against conventional natural gas and air conditioner systems with regard to their annual energy consumption and Carbon Dioxide (CO_2) emissions. We analyze twelve system-in-house scenarios across three climatic regions and utilize various EFs of the Midcontinent Independent Systems Operator (MISO) grid. Results show that the GSHP systems analyzed consume less energy than the conventional systems in all scenarios, but their site energy savings do not necessarily translate to CO_2 emission reductions due to the spatiotemporal variability of the grid fuel mix in certain locations. Findings reveal that applying the EFs with higher spatial and temporal resolutions and using marginal EFs (MEFs) instead of AEFs both give more accurate emission estimates. Our study highlights the importance of applying the accurate EF metric to emissions performance assessment and recommends policymaking to incentivize distributed electrification technologies that meet today's grid realities and a renewable-integrated grid of tomorrow.

3.1 Introduction

Energy use is one of the main drivers of anthropogenic greenhouse gases emissions and the consequential global warming effects (Pachauri et al., 2015). Structural reforms in various energy end-use sectors are required to achieve the climate change mitigation goal, such as improvement of energy efficiency, electrification of energy end uses and decarbonization of electric power generation (Williams et al., 2014). In the United States (U.S.), the residential sector consumed about 20% (or about 18 quadrillion British thermal units) of total energy use in 2017 (U.S. Energy Information Administration, 2018). Heating, ventilation, and air conditioning (HVAC) account for almost 50% of the onsite energy use in U.S. homes (U.S. Energy Information Administration (EIA), 2013). Therefore, applications of the most efficient residential HVAC systems are urgently needed to help reduce energy consumption and related environmental impacts. Many studies have investigated innovative HVAC technologies from the perspective of reducing energy use and emissions (Fiorentini, Cooper, & Ma, 2015; Graditi et al., 2015; Gustafsson et al., 2014; Ippolito, Zizzo, Piccolo, & Siano, 2014; J. W. Lund & Boyd, 2016). Ground source heat pump (GSHP) system has been found being a good alternative for space heating and cooling, because it utilizes renewable geothermal energy and has higher efficiency than the conventional HVAC systems (Curtis, Lund, Sanner, Rybach, & Hellström, 2005; Lucia, Simonetti, Chiesa, & Grisolia, 2017; Sarbu & Sebarchievici, 2014).

Previous research has found GSHP systems can significantly reduce energy use and CO_2 emissions when compared against conventional HVAC systems in many situations and at different spatial scales (Cassidy, 2003; Curtis et al., 2005; Huelman et al., 2016; M. Li, 2013; LIENAU, 1997; J. W. Lund, 1988; Meyer, Pride, O'Toole, Craven, & Spencer, 2011). Energy performance of GSHP systems was evaluated in specific regions including Alaska in the U.S., Minnesota in the U.S., southern Germany, northern Tunisia, and Ireland, and cities, such as Shenyang in China and a Himalayan city in India; results showed the systems could achieve energy savings due to their relatively stable coefficient of performance (COP) (Cassidy, 2003; Dai et al., 2015; M. Li, 2013; Liu, Xu, Zhai, Qian, & Chen, 2017; Luo et al., 2015; Meyer et al., 2011; Naili, Hazami, Attar, & Farhat, 2016; Sivasakthivel, Murugesan, Kumar, Hu, & Kobiga, 2016). Shen and Lukes investigated

the performance of GSHP technologies across U.S. climate zones and found global warming could decrease GSHP's energy efficiency due to soil temperature rise Particularly in cooling dominated locations (Shen & Lukes, 2015). Environmental performance of GSHP systems have largely been assessed within a life-cycle framework, using historical annual average emission factors (EFs, in kg CO_2 e/kWh) of the electric power grid were used to estimate life-cycle emissions from operational electricity consumption by GSHP systems (Bayer, Saner, Bolay, Rybach, & Blum, 2012; Blum, Campillo, Münch, & Kölbel, 2010; Huang & Mauerhofer, 2016; Koroneos & Nanaki, 2017; Saner et al., 2010) In all studies, electricity in the use phase was found to play the dominant role in the climate impacts over the lifespan of GSHP systems; thus, carbon intensity of the electricity production substantially affects GSHP systems' life-long emission (Mattinen, Nissinen, Hyysalo, & Juntunen, 2015).

Existing research that calculates the emissions from deploying and operating the GSHP technologies are mainly carried out in the life cycle assessment (LCA) context, where the annual average emission factor (AEF) is the most commonly used metric in the calculation. However, power grids' instant EFs are much more volatile than their annual AEF due to the fact that, in practice, generation profiles in power grids are constantly changing over time to balance the changes in demand. Furthermore, because GSHP systems have not been widely adopted in U.S. homes (Hughes, 2009), their electricity use due to daily operation can be considered as marginal demand for the entire power system. Hence, marginal emission factors (MEFs), which estimate the emission intensity of power generation that responds to incremental demand, are a more appropriate metric to assess emissions related to GSHP systems' operational electricity use (M. Li, Smith, Yang, & Wilson, 2017). In other words, using annual average EFs can practically misestimate the total emissions from GSHP systems' long-term electricity consumption. Such misestimation would lead to fallacious conclusions regarding GSHPs' actual environmental benefits. This will not only impact homeowners who live in a particular region and wonder how much exactly they can reduce CO_2 by installing GSHP systems at home, but also influence policymakers who care about where, across various regions, they should deploy more GSHP systems to propel effective demand-side energy transition.

In this study, we first simulate and compare the heating and cooling energy consumption by GSHP and GFAC (natural gas furnace and air conditioner) systems hypothetically installed in residential houses with different house and technology configurations in Minneapolis, St. Louis, and New Orleans, then we calculate and compare the annual CO_2 emissions from the GSHP and GFAC systems. Results show that the annual energy consumption and CO_2 emissions vary substantially across cities and technologies, because 1) the cities are located in cold, mixed-humid, and hot-humid climate regions in the U.S., respectively; and 2) the technologies use electricity supplied by the North, Central, and South subregional power grids, which have different generation fuel mix profiles, in the Midcontinent Independent System Operator (MISO) system, respectively (Figure 3.1).

In the CO_2 emissions calculation, we use four types of emission factors (EFs) that have various spatial and temporal resolutions and account for total or marginal generation: 1) the MISO annual AEF, 2) the MISO subregional, i.e. North, Central, and South, annual AEFs, 3) the MISO spatiotemporal (subregional, month-hour) AEFs, and 4) the MISO spatiotemporal (subregional, month-hour) MEFs. Findings indicate that applying the EFs with higher spatial and temporal resolutions gives more accurate emission estimates, as their higher spatial and temporal granularities account for the variation in electricity consumption across space and time. We also find that using MEFs instead of AEFs in the calculation is more appropriate, because the electricity consumption from the modeled scenarios (GFAC and GSHP) is the marginal demand to the grid and MEFs reflect the emission intensity of the generation that responds to such marginal demand, whereas AEFs characterize the grid's average emission intensity which cannot reflect the fuel mix in marginal generation.

This study comprehensively assesses the performances of two different residential heating and cooling technologies, i.e. GFAC and GSHP, in the context of various house insulation configurations. The assessment and comparison between technologies and among scenarios provide broad policy implications for electrification in the residential sector.

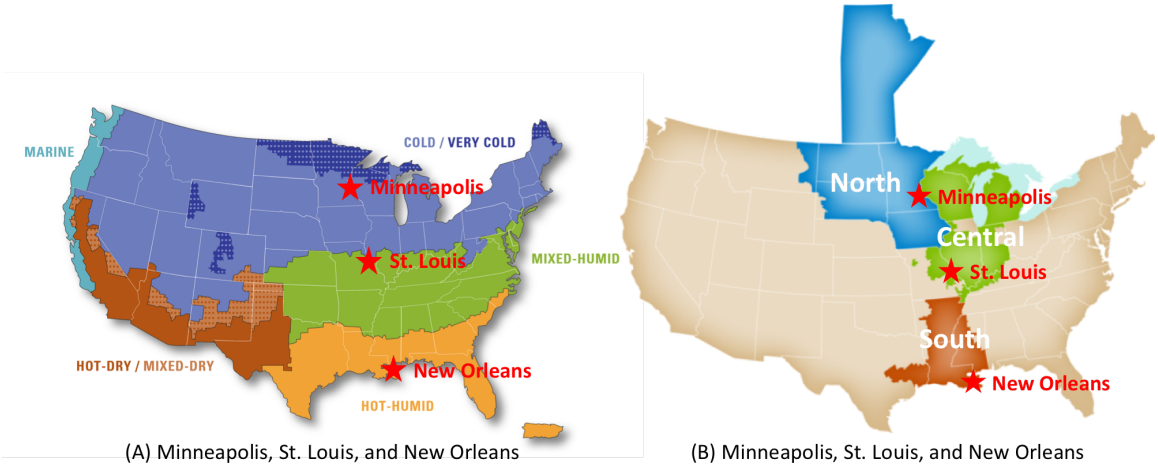

(A) Minneapolis, St. Louis, and New Orleans in the U.S. climatic regions

(B) Minneapolis, St. Louis, and New Orleans in the MISO sub-regional power grids

Figure 3. 1. Minneapolis, St. Louis, and New Orleans in the U.S. climatic regions (A) and the MISO subregional power grids (B).
Adopted from the U.S. Energy Information Administration (U.S. Energy Information Administration (EIA), 2009) and MISO (MISO, 2015c).

3.2 Methods

Hourly heating and cooling energy consumption of residential GFAC and GSHP systems in Minneapolis, St. Louis, and New Orleans are simulated using the Building Energy Optimization Tool (BEopt v2.8.0) developed by the National Renewable Energy Laboratory (NREL) (NREL, 2018). Beopt is a residential-specific modeling program that provides a graphical user interface for EnergyPlus, the flagship hourly-level energy use simulation engine which is well developed and documented by the U.S. Department of Energy (DOE) and widely used and respected by researchers and practitioners (DOE, 2018). The tool enables users to evaluate energy consumed by various HVAC technologies and consider the complex interactions of all building and climate variables. This study uses the site energy consumption simulated by the BEopt model.

Carbon dioxide emissions from the simulated hourly energy consumption are then calculated using four types of electric power grid's emissions factors that have different spatial and temporal granularities.

3.2.1 Residential heating and cooling system scenarios and energy consumption

For each city, we create twelve system-in-house scenarios to simulate and compare energy consumption and CO_2 emissions of the GFAC and GSHP technologies. In each

scenario, the cooling set point is 76 ºF and the heating set point is 71 ºF (Wilson, Engebrecht-Metzger, Horowitz, & Hendron, 2014). The Typical Meteorological Year, version 3 (TMY3) data at each city's airport is used as weather data in the energy use simulation model.

The residential houses in which the GFAC and GSHP technologies are hypothetically installed have different characteristics that frame low, medium and high house efficiency levels. To keep consistency and comparability, the twelve system-in-house scenarios are designed identical across the three cities. Details of the scenarios are displayed in Table 3.1 and Appendix B1.

Table 3. 1. Residential heating and cooling system-in-house scenario details.

Scenario component	Component description
System, GFAC	• Natural gas furnace: 90% AFUE[a] • Air conditioner: 13 SEER[b]
System, GSHP	• Low efficiency: COP 3.6[c]; EER 16.6[d] • Medium efficiency: COP 3.8[c]; EER 19.4[d] • High efficiency: COP 4.2[c]; EER 20.2[d]
House, 1984 square feet	• Low efficiency[e] • Medium efficiency[e] • High efficiency[e]

[a]AFUE is the annual fuel utilization efficiency of a natural gas furnace. Higher AFUE means higher efficiency.
[b]SEER is the seasonal energy efficiency ratio of an air conditioner. Higher SEER means higher efficiency.
[c]COP is the coefficient of performance that rates the heating efficiency of a ground source heat pump system. Higher COP means higher heating efficiency.
[d]EER is the energy efficiency ratio that rates the cooling efficiency of a ground source heat pump system. Higher EER means higher cooling efficiency.
[d]Detailed parameter selections about house efficiency are provided in Appendix B1.

3.2.2 CO_2 emissions

Based on the scenario design in this study, there are two sources of CO_2 emissions from residential heating and cooling systems: 1) on-site natural gas combustion in the GFAC system's gas furnace and 2) electricity consumption by the GFAC system's air conditioner and the GSHP system's heat pump. For natural gas combustion, we use EIA's CO_2 emissions coefficients for natural gas (U.S. Energy Information Administration (EIA), 2016) to calculate related emissions. For electricity consumption, we use four types of emission factors: 1) the MISO annual AEF, 2) the MISO subregional, i.e. North, Central, and South, annual AEFs, 3) the MISO spatiotemporal

(subregional, month-hour) AEFs, and 4) the MISO spatiotemporal (subregional, month-hour) MEFs to assess CO_2 emissions related to electricity demand by the GFAC and GSHP systems at different spatial and temporal resolutions. All emission factors are calculated using data from MISO and the EPA's Air Market Program Data (AMPD) database.

We first apply the 2016 annual AEF of the MISO grid to calculate the annual CO_2 emissions from electricity consumption of all scenarios, as annual AEF is the most commonly used metric in life cycle assessment to measure year-round and life-long emissions from electricity consumption.

Next, we consider the spatial factor about electricity generation, as Minneapolis, St. Louis, and New Orleans are located in and connected to MISO's North, Central, and South subregional grids, respectively (see Figure 3.1). We apply the 2016 subregional AEFs to the annual CO_2 calculations with the purpose of improving spatial accuracy of the AEF metric.

Then, we integrate the temporal factor with the spatial factor regarding electricity generation, as the generation in MISO's subregional grids and the electricity consumption by GSHP both vary from hour to hour. We apply the 2016 spatiotemporal AEFs to the annual CO_2 calculations in order to improve the spatial and temporal accuracy of the AEF metric.

Lastly, we utilize the MEF metric which measures the emission intensity of marginal generation and has been recommended as the more appropriate metric than AEF to estimate emissions from marginal demand (Doucette & McCulloch, 2011; Farhat & Ugursal, 2010; Hawkes, 2010; Marnay et al., 2002; Siler-Evans et al., 2012). The MEF used here is an improved metric adopted from Li et al., which includes renewable generation in the calculation and considers spatial and temporal variations (M. Li et al., 2017). We apply the 2016 spatiotemporal MEFs to the annual CO_2 calculations.

3.3 Results

3.3.1 Energy consumption

Annual energy consumption of all twelve scenarios in Minneapolis, St. Louis, and New Orleans are presented in Figure 3.2. Natural gas consumption by GFAC systems

were initially measured in MMBtu (thermal heat unit) but later converted to MWh (electric heat unit) in order to secure comparability against GSHP systems.

We find GFAC system's annual energy consumption ranging from 13.8 to 30.5 MWh in Minneapolis, from 8.1 to 18.5 MWh in St. Louis, and from 3.5 to 6.6 MWh in New Orleans. The higher the house efficiency is, the less energy the GFAC systems consumes year-round. All GSHP systems are found achieving energy savings compared to the GFAC system in the same house and city: annual energy consumption of GSHP ranges from 3.8 to 9.8 MWh (compared to 13.8 to 30.5 MWh of GFAC) in Minneapolis, from 2.5 to 6.2 MWh (compared to 8.1 to 18.5 MWh of GFAC) in St. Louis, and from 2.5 to 4.3 MWh (compared to 3.5 to 6.6 MWh of GFAC) in New Orleans. Under the same house efficiency, the higher the GSHP system efficiency is, the greater the energy savings are.

House efficiency improvement is found enhancing the annual heating and cooling energy savings by GSHPs compared to the GFAC system in Minneapolis, weakening those in New Orleans, and having a mixed effect on those in St. Louis. This is because such improvement is more effective in reducing heating energy use than reducing cooling energy use in all three cities, while the heating-cooling ratio is quite different across the cities: heating being dominant in Minneapolis, cooling being dominant in New Orleans, and heating-cooling being relatively balanced in St. Louis (Figure 3.2). In Minneapolis, GSHP systems at low, medium, and high efficiency levels save annual energy use by 67.7%, 69.3%, and 71.7% in the low-efficient house, by 67.8%, 69.4%, and 71.8% in the medium-efficient house (slight increase from the low-efficient house), and 68.2%, 69.9%, and 72.3% in the high-efficient house (slight increase from the medium-efficient house); in St. Louis, GSHP systems at low, medium, and high efficiency levels save annual energy use by 66.4%, 68.6%, and 70.9% in the low-efficient house, by 66.6%, 68.9%, and 71.2% in the medium-efficient house (slight increase from the low-efficient house), and 63.8%, 66.5%, and 68.9% in the high-efficient house (slight decrease from the medium-efficient house); in New Orleans, GSHP systems at low, medium, and high efficiency levels save annual energy use by 35.8%, 42.4%, and 44.9% in the low-efficient house, by 27.5%, 35.6%, and 38.1% in the medium-efficient house (slight decrease from

the low-efficient house), and 14.3%, 24.1%, and 26.9% in the high-efficient house (slight decrease from the medium-efficient house).

Homeowners can also save annual heating and cooling energy consumption by simply improving their house's efficiency without adopting the new technology (GSHP). For homeowners in Minneapolis, improving their house efficiency from low to medium saves annual heating and cooling energy consumption by 33.0% if they have an GFAC system and by 33.4% on average if they have an GSHP system; while improving their house efficiency from low to high saves annual heating and cooling energy consumption by 54.6% if they have an GFAC system and by 55.5% on average if they have an GSHP system. For homeowners in St. Louis, improving their house efficiency from low to medium saves annual heating and cooling energy consumption by 34.2% if they have an GFAC system and by 34.8% on average if they have an GSHP system; while improving their house efficiency from low to high saves annual heating and cooling energy consumption by 55.9% if they have an GFAC system and by 52.8% on average if they have an GSHP system. For homeowners in New Orleans, improving their house efficiency from low to medium saves annual heating and cooling energy consumption by 32.6% if they have an GFAC system and by 24.3% on average if they have an GSHP system; while improving their house efficiency from low to high saves annual heating and cooling energy consumption by 47.6% if they have an GFAC system and by 30.6% on average if they have an GSHP system.

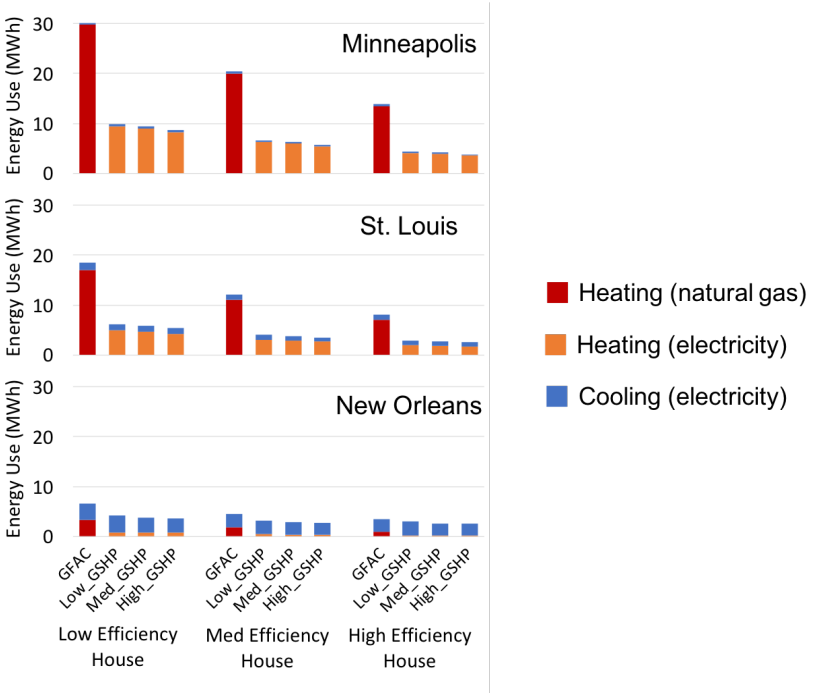

Figure 3. 2 Annual energy consumption of the system-in-house scenarios in Minneapolis, St. Louis, and New Orleans.

3.3.2 CO_2 emissions

As described in the method section, annual CO_2 emissions from the electricity consumption by the GFAC and GSHP systems in Minneapolis, St. Louis, and New Orleans are calculated using four types of emission factors with different spatial and temporal granularities to inspect and compare their effects on total emissions. Results show that the annual CO_2 emissions of a GFAC or a GSHP system are different when calculated using different EF metrics. As the EFs' spatial and temporal resolutions improve and the EFs characterize the marginal, renewable-included generation, the annual CO_2 emissions from electricity consumption by the GFAC and GSHP systems are more accurately and appropriately estimated.

As shown in Table 3.2, a medium-efficient GSHP system in a 1984-square-foot, medium-efficient house in Minneapolis causes less CO_2 emissions as the EFs' spatial and temporal resolution improves: by using the subregional AEFs, the spatiotemporal AEFs, and the spatiotemporal MEFs, annual CO_2 emissions of the GSHP system are reduced by 15.2%, 18.0%, and 18.2% from the emissions calculated using the MISO AEF,

respectively. For the same GSHP scenario in St. Louis, more spatial and temporal granularity in the EFs and the switch from AEFs to MEFs actually cause the GSHP's annual CO_2 emissions to increase by 19.0%, 17.7%, and 13.1% from the emissions calculated using the MISO AEF. For this GSHP scenario in New Orleans, more granular EFs and the switch from AEFs to MEFs lower the GSHP's annual CO_2 emissions by 22.7%, 21.1%, and 0.8% from the emissions calculated using the MISO AEF, but the switch from the spatiotemporal AEFs to MEFs actually causes an increase of 0.205 metric tons in annual CO_2 emissions.

The comparison among different AEF metrics, i.e. the MISO AEF, the subregional AEFs, and the spatiotemporal AEFs, reveals that the place and time of GSHP's operation are critical for its cumulative CO_2 emissions. Accounting for spatial and temporal factors in the AEF metrics lowers the GSHP's annual CO_2 emissions in Minneapolis, from 3.868 to 3.280 to 3.171 metric tons, and New Orleans, from 1.779 to 1.375 to 1.403 metric tons; but it raises the GSHP's annual CO_2 emissions in St. Louis, from 2.337 to 2.781 to 2.752 metric tons.

Table 3. 2 Annual heating and cooling energy use and CO_2 emissions of a medium-efficient GSHP system in a 1984-square-foot, medium-efficient house.
Numbers in brackets represent the overall CO_2 emission intensity (metric tons/MWh), which equals to annual CO_2 divided by annual electricity consumption.

City	Electricity (MWh)	CO_2 (MT) MISO AEF	CO_2 (MT) subregional AEFs	CO_2 (MT) spatiotemporal AEFs	CO_2 (MT) spatiotemporal MEFs
Minneapolis	6.256	3.868 (0.618)	3.280 (0.524)	3.171 (0.507)	3.164 (0.506)
St. Louis	3.780	2.337 (0.618)	2.781 (0.736)	2.752 (0.728)	2.643 (0.699)
New Orleans	2.878	1.779 (0.618)	1.375 (0.478)	1.403 (0.487)	1.765 (0.613)

We further inspect the effect of switching from the spatiotemporal AEFs to the renewables-included MEFs on when calculating the annual CO_2 emissions from this medium-efficient GSHP system in the 1984-square-foot, medium-efficient house (Figure 3.3). Figure 3.3 illustrates the GSHP's heating and cooling CO_2 emissions in a month-hour context. It shows that the spatiotemporal AEFs lead to few emission variations

across hours in the same month (Figure 3.3A), which partially reflects the fairly constant grid average fuel mix profile in MISO's subregions. However, the CO_2 emissions calculated using the MEFs are found varying much more substantially from hour to hour in the same month, especially during the heating season in Minneapolis (Figure 3.3B). The observation implies the EFs of renewables-included marginal generation are substantially different from the EFs of grid total generation, even in the same spatial and temporal context. Moreover, the variation of the annual CO_2 emissions calculated using MEFs (Figure 3.3B) reveals critical opportunities for mitigating emissions from the GSHP by better strategizing the operation of GSHP, such as shifting load from high-emission hours to low-emission hours while maintaining the heating or cooling requirement.

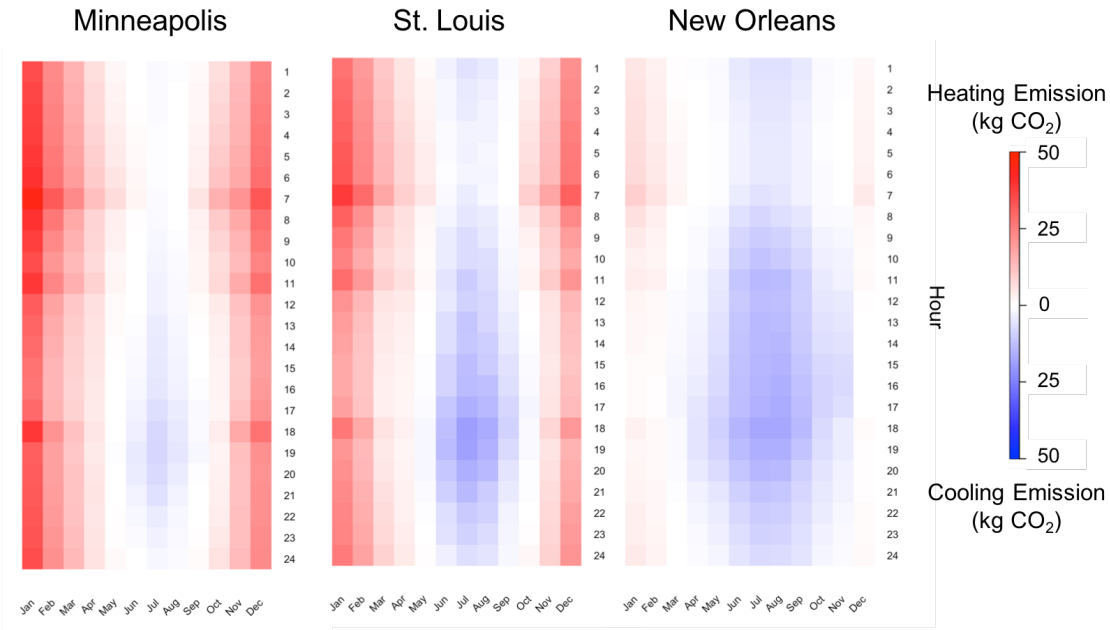

(A) Monthly and hourly CO_2 emissions calculated by AEFs

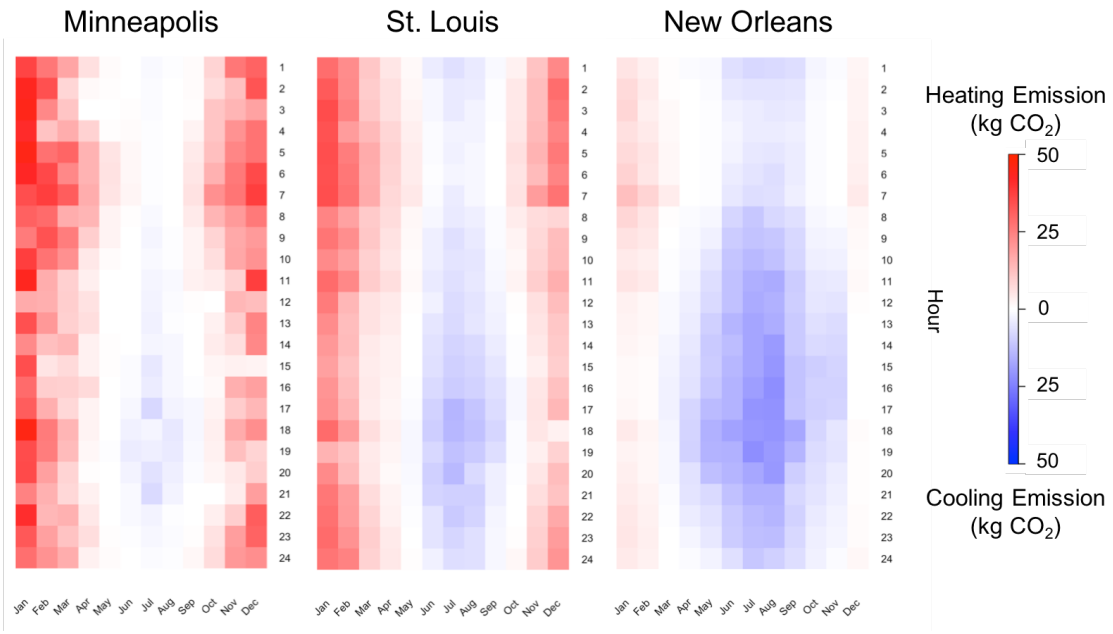

(B) Monthly and hourly CO_2 emissions calculated by MEFs

Figure 3. 3. Monthly and hourly CO_2 emissions from a medium-efficient GSHP system in a 1984-square-foot, medium-efficient house calculated using spatiotemporal AEFs (A) and MEFs (B).

Annual CO_2 emissions from the energy (natural gas and electricity) consumption by all residential heating and cooling scenarios in Minneapolis, St. Louis, and New Orleans are presented in Figure 3.4. Results show the high-efficient GSHP system always reduces annual CO_2 emissions compared to the GFAC system in the same house regardless of the city location, but the amount of reduction varies from city to city. The low- and medium-efficient GSHP systems are found having a mixed outcome: some have increased whereas others have decreased emissions compared the GFAC system. The increase and decrease are essentially dependent on which EF metric is used in the calculation as well as the city where the inspection focuses on.

In Minneapolis, using the MISO AEF to calculate annual CO_2 emissions (Figure 3.4A) leads to the low-efficient GSHP systems having 1% to 5% more emissions than the GFAC system in the same house, dependent on the house efficiency, while the medium- and high-efficient GSHP system having 1% to 12% less emissions than the GFAC system in the same house, dependent on the house efficiency. Switching from the MISO AEF to the subregional AEFs (Figure 3.4B) decreases annual emissions for all GSHP scenarios and makes them have less emissions than the GFAC: 10%, 14%, and 21% lower in the low-efficient house, 10%, 15%, and 22% lower in the medium-efficient house, and 13%,

18%, and 24% lower in the high-efficient house. Applying the spatiotemporal AEFs (Figure 3.4C) and MEFs (Figure 3.4D) also makes all GSHP scenarios capable of reducing emissions compared to the GFAC system in the same house: the AEFs lead to reductions of 14%, 18%, and 25% in the low- and medium-efficient houses and reductions of 17%, 21%, and 27% in the high-efficient house; meanwhile the MEFs lead to slightly smaller reductions of 13%, 17%, and 24% in the low- and medium-efficient houses and reductions of 15%, 20%, and 26% in the high-efficient house.

In St. Louis, using the MISO AEF to calculate annual CO_2 emissions (Figure 3.4A) leads to all GSHP scenarios having less emissions than the GFAC system: 4%, 10%, and 17% lower in the low-efficient house, 7%, 13%, and 20% lower in the medium-efficient house, and 6%, 13%, and 19% lower in the high-efficient house. However, switching from the MISO AEF to the subregional AEFs (Figure 3.4B) makes the low-efficient GSHP systems have more annual emissions than the GFAC system: 9%, 5%, and 5% in the low-, medium-, and high-efficient houses; the medium-efficient GSHP systems are found increasing the annual emissions by 2% in the low-efficient house while reducing those by 2% and 3% in the medium- and high-efficient houses; the high-efficient GSHP systems lower annual emissions by 5%, 9%, and 10% in the low-, medium-, and high-efficient houses. Applying the spatiotemporal AEFs (Figure 3.4C) and MEFs (Figure 3.4D) gives similar emission increase or decrease rates of comparing the GSHPs against those of the GFACs: for the low-efficient GSHP system, the AEFs lead to increases of 7%, 3% and 3% in the low-, medium- and high-efficient houses, respectively, while the MEFs lead to increases of 8%, 5% and 4% in the low-, medium- and high-efficient houses, respectively; for the for the medium-efficient GSHP system, the AEFs lead to reductions of 0.02%, 4% and 5% in the low-, medium- and high-efficient houses, respectively, while the MEFs lead to an increase of 2% in the low-efficient house and reductions of 2% and 3% in the medium- and high-efficient houses, respectively; for the high-efficient GSHP system, the AEFs lead to increases of 7%, 11% and 12% in the low-, medium- and high-efficient houses, respectively, while the MEFs lead to increases of 6%, 10% and 10% in the low-, medium- and high-efficient houses, respectively.

In New Orleans, using the MISO AEF (Figure 3.4A) leads to the low-efficient GSHP systems having 1%, 1%, and 5% more annual emissions compared to the GFAC

system in the low-, medium- and high-efficient houses, respectively; the medium-efficient GSHP systems are found reducing emissions by 10%, 10%, and 7% while the high-efficient GSHP systems are found reducing emissions 14%, 13%, and 11% in the low-, medium- and high-efficient houses, respectively. Switching from the MISO AEF to the subregional AEFs (Figure 3.4B) and spatiotemporal AEFs (Figure 3.4C) leads to quite similar outcomes: all GSHP scenarios reduce annual emissions by 3% to 19% compared to the GFAC system, except for the low-efficient GSHP system in the high-efficient house which has 2% more emissions than the GFAC system installed in the same house. Under the spatiotemporal MEFs, all GSHP scenarios reduce annual emissions by 1% to 15% compared to the GFAC system, except for the low-efficient GSHP systems in the medium- and high-efficient houses which have 0.44% and 4% more emissions than the GFAC system installed in the same house.

Similar to how house efficiency improvement saves energy consumption without technological replacement, the medium- and high-efficient houses, when compared to the low-efficient house, are found reducing about 33% and 55% of annual CO_2 emissions in Minneapolis, reducing about 34% and 52% of annual CO_2 emissions in St. Louis, and reducing about 25% and 31% of annual CO_2 emissions in New Orleans. This provides another potential solution for mitigating emissions from residential energy use besides adopting alternative technologies.

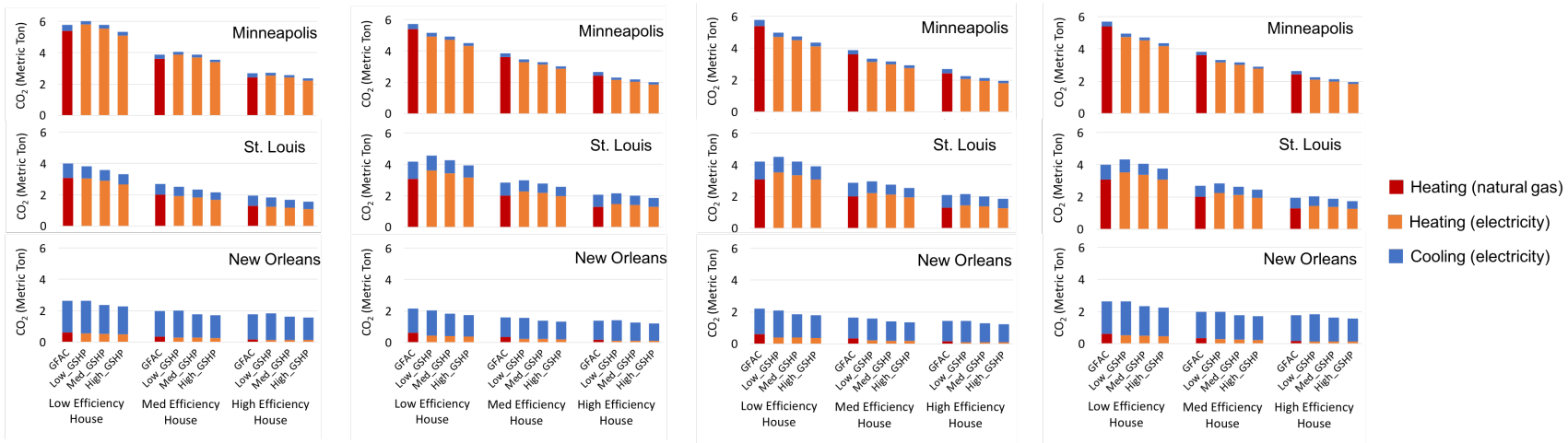

(A) CO_2 emissions (MISO AEF)

(B) CO_2 emissions (subregional AEFs)

(C) CO_2 emissions (spatiotemporal AEFs)

(D) CO_2 emissions (spatiotemporal MEFs)

Figure 3. 4. Annual CO_2 emissions of the heating and cooling scenarios in Minneapolis, St. Louis, and New Orleans.

3.4. Discussion

3.4.1 Average emission factors (AEFs) versus marginal emission factors (MEFs)

Marginal emission factors (MEFs) have been acknowledged as a more appropriate metric than average emission factors (AEFs) in evaluating emissions from electricity consumption by electric-powered technologies. AEFs may suffice to assess the emissions from technologies that have constant electricity consumption over time such as baseload demand. However, they would neglect the temporal variations in grid's generation fuel mix therefore significantly misestimate the amount of emissions from temporally varying electricity consumption, such as residential heating and cooling. Comparison between Figure 3.3A and Figure 3.3B shows that CO_2 emissions caused by GSHP system consuming electricity can vary significantly from hour to hour in all three cities if they are calculated using MEFs, whereas using AEFs to calculate the CO_2 emissions does not show great hour-to-hour variances. The variation of CO_2 emissions displayed in Figure 3.3B can serve as an informative tool to assist smarter operation of GSHP or any electric-powered appliances to reduce overall CO_2 emissions by potentially shifting the operation away from carbon-heavy hours. With regard to annual CO_2 emissions, we find using AEFs, especially the MISO AEF, may misestimate the emissions of all system-in-house scenarios. Such misestimation by using AEFs instead of MEFs could potentially conceal the environmental benefits, i.e. CO_2 emissions reduction, GSHP systems could have provided by replacing GFAC systems in Minneapolis and St. Louis, yet it exaggerates the benefits in New Orleans.

3.4.2 Policy implications

Our findings have important implications for residential energy transition and electricity system policy making at federal and state governments. The transition from natural gas to electricity for residential heating and cooling is found capable of significantly saving energy consumption in various system and house scenarios across different climate zones. But the lifetime economic cost of residential GSHP system may not be as competitive against the more conventional GFAC system, specifically due to

GSHP system's relatively high capital cost (Self, Reddy, & Rosen, 2013). Therefore, availability of financial incentives can play a crucial role in overcoming market barriers for the residential GSHP technology. According to the Database of State Incentives for Renewables & Efficiency (DSIRE), homeowners who are interested in investing in GSHP technologies can be incentivized by three loan programs (one federal, one state, one local) and one rebate program by local utility if they reside in Minneapolis (DSIRE, 2018a, 2018c, 2018d, 2018f), or two loan programs (one federal and one local) if they reside in St. Louis or New Orleans (DSIRE, 2018a, 2018e, 2018b). However, none of the programs incentivizes residential GSHP technologies based on their efficiency levels. This potentially encourages consumers to purchase the least-efficient GSHP systems, because they usually are the cheapest, and consequently lose the energy savings that could have been gained by GSHP systems at higher efficiency levels: 227 to 747 kWh in Minneapolis, 196 to 435 kWh in St. Louis, and 96 to 445 kWh in New Orleans. Therefore, energy transition policy aiming at reducing energy consumption should be made more explicit with regard to technologies' efficiency levels and maximize energy-saving benefits of the technologies.

We also find the gas-to-electricity transition for residential heating and cooling can reduce annual CO_2 emissions in various house scenarios and across different climate zones, except for the transition from GFAC system to low-efficient GSHP systems in St. Louis. The CO_2 emissions reduction is not as substantial as the energy savings for each transition scenario. We attribute this to the power grid that supplies electricity for energy use after the transitions. Grid with more renewable energy for marginal generation tends to have lower MEFs and leads to less CO_2 emissions from residential electricity consumption than the grid with more fossil energy in the fuel mix. This requires more coordinated policy making about residential gas-to-electricity transition and power grid decarbonization, because environmental, economic, and societal benefits of the energy transition are profoundly impacted by the grid's profile (Dennis, Colburn, & Lazar, 2016; Williams et al., 2014).

3.4.3 House renovation without technological upgrade

As for homeowners, our findings show that replacing GFAC with GSHP system may not be the only option to cut energy bills and emit less CO_2. Retrofitting houses by improving insulation is one relatively inexpensive option compared to adopting new technologies like GSHP. We find that homeowners having GFAC system can reduce heating and cooling energy consumption by 33% to 55% and associated CO_2 emissions by 25% to 55% if their houses become more efficient. Improving house efficiency alone may not be able to reduce as much energy use and CO_2 emissions as switching to GSHP systems in most scenarios, but it certainly can be fairly cost-effective and having short payback time compared to purchasing and installing new GSHP systems. However, if homeowners choose to invest in house retrofit first, the likelihood of them spending another greater amount of money on replacing GFAC with GSHP will be lessened. In addition, as their houses become more efficient, the energy savings and CO_2 emissions reduction they could have receive from only switching to GSHP systems will be shrunk. This will potentially depreciate the benefits of replacing GFAC with GSHP and suppress the gas-to-electricity transition.

3.4.4 Limitation and future work

Our study focuses on building-level energy transition in the residential heating and cooling sector, therefore it has some limitation considering the fact that large-scale gas-to-electricity transitions in various sectors will cause foreseeable increase in electricity demand and require substantial expansion of power grid infrastructure and power generation capacity. Future work examining extensive energy transitions should account for such effects on the power grids. Meanwhile, the deployment of energy-transitioning technologies like GSHP and the planning of grid expansion should be carefully coordinated by effective policymaking.

Chapter 4

Locating Locational Marginal Prices in the Midcontinent Independent System Operator (MISO): Economic and Environmental Impacts of Emerging Grid-scale Electricity Storage across the Landscape

Energy storage technologies are recognized as important instruments to assist decarbonization and modernization of electricity system. As regulations mandate and policies incentivize additional energy storage installation, stakeholders are concerned about where and how new storage might be deployed and its impact on electricity markets. To address these concerns, we utilize a novel dataset of spatialized locational marginal prices (LMP) of electricity to estimate cash flows and emissions of grid-scale battery storage that are sited at 358 locations and arbitrage as price takers in the Midcontinent Independent System Operator (MISO) wholesale market. We find annual net operating revenue associated with a 0.5 MW/2.1 MWh battery storage ranging from $11,177 to $39,677. In addition, annual net CO_2, SO_2, and NO_x emissions range from -30 to 194 metric tons, from -87 to 372 kg, and from -428 to 96 kg, respectively. Our findings demonstrate specific locations where battery storage might initially be most profitable, which offers projection of future storage and has significant policy implications and the marginal environmental implications associate with these near-term adoptions.

4.1 Introduction

Electric power system is expected to play a pivotal role in realizing the global decarbonization goal that many countries committed to the 2015 Paris Agreement (Cleetus, Bailie, & Clemmer, 2016). In the United States (U.S.), Department of Energy (DOE) launched the Grid Modernization Initiative (GMI) in 2014 to accelerate the adoption of innovative technologies and the development of next-generation smart power grid across the country (U.S. DOE, 2017). Energy storage technology, such as electrochemical battery, pumped hydroelectric, and compressed air energy storage, has been recognized as an effective means to improve grid reliability, shave peak load, and hedge intermittency of renewables (Eyer & Corey, 2010; White House, 2016).

With a recent order issued by the Federal Energy Regulation Committee (FERC), pathways for more storage deployment in the grid have just been broadened. In February 2018, FERC issued Order 841 to "remove barriers to the participation of electric storage resources in the capacity, energy and ancillary services markets operated by Regional Transmission Organizations (RTOs) and Independent System Operators (ISOs)" (FERC, 2018). This certainly opens up market access for storage technologies and provides new opportunities for various revenue streams. It is foreseeable that more subsidies will likely to come from policies for storage projects, and more private funding will be invested into the market in addition to growing utility-owned storage capacity. Although RTOs/ISOs are given considerable flexibility in implementing FERC's regulation, it is difficult to predict how much, where, and in what form storage will be deployed without a thorough understanding of market and established market rules.

Despite the fact that adding energy storage in the current power grid may cause increased system-wide emissions (E. S. Hittinger & Azevedo, 2015b), U.S. legislation has pushed for more deployment of storage. In the Western U.S., the Governor of California signed AB2514 in 2010 directing the California Public Utility Commission (CPUC) to determine appropriate energy storage goals (California, 2010), which led to a mandate later in 2013 requiring three large California investor-owned utilities to procure 1325 MW of storage capacity by 2020 (California Public Utilities Commission, 2013). In 2016, Oregon followed California's step to require major utilities have at least 5 MWh of energy storage capacity in 2020 (Oregon, 2016). On the U.S. east coast, Massachusetts

was the first state to set an energy storage goal of 200 megawatt-hour (MWh) by 2020 (State of Massachusetts, 2017). The State of New York established a storage procurement goal for 2030 (State of New York, 2017). Most recently, New Jersey is set to reach 600 megawatts (MW) of storage capacity by 2021 and 2 gigawatts (GW) by 2030 (State of New Jersey, 2018). Many utilities have implemented new storage deployment under such mandates. In 2017, for example, California utilities Southern California Edison and San Diego Gas & Electric unveiled grid-scale battery storage facilities of 80 MWh (partnered with Tesla) and 120 MWh (partnered with AES Energy Storage), respectively, aiming to pick up the unmet demand after the Aliso Canyon natural gas leak (San Diego Gas & Electric, 2017; Southern California Edison, 2018).

Prior studies have extensively examined energy storage technologies from the perspectives of arbitrage opportunities, optimal sizing, and benefits from integrating with renewables. (Barton & Infield, 2004; Beaudin, Zareipour, Schellenberglabe, & Rosehart, 2010; Garcia-Gonzalez, Muela, Santos, & Gonzalez, 2008; Korpaas, Holen, & Hildrum, 2003; N. Li & Hedman, 2015; Marzband, Ghazimirsaeid, Uppal, & Fernando, 2017; Paine, Homans, Pollak, Bielicki, & Wilson, 2014; Staffell & Rustomji, 2016; Swider, 2007; Zhao, Wu, Hu, Xu, & Rasmussen, 2015). Real-time electricity prices are used in many studies to inspect storage's optimal operation strategy, environmental impacts, and economic feasibility in the U.S. (Bradbury, Pratson, & Patiño-Echeverri, 2014; E. Hittinger & Azevedo, 2017; E. S. Hittinger & Azevedo, 2015b; Krishnamurthy, Uckun, Zhou, Thimmapuram, & Botterud, 2018), Spain (Lujano-Rojas, Dufo-López, Bernal-Agustín, & Catalão, 2017), and Denmark (Hu, Chen, & Bak-Jensen, 2010). Real-time prices used in the studies are usually at hourly intervals, which is fairly fine temporal resolution, but spatially, the prices are only at regional- or state-level. Prices at such spatial granularity could be used to determine optimal operation for storage if it has been built up in the region or state. In reality, however, the emergence of these technologies is unlikely to be distributed equally across geographies due largely to economic conditions particular to individual locations. Within the same region or state, real-time electricity prices can vary drastically, even among nearby locations. As such, net operating revenues of storage are also expected to vary significantly, with the most profitable locations attracting early storage adaptors first. More importantly, the lack of finer spatial

granularity restrains prediction for siting of future storage, which is one of the matters that most concerns stakeholders, such as RTOs/ISOs, utility companies, and storage investors, especially after FERC issued Order 841 (Zidar, Georgilakis, Hatziargyriou, Capuder, & Škrlec, 2016).

In this study, we utilize a unique spatiotemporal, real-time electricity price dataset to identify the most profitable locations for grid-scale battery energy storage systems if they could, as price takers, participate in the current Midcontinent Independent System Operator (MISO) wholesale market. The dataset is unique in that it not only provides the finest known and publicly available temporal resolution (five-minute) of real-time locational marginal prices (LMPs) in MISO, but more importantly, it reveals the exact latitude and longitude of all MISO LMP locations shown on the real-time LMP map (MISO, 2018b). Such detailed geographic information of MISO LMP has not been published by previous studies, or made easily available in MISO's historical LMP market data archive (MISO, 2018a). The improved spatial resolution can facilitate more precise, location-specific analyses than those dependent on region- or state-level LMP (E. Hittinger & Azevedo, 2017; E. S. Hittinger & Azevedo, 2015b; Khani & Zadeh, 2015).

In the sections that follow, we assume that grid-scale battery storage has perfect information about real-time LMP in the MISO market. We analyze their optimal hourly operation strategy, aiming to maximize annual net operating revenue, for 393 different locations throughout the MISO region. By projecting the locations of battery storage and their maximized annual net operating revenue on a map, we address the "where to expect new storage facilities to appear first" question for stakeholders including MISO, utility companies, and storage investors. We then calculate annual net CO_2, SO_2, and NO_x emissions induced by economic-optimally operating the battery storage according to their locations in MISO's North, Central, and South subregions. We also calculate some metrics related to net operating profitability, such as capital cost and return on investment, of the battery storage, as these factors fundamentally affect how storage project will be financed. We conclude with a discussion about the broad policy and market implications of investigating grid-scale battery storage at fine spatial and temporal granularity in current electricity wholesale market.

4.2 Methods and Data

We develop an optimization model to determine the revenue-maximizing hourly operation of battery storage system when participating, as a price taker, in the MISO real-time wholesale market at each of the 393 MISO LMP locations (366 generators, 20 load zone nodes, and 7 hubs). To reflect the realistic operational patterns of energy storage, we set the battery system to only charge from and discharge to the grid, even if it is collocated with other generation facilities; therefore, its annual net operating revenue is maximized from energy arbitrage. Location-specific prices and emission factors are used in our analysis to reveal the optimal siting of foreseeable battery storage systems and consequential climate impacts.

The battery storage system is designed based upon the Tesla Powerpack battery, as it represents the state-of-the-art technology for grid-scale battery storage (Tesla, 2018). Each system contains 10 units of the Tesla Powerpack battery and has energy capacity of 2.1 MWh, alternating current (AC) power of 0.5 MW, round-trip efficiency of 88%, and depth of discharge (DoD) rate of 100%. The system operates on an hourly basis to maximize annual net operating revenue on an hourly basis over a year. We use a linear programming model to find the maximized annual net operating revenue and corresponding hourly operation patterns of the battery (Equation 6, where P_t is the price, Q_t^{inflow} and $Q_t^{outflow}$ are the energy flows in and out of the battery at time *t*) subject to constraints (Equations 6-12).

Maximize:

$$\sum_{t=1}^{T} P_t \times Q_t^{outflow} - \sum_{t=1}^{T} P_t \times Q_t^{inflow} \tag{6}$$

Subject to:

$$S_t^{battery} = \sum_{t=1}^{t} Q_t^{inflow} \times \sqrt{\eta} - \sum_{t=1}^{t} Q_t^{outflow} \times \frac{1}{\sqrt{\eta}} \tag{7}$$

$$S_0^{battery} = 0 \tag{8}$$

$$\forall\, t,\ S_t^{battery} \geq 0 \tag{9}$$

$$\forall\, t,\ S_t^{battery} \leq Q^{battery} \tag{10}$$

$$\forall\, t,\ Q_t^{inflow} \in [0,\ 0.5] \tag{11}$$

$$\forall\, t,\ Q_t^{outflow} \in [0,\ 0.5] \tag{12}$$

In the model, the round-trip efficiency η is split geometrically between the processes of charge and discharge (Equation 7). Net energy stored in the battery system $S_t^{battery}$ is initialized at zero (Equation 8) and is constrained to be between zero and the system's designed energy capacity $Q^{battery}$ (Equations 9 and 10) at time *t*. Equations 11 and 12 set the lower and upper bounds of charge and discharge rate at time *t*. Because the battery system is modeled to operate on an hourly basis, the energy flow, either Q_t^{inflow} or $Q_t^{outflow}$, in a timestep (in MWh) always equals to the power flow (in MW). Although the battery system is not constrained to permit only charge or discharge in a single timestep, efficiency losses naturally drives the system to either charge or discharge at any time.

The real-time, hourly wholesale electricity prices used in this study are the locational marginal prices (LMPs) throughout MISO region for the year 2016. The LMP data was obtained at five-minute level from the MISO real-time LMP contour map, an open-access portal of MISO system operation (MISO, 2018b). The five-minute LMP data has a mean of 25.60 $/MWh, a standard deviation of 23.53 $/MWh, and a very wide spread from -1979.36 $/MWh to 2016.72 $/MWh. Statistical distribution details of the data are illustrated in Figure 4.1. Because real-time LMP is location sensitive, we also inspect statistics of the five-minute LMP at each of the 393 locations (Figure 4.2). From location to location, the LMP's means range from 15.53 to 31.84 $/MWh while their standard deviation ranges from 8.69 to 83.71 $/MWh.

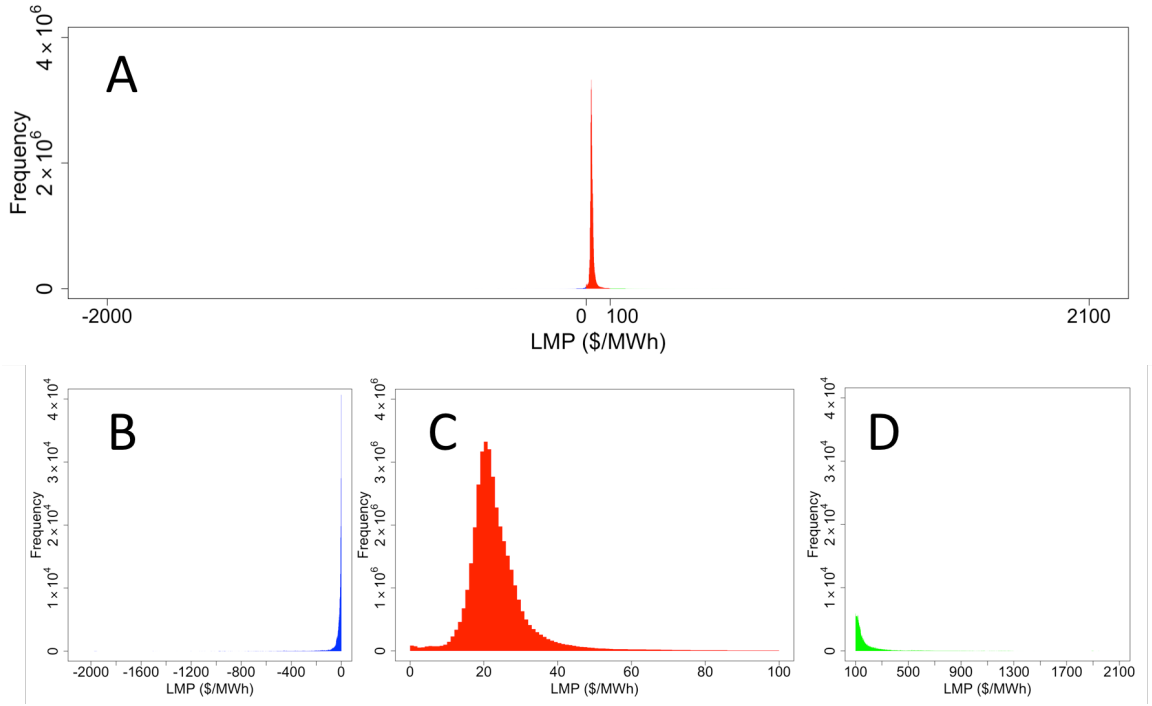

Figure 4. 1. Statistical distribution of 2016 five-minute LMP in MISO: overview of all five-minute LMP (A), separate view of all negative five-minute LMP (B), separate view of five-minute LMP ranging from 0 to 100 $/MWh (C), and separate view of five-minute LMP larger than 100 $/MWh (D).

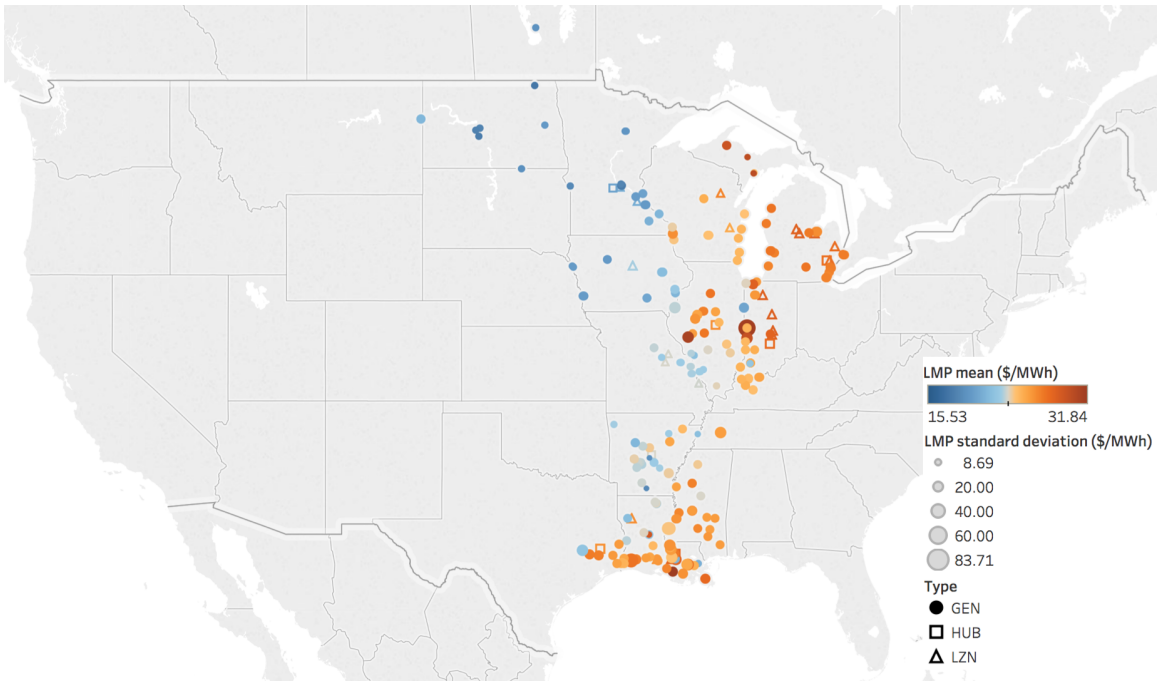

Figure 4. 2. Statistical distribution of 2016 five-minute LMP at 393 locations throughout MISO geographical footprint.
Under Type in the legend, GEN represents generator, HUB represents hub, and LZN represents load zone node.

Due to computational constraints of the optimization software, we use hourly LMP, averaged from the five-minute LMP, in the optimization model for battery storage. We were able to collect 99.2% of the 2016 hourly LMPs (8715 out of 8784 hours). To fill in the missing 69 hours, we apply a logic-based imputation approach to assign estimated values to each of the missing hours: 1) if the missing hour *h* is discrete, the LMP in hour *h* is the average of that in hour *h-1* and *h+1*; 2) if the previous or next hour of missing hour *h* is missing, the LMP in hour *h* is the average of that in hour *h-24* (same hour in previous day) and *h+24* (same hour in next day); and 3) if the previous or next hour and the same hour in previous or next day of missing hour h are missing, the LMP in hour *h* is the average of that in hour *h-24*, *h-48* (same hour in previous two days), *h+24* and *h+48* (same hour in next two days).

After applying the optimization model at each of the 393 LMP locations throughout MISO, we identify the revenue-maximizing hourly operation of a battery storage system at each location. We then calculate net emissions resulting from the system's year-round operation: when battery charges, it stores the emissions from the grid's marginal generator(s); when it discharges, it displaces emissions from the grid's marginal generator(s). Battery systems at the 393 LMP locations are classified into MISO's North, Central, and South subregions, according to the state in which each battery system is located and are assumed being connected to corresponding subregional grids. Hourly charge and discharge patterns of the battery systems are then matched with the marginal emission factors (MEFs) of corresponding subregional grids by time of day and month.

Marginal emission factors (MEFs) have been widely acknowledged as a more appropriate metric, than average emission factors (AEFs), to assess emissions caused by increase or decrease of grid generation in response to a change in demand (E. Hittinger & Azevedo, 2017; M. Li et al., 2017; Siler-Evans et al., 2012; Thind, Wilson, Azevedo, & Marshall, 2017). We use the method of calculating MEFs from Li et al., because they consider renewable sources in the MEF estimates and reflect the current marginal fuel mix in the MISO grid (M. Li et al., 2017). Specifically, we use 2016 electricity system data that comes from MISO and Air Market Program Data (AMPD) archive of the U.S. Environmental Protection Agency (EPA) (MISO, 2016a, 2016b; U.S. EPA, 2018), then apply 288 separate linear regression (Equation 13) approaches of change in emissions

$\Delta E_{m,h}$ against change in grid generation $\Delta G_{m,h}$ for MISO North, Central, and South subregions, where the slope $\beta_{m,h}$ is the MEF estimate (in metric tons of pollutant per megawatt-hour) for month m and hour h:

$$\Delta E_{m,h} = \beta_{m,h} \Delta G_{m,h} \tag{13}$$

Lastly, we calculate the annual total emissions by multiplying the hourly battery energy inflow (charge) and outflow (discharge) by corresponding subregional MEFs for the hour of day and month (Equation 14).

$$Emission_{annual} = \sum_{t=1}^{T} MEF_{h,m} \times Q_t^{outflow} - \sum_{t=1}^{T} MEF_{h,m} \times Q_t^{inflow} \tag{14}$$

4.3 Results

4.3.1 Annual net operating revenue

Hourly operation of battery storage is optimized, under specific technical constraints, to maximize net operating revenue for the year of 2016 at 393 LMP locations. We note that 35 locations have LMP data for less than 8784 hours thus are not included in the annual net operating revenue comparison. For the remaining 358 locations, results show that annual net operating revenue of battery storage varies substantially across locations from $11,177 to $39,677 (Figure 4.3). Battery storage located in and around the states of Illinois, Indiana, and Louisiana are found to generally make more annual net operating revenue than in other states. This is unsurprising because in Figure 4.2 we observe greater LMP variability in and around these states than in other states. To predict where new battery storage would be deployed first, we present 9 locations where battery storage can make the most annual net operating revenue for more than $ 25,000 in Figure 4.4. We find the locations are in the states of Illinois, Indiana, Iowa, Wisconsin, and Louisiana. It is noted that the California Ridge Wind Farm physically locates in Champaign County, Illinois, but its production is purchased by the Tennessee Valley Authority (TVA) company, so its LMP is shown at TVA's bus station in Tennessee instead of wind farm in Illinois (Tennessee Valley Authority, 2012). All of the 9 locations are found to be generators (GEN), including 6 coal-fired generating units,

1 peaking natural gas turbine, 1 hydroelectric station, and 2 wind farms. We also present annual net CO_2, SO_2, and NO_x emissions resulting from the optimal operation of battery storage at each of those location (Figure 4.4). Because seven out of the nine locations are in the Central subregion of MISO, annual net emissions of battery storage at these locations are found much higher than at the other two locations: CO_2 emissions ranging from 178 to 191 metric tons (compared to -22 and 77 metric tons at the other two locations), SO_2 emissions ranging from 318 to 353 kg (compared to -61 and 138 kg at the other two locations), and NO_x emissions ranging from 73 to 96 kg (compared to -399 and 48 kg at the other two locations).

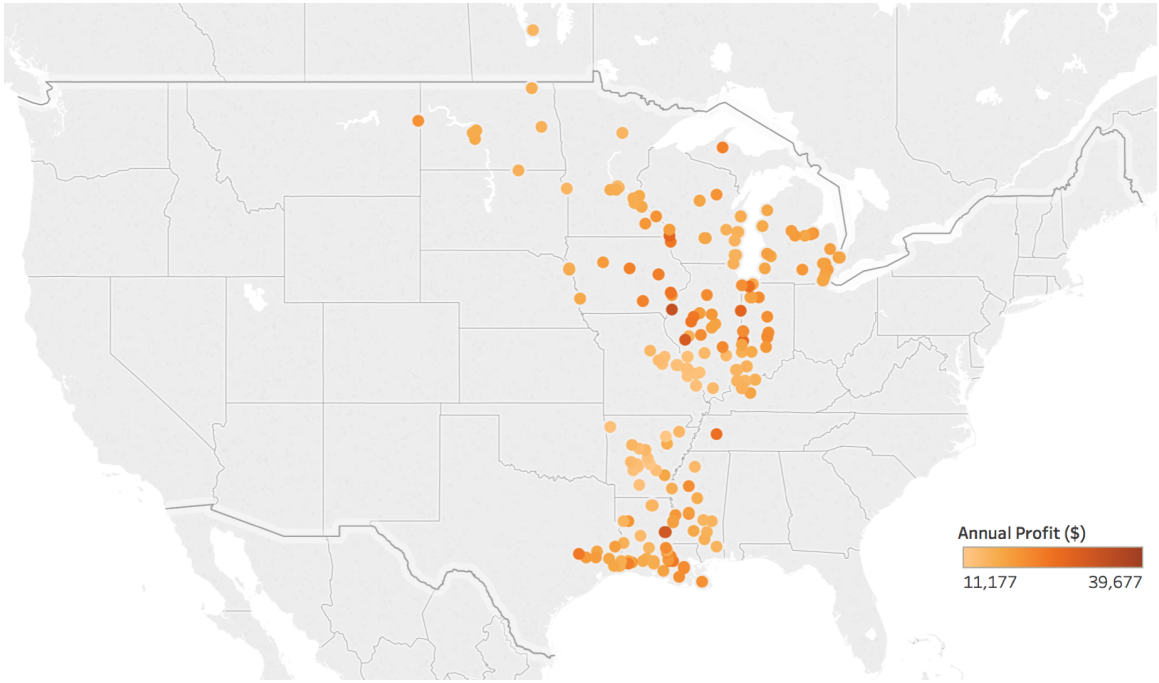

Figure 4. 3. Annual maximized net operating revenue of battery storage at 358 locations throughout MISO geographical footprint.

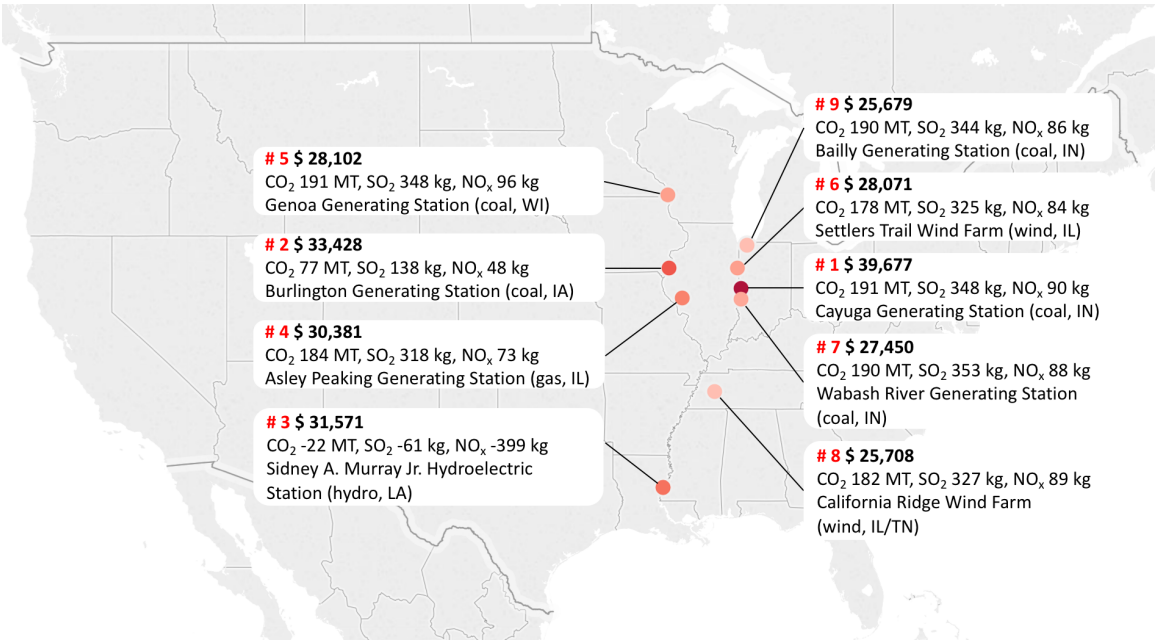

Figure 4. 4. Nine locations where battery storage can make annual net operating revenue for more than $ 25,000 in MISO.
Note that #8 California Ridge Wind Farm is physically located in Champaign County, Illinois, but its production is purchased by the company Tennessee Valley Authority (TVA), so its LMP is shown in TVA's bus station in Tennessee instead of the wind farm in Illinois (Tennessee Valley Authority, 2012).

4.3.2 Annual net emissions

In Figure 4.5, we present the annual net CO_2, SO_2, and NO_x emissions associated with deploying revenue-maximizing battery storage across 358 LMP locations in MISO. Emissions are expressed in metric tons for CO_2 (Figure 4.5A), kg for SO_2 (Figure 4.5B), and kg for NO_x (Figure 4.5C). Battery storage located in MISO's North and Central subregions are found causing increase in annual net CO_2, SO_2, and NO_x emissions, whereas battery storage located in the South subregion are found leading to reduction in annual CO_2, SO_2, and NO_x emissions. This is because in the North and Central subregions, emission rates of grid marginal generation (i.e. MEFs) are higher during the daily periods of low LMP when the batteries charge and lower during daily periods of high LMP when the batteries discharge (Figure 4.6-4.10), which means battery storage's economically optimal operation essentially displaces low-emission electricity with high-emission electricity in the grid. In the South subregion, however, MEFs are lower during the charging hours of battery storage but higher during the discharging hours of battery storage; therefore, battery storage that moves electricity in an economically optimal

pattern actually displaces high-emission electricity with low-emission electricity (Figure 4.6-4.10).

Annual net CO_2 emissions resulting from the optimal operation of battery storage vary between 75 and 89 metric tons in the North subregion, between 178 and 194 metric tons in the Central subregion, and between -30 and -10 metric tons in the South subregion (Figure 4.5). Battery storage in North causes moderate increases in annual CO_2 emissions primarily because both battery-charging and -discharging hours have a good mixture of high and low MEFs for CO_2 (Figure 4.8), which leads to the overall difference in MEFs for CO_2 not varying greatly between battery-charging and -discharging hours. In Central, MEFs for CO_2 during battery-charging hours are generally higher than those during battery-discharging hours (Figure 4.8), so the operation of battery storage has the greatest annual net CO_2 emissions. In contrast, MEFs for CO_2 in South are found to be lower during battery-charging hours but higher during battery-discharging hours (Figure 4.8), so battery storage in South are capable of reducing annual CO_2 emissions.

Annual net SO_2 emissions induced by battery storage range from 127 to 157 kg in the North subregion, from 318 to 372 kg in the Central subregion, and from -87 to -2 kg in the South subregion (Figure 4.5). Similar to the temporal trend of MEFs for CO_2, MEFs for SO_2 do not vary greatly between battery-charging and -discharging hours in North but are clearly higher during battery-charging hours and lower during battery-discharging hours in Central (Figure 4.9). Therefore, annual net SO_2 emissions in North are found relatively moderate compared to those in Central. The temporal trend of MEFs for SO_2 is reversed again in South (Figure 4.9) and leads to decrease in annual SO_2 emissions.

Annual net NO_x emissions caused by battery storage vary between 48 and 61 kg in the North subregion, between 73 and 96 kg in the Central subregion, and between -428 and -328 kg in the South subregion (Figure 4.5). Battery storage in North and Central are associated with less than 100 kg increase in annual net NO_x emissions because MEFs for NO_x do not varying strongly between battery-charging and -discharging hours in the two subregions (Figure 4.10). In South, however, MEFs for NO_x vary significantly between battery-charging and -discharging hours (Figure 4.10), which results in considerable reduction in annual NO_x emissions. Because NO_x emissions are most damaging in

summer, the environmental benefit of deploying battery storage in South becomes more valuable as battery storage can displace high-NO_x marginal generation in summer afternoons with energy stored during low-NO_x night hours.

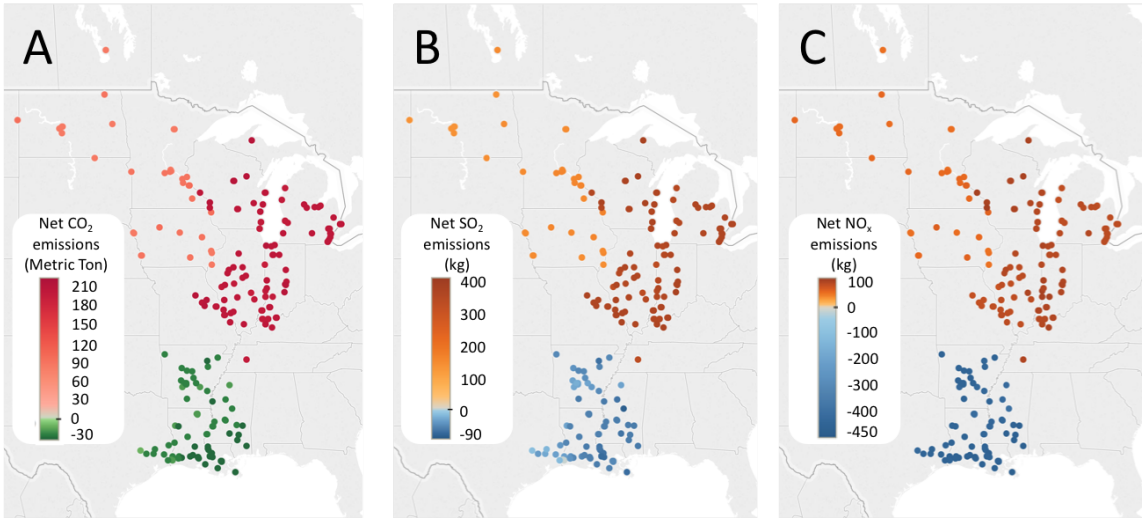

Figure 4. 5. Annual net CO_2 (A), SO_2 (B), and NO_x emissions (C) associated with the revenue-maximizing operation of battery storage across 358 locations in MISO.

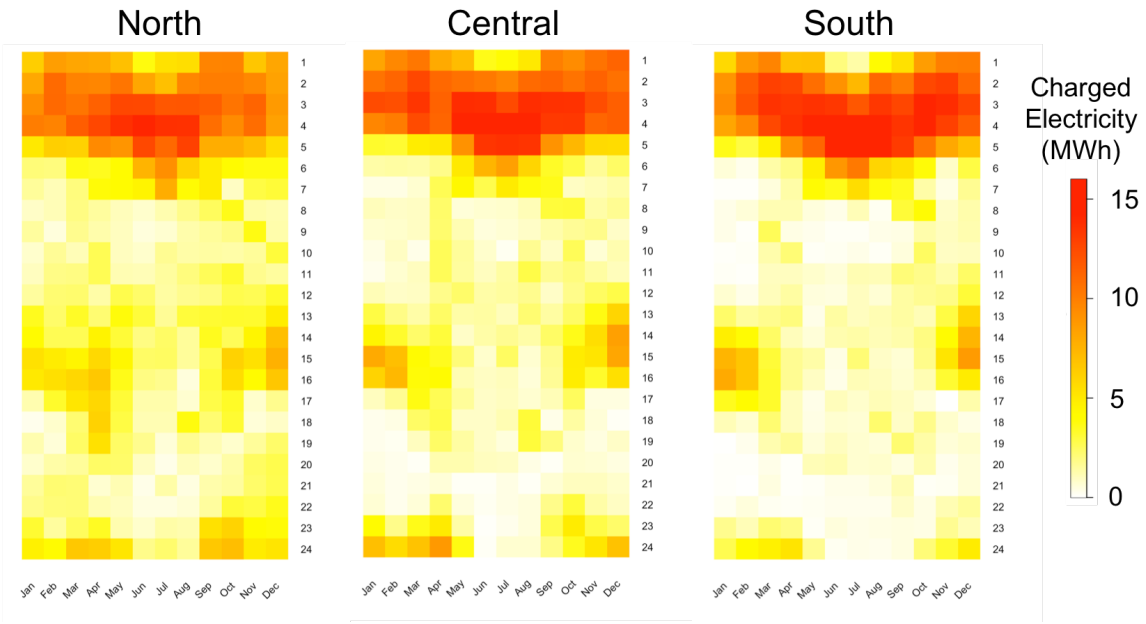

Figure 4. 6. Battery storage charging patterns in the North, Central, and South subregions in MISO.

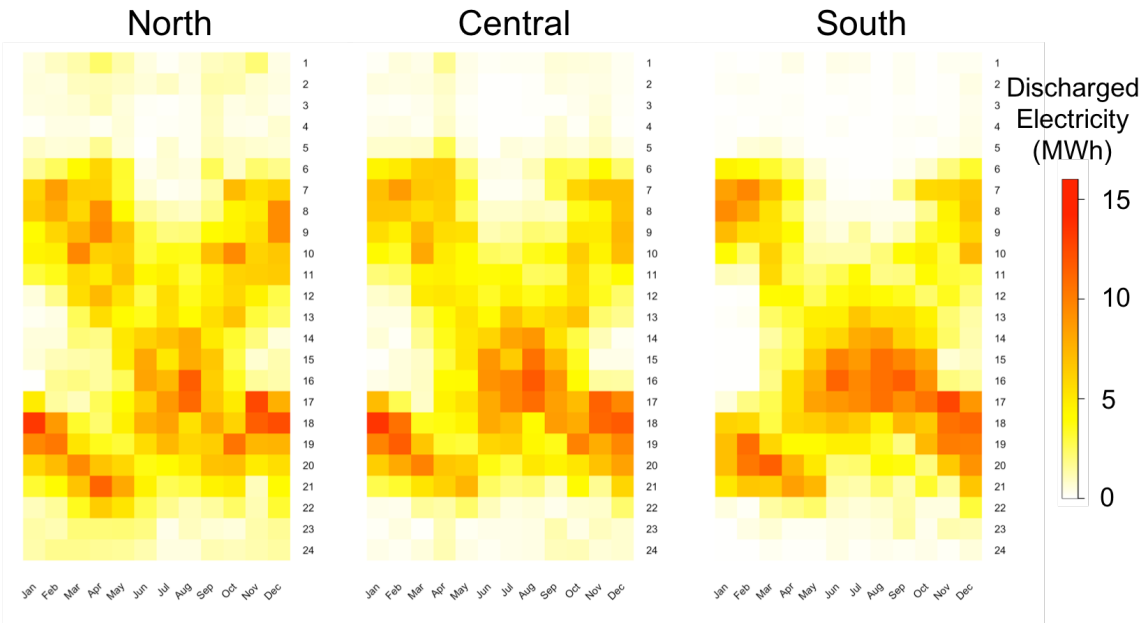

Figure 4. 7. Battery storage discharging patterns in the North, Central, and South subregions in MISO.

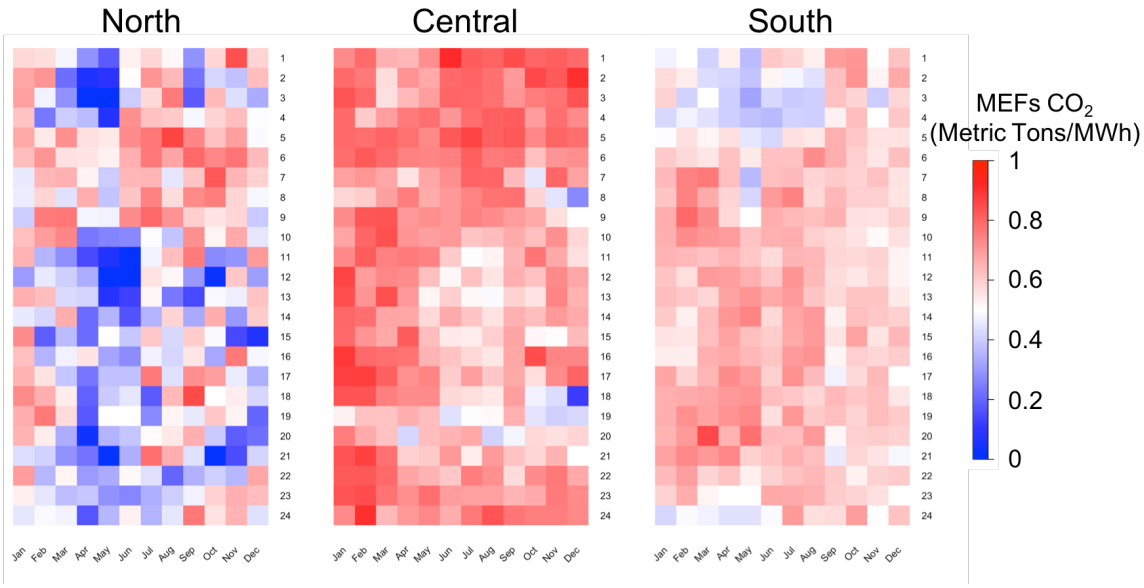

Figure 4. 8. Marginal emission factors (MEFs) for CO_2 in MISO's North, Central, and South subregional grids.

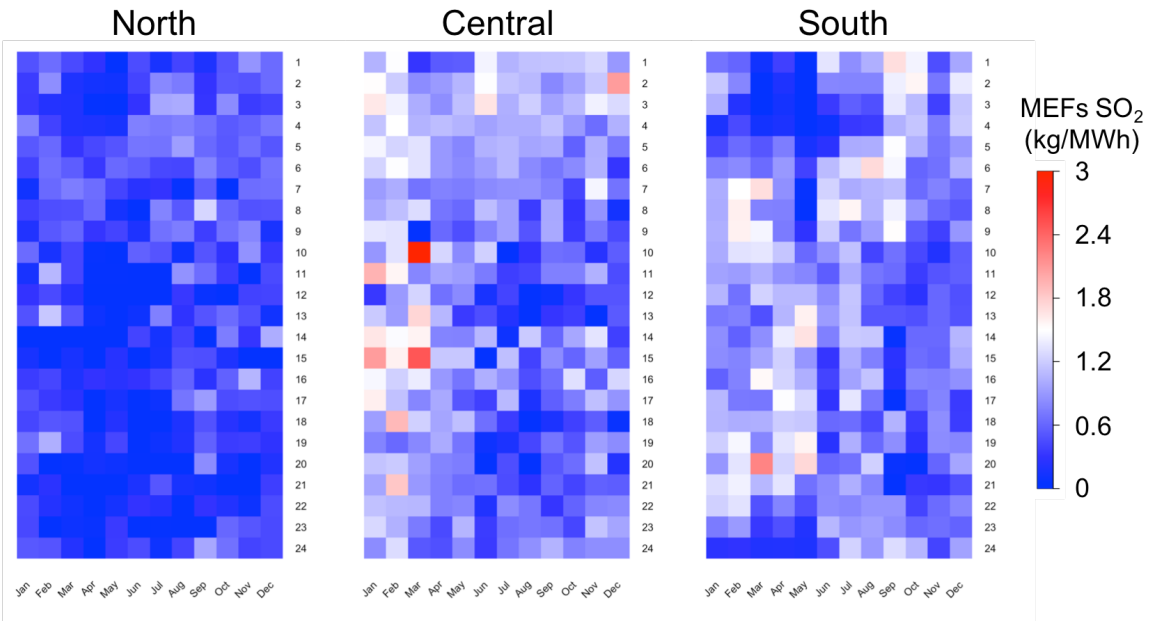

Figure 4. 9. Marginal emission factors (MEFs) for SO_2 in MISO's North, Central, and South subregional grids.

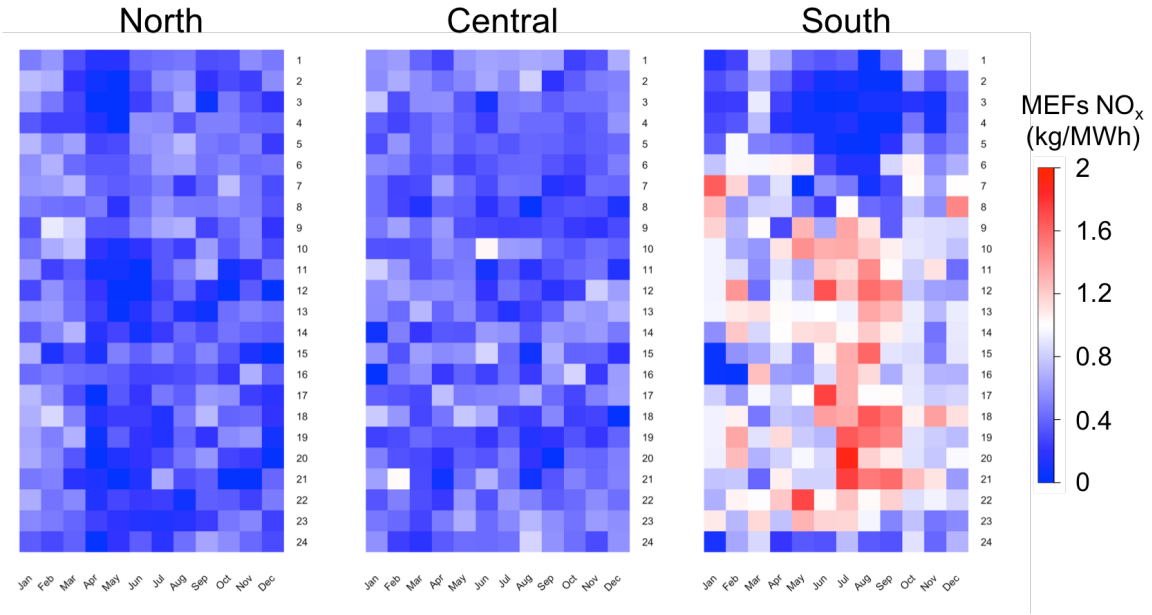

Figure 4. 10. Marginal emission factors (MEFs) for NO_x in MISO's North, Central, and South subregional grids.

4.3.3 Economic feasibility

Like any energy technology, battery storage adoption is significantly dependent on its economic feasibility, which is particularly determined by a series of factors including

annual cash inflow, capital cost, internal rate of return (IRR), and investment time horizon. Our revenue-maximizing model reveals that the annual financial return of a 0.5 MW/2.1 MWh battery storage, assuming it arbitrages as a price taker, varies between $11,000 and $40,000 in the MISO market in 2016. Capital cost of the battery storage was $990,000 when it started to deliver in September 2016, then it dropped by 10% to $891,300 two months later (Lambert, 2016). As its price continues to fall, battery storage will soon be able to compete widely against other resources in the market. In order to assess the economic feasibility of the battery storage under different investment strategies, we conduct a sensitivity analysis of the capital cost needed to secure the return on investment under a 20-year time horizon, given different levels of annual cash flow and investment IRR. A U.S. Dollar annual inflation rate of 2% is used to estimate future annual cash flow of the battery storage investment (Statista, 2018). In Figure 4.11, we observe that the capital cost of battery will need to be lower than $ 630,000 to secure the return on investment under a 20-year time horizon if the investors require an annual IRR of 5%; or lower than $ 225,000 to secure the return under the same time horizon if the investors require an annual IRR of 20%. These desired capital costs seem to be dramatic reductions from the battery's announced price in 2016, but with continued decrease in price and government subsidies for battery technologies (Hart & Sarkissian, 2016), the investment under a 20-year time horizon may become economically feasible in the next decade.

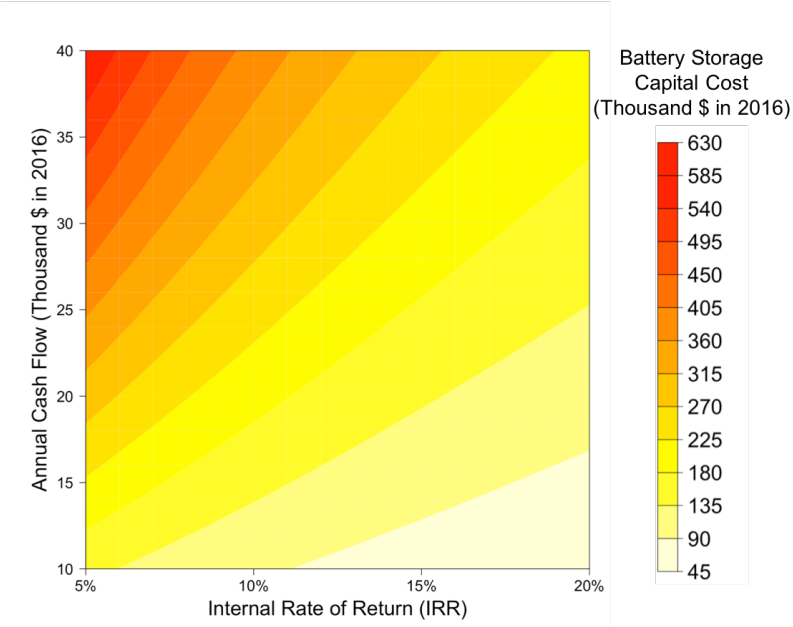

Figure 4. 11. Capital cost required for 0.5 MW/2.1 MWh battery storage to secure the return of investment under a 20-year time horizon.

4.4 Discussion

Grid services, economic benefits, and environmental impacts of energy storage are well studied, but there is a lack of information available to better forecast where future storage is likely to be sited. As policies incentivize or mandate installation of energy storage, stakeholders are concerned about where and how energy storage should be deployed to participate in the current electricity market. To address these concerns, we apply spatiotemporal, real-time LMP data in a revenue-maximizing model to assess and evaluate the operational decisions of battery storage in the MISO electricity wholesale market. Our findings demonstrate specific locations where battery storage can be most profitable in MISO, which offers policy implications for promoting and deploying storage technologies. It is noted that we model the battery storage at small capacity (2.1 MWh) and as price takers when arbitraging in the market. Factors like larger capacity or renewable integration will change the current economics of battery storage.

Thanks to the high spatial and temporal resolution of our real-time LMP data, we are able to simulate optimal operation and compare annual net operating revenue of battery storage at 393 different locations throughout MISO. Because we have the geographic coordinates associated with the locational marginal prices, the results from

the revenue-maximizing model intuitively display which locations are the most profitable for battery storage and offer guidance for stakeholders regarding where to expect or invest in new storage. In addition, we estimate annual net CO_2, SO_2, and NO_x emissions resulting from deploying battery storage at the 393 locations based upon the subregional grids in MISO. Results show some heterogeneity in economics and emissions: battery storage installed in the North and Central subregions of MISO cause increases in CO_2, SO_2, and NO_x emissions, while those in the South subregion lead to reduction in the emissions. However, many of the most profitable locations for battery storage are in the Central subregion. Although profitability and environmental impacts are critical factors for evaluating storage projects, there are other valuable services storage technologies can provide, such as mitigating grid congestion and adding operating reserve in ancillary service markets. These services are not examined in this study but could be further analyzed using the spatiotemporal, real-time LMP data.

This study gives a glimpse of where the economics of wholesale power are most favorable in the MISO market to attract storage projects. But there are many other revenue streams for storage in addition to arbitraging electricity prices. For example, ancillary services be attractive to investors and require new policies. As more energy storage enters the market, frequent intersections between policy and technology will occur. Regulators would anticipate new storage projects implemented in various forms: privately-owned energy storage, for example, would grow and become complementary for or competitive against utility-owned storage. Grid operators would foresee more distributed storage appear as they are coupled with small-scale renewables like rooftop photovoltaics and operate completely behind the meter. Consequently, institutional framework, as well as market design and tariff structure, is extremely important.

It should be noted that findings about annual net operating revenue in this study only hold when battery storage operates as a price taker. As more storage are introduced into the grid, real-time price volatility would decrease and lead to narrower room for storage to capture arbitrage opportunities. Similarly, when more renewable resources become integrated with storage, the price-taking assumption of storage will become less realistic. Our sensitivity analysis about economic feasibility of battery storage looks at annual income cashflow ranging from $10,000 to $40,000, which, to some extent,

imitates the reduced arbitrage opportunities for storage in the future. It is clear that as annual net operating revenue shrinks, the capital cost of battery has to be further lowered in order to secure financial return of the investment. Therefore, effective incentives and significant cost reductions are extremely important for the prosperity of battery storage industry.

Energy storage can stimulate development of renewable energy primarily because renewable generation is variable and tend to cause increased price fluctuations, while energy storage can hedge the variability of renewable generation and tend to suppress price fluctuations. Although additional energy storage may lead to an increase in system-wide emissions, the induced renewable generation could displace emission-heavy, fossil-fueled power production and neutralize the direct emission effect of storage. Policymakers should be cognizant of the fact that financial profitability of energy storage may be diminished by growing renewable generation, but environmental benefits of energy storage are dependent on its ability to facilitate new renewable power generation.

Chapter 5

Conclusion

This dissertation has demonstrated the approaches to explore possible solutions for decarbonization and modernization of electricity systems by considering aspects of materiality, comparability and multi-metric dimensionality in the design of methods and utilization of spatiotemporal data. The improved methods and spatiotemporal data enable comprehensive inspection of current systems in terms of generation profile and emission intensity and empower thorough examination of advanced technologies with regard to environmental and economic effects. Consequently, this research provides critical implications for policy and practice and significantly expands the literature about electricity system and energy policy.

The MISO electricity system is studied from different perspectives in the three separate case studies. In the first case study, the assessment of conventional and expanded marginal emission factors reveals crucial gaps between current metrics and what is needed to accurately and comprehensively measure emission intensity of electricity generation in the MISO system. The MEFs only considering emitting resources may provide a good estimate for the MISO grid and in the Central and South subregional grids because the share of renewable generation in these grids is relatively low; however, neglecting nonemitting sources can significantly overestimate MEFs for CO_2, SO_2, and NO_x in the North subregional grid where wind has contributed remarkably to the grid generation. Our expanded MEFs considering both emitting and nonemitting sources on the margin accounts for the increasing renewable installation and dispatchment in the grid and provides more accurate estimates of the avoided emissions from interventions including bulk energy storage, PHEVs, and demand response. Findings in this study have important implications for regional electricity system policy making.

The second case study demonstrates an application of the expanded MEFs to the electricity consumption by residential heating and cooling technologies. By considering regional climate differences and regional grid fuel mix differences, energy use and CO_2 emissions related to the GSHP and conventional HVAC systems are investigated in a

system-in-house scenario context. Results show that GSHPs consume less energy than the conventional systems but not necessarily reducing CO_2 emissions in all scenarios because the grid fuel mix varies drastically across space and time in certain locations. Findings reveal that applying EFs with higher spatial and temporal resolutions and using MEFs instead of AEFs both give more accurate emission estimates. Using static AEFs is found overestimating total emissions compared to using MEFs. This study emphasizes the importance of applying accurate EFs to emissions performance assessment and recommends policymaking to properly incentivize the technologies that meet today's grid realities and renewable-integrated grid of tomorrow.

The third case study explores the possibility of energy storage technologies participating in the MISO wholesale electricity market. By utilizing spatiotemporal, real-time locational marginal prices (LMP) of electricity, annual net operating revenues and emissions are estimated for grid-scale battery storage that arbitrage as price takers in the MISO market at various locations. Benefiting from the unique LMP data set that has the finest temporal resolution (five-minute) and exact geographic information (latitude and longitude) for the pricing metrics, findings in this study illustrate specific locations where battery storage can be most profitable. This offers projection of future storage siting and has significant implications for policy and practice. Affected by regulatory mandates, energy storage technologies will thrive via many other revenue streams, such as frequency control and capacity reserve. The fine spatial and temporal granularity the LMP data could assist further investigation on how energy storage can compete against conventional generation.

Overall, this dissertation address sustainability challenges in the MISO electricity system in three approaches, including measuring emissions from generation and demand, assessing economic feasibility of advanced technologies, and discussing policy implications of different strategies. Although several limitations and areas of uncertainty exist within each of the approaches, as described in the respective case studies, these approaches provide a viable path forward for improving measurement criteria for electricity systems and assisting policymaking for advanced technologies to enable system decarbonization and modernization. To further understand the broader implications of the proposed methods and demonstrated findings, future research should

focus on expanding the assessments to additional electricity systems and markets. Improved transparency of data and information disclosure will enable proper assessment of policy and technology interventions in terms of their societal impacts and will help to inform effective investment and policy decisions.

Bibliography

Anderson, D., & Leach, M. (2004). Harvesting and redistributing renewable energy: on the role of gas and electricity grids to overcome intermittency through the generation and storage of hydrogen. Energy Policy, 32(14), 1603–1614. https://doi.org/10.1016/S0301-4215(03)00131-9

Archsmith, J., Kendall, A., & Rapson, D. (2015). From cradle to junkyard: assessing the life cycle greenhouse gas benefits of electric vehicles. Research in Transportation Economics, 52, 72–90.

Axsen, J., Kurani, K. S., McCarthy, R., & Yang, C. (2011). Plug-in hybrid vehicle GHG impacts in California: Integrating consumer-informed recharge profiles with an electricity-dispatch model. Energy Policy, 39(3), 1617–1629. https://doi.org/10.1016/j.enpol.2010.12.038

Barton, J. P., & Infield, D. G. (2004). Energy storage and its use with intermittent renewable energy. IEEE Transactions on Energy Conversion, 19(2), 441–448. https://doi.org/10.1109/TEC.2003.822305

Beaudin, M., Zareipour, H., Schellenberglabe, A., & Rosehart, W. (2010). Energy storage for mitigating the variability of renewable electricity sources: An updated review. Energy for Sustainable Development, 14(4), 302–314. https://doi.org/10.1016/j.esd.2010.09.007

Bettle, R., Pout, C. H., & Hitchin, E. R. (2006). Interactions between electricity-saving measures and carbon emissions from power generation in England and Wales. Energy Policy, 34(18), 3434–3446. https://doi.org/10.1016/j.enpol.2005.07.014

Blumsack, S., Samaras, C., & Hines, P. (2008). Long-term electric system investments to support plug-in hybrid electric vehicles. In Power and Energy Society General Meeting-Conversion and Delivery of Electrical Energy in the 21st Century, 2008 IEEE (pp. 1–6). IEEE. Retrieved from http://ieeexplore.ieee.org/xpls/abs_all.jsp?arnumber=4596906

Bradbury, K., Pratson, L., & Patiño-Echeverri, D. (2014). Economic viability of energy storage systems based on price arbitrage potential in real-time U.S. electricity markets. Applied Energy, 114, 512–519. https://doi.org/10.1016/j.apenergy.2013.10.010

California. (2010, August 23). AB 2514 Assembly Bill - Bill Analysis. Retrieved May 22, 2018, from http://www.leginfo.ca.gov/pub/09-10/bill/asm/ab_2501-2550/ab_2514_cfa_20100823_113407_sen_floor.html

California Public Utilities Commission. (2013, October 17). Order Instituting Rulemaking Pursuant to Assembly Bill 2514 to Consider the Adoption of Procurement Targets for Viable and Cost-Effective Energy Storage Systems. Retrieved May 22, 2018, from https://www.sce.com/wps/wcm/connect/435ea164-60d5-433f-90bc-

b76119ede661/R1012007_StorageOIR_D1310040_AdoptingEnergyStorageProcurement FrameworkandDesignProgram.pdf?MOD=AJPERES

Carson, R. T., & Novan, K. (2013). The private and social economics of bulk electricity storage. Journal of Environmental Economics and Management, 66(3), 404–423. https://doi.org/10.1016/j.jeem.2013.06.002

Cassidy, S. F. (2003). Recent Large-Scale Ground-Source Heat Pump Installations in Ireland.

Choi, D. G., Kreikebaum, F., Thomas, V. M., & Divan, D. (2013). Coordinated EV Adoption: Double-Digit Reductions in Emissions and Fuel Use for $40/Vehicle-Year. Environmental Science & Technology, 130829161516000. https://doi.org/10.1021/es4016926

Cleetus, R., Bailie, A., & Clemmer, S. (2016). The US Power Sector in a Net Zero World Analyzing pathways for deep carbon reductions. Retrieved from https://www.ucsusa.org/sites/default/files/attach/2016/11/UCS-Deep-Decarbonization-working-paper.pdf

Curtis, R., Lund, J., Sanner, B., Rybach, L., & Hellström, G. (2005). Ground source heat pumps–geothermal energy for anyone, anywhere: current worldwide activity. In Proceedings World Geothermal Congress, Antalya, Turkey (pp. 24–29). Retrieved from http://www.academia.edu/download/34086567/1437.pdf

Dai, L., Li, S., DuanMu, L., Li, X., Shang, Y., & Dong, M. (2015). Experimental performance analysis of a solar assisted ground source heat pump system under different heating operation modes. Applied Thermal Engineering, 75, 325–333. https://doi.org/10.1016/j.applthermaleng.2014.09.061

Denholm, P., & Kulcinski, G. L. (2004). Life cycle energy requirements and greenhouse gas emissions from large scale energy storage systems. Energy Conversion and Management, 45(13–14), 2153–2172. https://doi.org/10.1016/j.enconman.2003.10.014

Dennis, K., Colburn, K., & Lazar, J. (2016). Environmentally beneficial electrification: The dawn of 'emissions efficiency.' The Electricity Journal, 29(6), 52–58. https://doi.org/10.1016/j.tej.2016.07.007

Diem, A., & Quiroz, C. (2012a). How to use eGRID for Carbon Footprinting Electricity Purchases in Greenhouse Gas Emission Inventories. U.S. EPA. Retrieved from https://www.epa.gov/sites/production/files/2015-01/documents/adiem.pdf

Diem, A., & Quiroz, C. (2012b). How to Use eGRID for Carbon Footprinting Electricity Purchases in Greenhouse Gas Emission Inventories. Environmental Protection Agency. Https://Www. Epa. Gov/Sites/Production/Files/2015-01/Documents/Adiem. Pdf.

DOE. (2018). EnergyPlus | EnergyPlus. Retrieved August 24, 2018, from https://energyplus.net/

Doucette, R. T., & McCulloch, M. D. (2011). Modeling the CO2 emissions from battery electric vehicles given the power generation mixes of different countries. Energy Policy, 39(2), 803–811. https://doi.org/10.1016/j.enpol.2010.10.054

DSIRE. (2018a). DSIRE - Federal FHA PowerSaver Load Program. Retrieved January 31, 2018, from http://programs.dsireusa.org/system/program/detail/5631

DSIRE. (2018b). DSIRE - Louisiana Home Energy Loan Program (HELP). Retrieved January 31, 2018, from http://programs.dsireusa.org/system/program/detail/1206

DSIRE. (2018c). DSIRE - Minnesota Home Energy Loan Program. Retrieved January 31, 2018, from http://programs.dsireusa.org/system/program/detail/1188

DSIRE. (2018d). DSIRE - Minnesota Xcel Energy (Electric) - Residential Energy Efficiency Rebate Programs. Retrieved January 31, 2018, from http://programs.dsireusa.org/system/program/detail/1590

DSIRE. (2018e). DSIRE - Missouri Local Option - Clean Energy Development Boards PACE Financing. Retrieved January 31, 2018, from http://programs.dsireusa.org/system/program/detail/4248

DSIRE. (2018f). DSIRE - Saint Paul Port Authority PACE Program. Retrieved January 31, 2018, from http://programs.dsireusa.org/system/program/detail/5753

Du, L., & Mao, J. (2015). Estimating the environmental efficiency and marginal CO2 abatement cost of coal-fired power plants in China. Energy Policy, 85, 347–356. https://doi.org/10.1016/j.enpol.2015.06.022

EIA. (2016). U.S. Electric System Operating Data. Retrieved July 14, 2017, from https://www.eia.gov/beta/realtime_grid/#/data/table?end=20161030&start=20160930&frequency=Daily&dataTypes=mc&bas=00000000000g

EIA. (2018). Annual Electric Generator data - EIA-860 data file. Retrieved November 10, 2016, from http://www.eia.gov/electricity/data/eia860/

Eyer, J., & Corey, G. (2010). Energy storage for the electricity grid: Benefits and market potential assessment guide. Sandia National Laboratories, 20(10), 5.

Farhat, A. A. M., & Ugursal, V. I. (2010). Greenhouse gas emission intensity factors for marginal electricity generation in Canada. International Journal of Energy Research, 34(15), 1309–1327. https://doi.org/10.1002/er.1676

FERC. (2018, February 15). FERC Issues Final Rule on Electric Storage Participation in

Regional Markets. Retrieved May 15, 2018, from https://www.ferc.gov/media/news-releases/2018/2018-1/02-15-18-E-1.asp#.WvrwXdOUuEI

Fiorentini, M., Cooper, P., & Ma, Z. (2015). Development and optimization of an innovative HVAC system with integrated PVT and PCM thermal storage for a net-zero energy retrofitted house. Energy and Buildings, 94, 21–32. https://doi.org/10.1016/j.enbuild.2015.02.018

Garcia-Gonzalez, J., Muela, R. M. R. de la, Santos, L. M., & Gonzalez, A. M. (2008). Stochastic Joint Optimization of Wind Generation and Pumped-Storage Units in an Electricity Market. IEEE Transactions on Power Systems, 23(2), 460–468. https://doi.org/10.1109/TPWRS.2008.919430

Graditi, G., Ippolito, M. G., Lamedica, R., Piccolo, A., Ruvio, A., Santini, E., … Zizzo, G. (2015). Innovative control logics for a rational utilization of electric loads and air-conditioning systems in a residential building. Energy and Buildings, 102, 1–17. https://doi.org/10.1016/j.enbuild.2015.05.027

Graff Zivin, J. S., Kotchen, M. J., & Mansur, E. T. (2014). Spatial and temporal heterogeneity of marginal emissions: Implications for electric cars and other electricity-shifting policies. Journal of Economic Behavior & Organization, 107, 248–268. https://doi.org/10.1016/j.jebo.2014.03.010

Gustafsson, M., Dermentzis, G., Myhren, J. A., Bales, C., Ochs, F., Holmberg, S., & Feist, W. (2014). Energy performance comparison of three innovative HVAC systems for renovation through dynamic simulation. Energy and Buildings, 82, 512–519. https://doi.org/10.1016/j.enbuild.2014.07.059

Hadley, S. W., & Van Dyke, J. W. (2003). Emissions benefits of distributed generation in the Texas market (No. ORNL/TM-2003/100). Oak Ridge, TN: Oak Ridge National Laboratory. Retrieved from http://citeseerx.ist.psu.edu/viewdoc/download?doi=10.1.1.196.1305&rep=rep1&type=pdf

Hart, D., & Sarkissian, A. (2016). Deployment of Grid-Scale Batteries in the United States. Unpublished Case Study Prepared for DOE Office of Energy Policy and Strategic Analysis, Washington, DC.

Hawkes, A. D. (2010). Estimating marginal CO2 emissions rates for national electricity systems. Energy Policy, 38(10), 5977–5987. https://doi.org/10.1016/j.enpol.2010.05.053

Hawkes, A. D. (2014). Long-run marginal CO2 emissions factors in national electricity systems. Applied Energy, 125, 197–205. https://doi.org/10.1016/j.apenergy.2014.03.060

Hittinger, E., & Azevedo, I. M. L. (2017). Estimating the Quantity of Wind and Solar Required To Displace Storage-Induced Emissions. Environmental Science & Technology, 51(21), 12988–12997. https://doi.org/10.1021/acs.est.7b03286

Hittinger, E. S., & Azevedo, I. M. L. (2015a). Bulk Energy Storage Increases United States Electricity System Emissions. Environmental Science & Technology, 49(5), 3203–3210. https://doi.org/10.1021/es505027p

Hittinger, E. S., & Azevedo, I. M. L. (2015b). Bulk Energy Storage Increases United States Electricity System Emissions. Environmental Science & Technology, 49(5), 3203–3210. https://doi.org/10.1021/es505027p

Hittinger, E., Whitacre, J. F., & Apt, J. (2010). Compensating for wind variability using co-located natural gas generation and energy storage. Energy Systems, 1(4), 417–439. https://doi.org/10.1007/s12667-010-0017-2

Holland, S. P., & Mansur, E. T. (2008). Is real-time pricing green? The environmental impacts of electricity demand variance. The Review of Economics and Statistics, 90(3), 550–561.

Holland, S. P., Mansur, E. T., Muller, N. Z., & Yates, A. J. (2015). Environmental benefits from driving electric vehicles? National Bureau of Economic Research. Retrieved from http://www.nber.org/papers/w21291

Holland, S. P., Mansur, E. T., Muller, N. Z., & Yates, A. J. (2016). Distributional Effects of Air Pollution from Electric Vehicle Adoption. National Bureau of Economic Research. Retrieved from http://www.nber.org/papers/w22862

Hu, W., Chen, Z., & Bak-Jensen, B. (2010). Optimal operation strategy of battery energy storage system to real-time electricity price in Denmark. In IEEE PES General Meeting (pp. 1–7). https://doi.org/10.1109/PES.2010.5590194

Huelman, P., Schirber, T., Mosiman, G., Jacobson, R., Smith, T. M., & Li, M. (2016). Residential Ground Source Heat Pump Study: A Comprehensive Assessment of Performance, Emissions, and Economics (Minnesota Conservation Applied Research & Development (CARD) Final Report No. OES-01192010-B44645). Retrieved from http://mn.gov/commerce-stat/pdfs/card-residential-gound-source-heat-pump-study.pdf

Hughes, P. J. (2009). Geothermal (Ground-Source) Heat Pumps: Market Status, Barriers to Adoption, and Actions to Overcome Barriers. Retrieved from https://digitalcommons.unl.edu/cgi/viewcontent.cgi?referer=https://www.google.com/&httpsredir=1&article=1017&context=usdoepub

Ippolito, M. G., Zizzo, G., Piccolo, A., & Siano, P. (2014). Definition and application of innovative control logics for residential energy optimization (pp. 1272–1277). IEEE. https://doi.org/10.1109/SPEEDAM.2014.6872124

ISO New England. (2016). 2014 ISO New England Electric Generator Air Emissions Report. Retrieved from https://www.iso-ne.com/static-assets/documents/2016/01/2014_emissions_report.pdf

Jansen, K. H., Brown, T. M., & Samuelsen, G. S. (2010). Emissions impacts of plug-in hybrid electric vehicle deployment on the U.S. western grid. Journal of Power Sources, 195(16), 5409–5416. https://doi.org/10.1016/j.jpowsour.2010.03.013

Kanoria, Y., Montanari, A., Tse, D., & Zhang, B. (2011). Distributed storage for intermittent energy sources: Control design and performance limits. In Communication, Control, and Computing (Allerton), 2011 49th Annual Allerton Conference on (pp. 1310–1317). IEEE. Retrieved from http://ieeexplore.ieee.org/xpls/abs_all.jsp?arnumber=6120319

Keith, G., Biewald, B., Sommer, A., Henn, P., & Breceda, M. (2003). Estimating the emission reduction benefits of renewable electricity and energy efficiency in North America: experience and methods. Energy, 5255, 5264–7181.

Khani, H., & Zadeh, M. R. D. (2015). Real-Time Optimal Dispatch and Economic Viability of Cryogenic Energy Storage Exploiting Arbitrage Opportunities in an Electricity Market. IEEE Transactions on Smart Grid, 6(1), 391–401. https://doi.org/10.1109/TSG.2014.2357253

Kim, J. D., & Rahimi, M. (2014). Future energy loads for a large-scale adoption of electric vehicles in the city of Los Angeles: Impacts on greenhouse gas (GHG) emissions. Energy Policy, 73, 620–630. https://doi.org/10.1016/j.enpol.2014.06.004

Kintner-Meyer, M., Schneider, K., Pratt, R., & Pacific Northwest National Laboratory. (2007). Impacts Assessment of Plug-In Hybrid Vehicles on Electric Utilities and Regional U.S. Power Grids Part 1: Technical Analysis. Retrieved from https://www.ferc.gov/about/com-mem/5-24-07-technical-analy-wellinghoff.pdf

Korpaas, M., Holen, A. T., & Hildrum, R. (2003). Operation and sizing of energy storage for wind power plants in a market system. International Journal of Electrical Power & Energy Systems, 25(8), 599–606. https://doi.org/10.1016/S0142-0615(03)00016-4

Krishnamurthy, D., Uckun, C., Zhou, Z., Thimmapuram, P. R., & Botterud, A. (2018). Energy Storage Arbitrage Under Day-Ahead and Real-Time Price Uncertainty. IEEE Transactions on Power Systems, 33(1), 84–93. https://doi.org/10.1109/TPWRS.2017.2685347

Lambert, F. (2016, November 14). Tesla slashes price of the Powerpack system by another 10% with new generation. Retrieved April 30, 2018, from https://electrek.co/2016/11/14/tesla-powerpack-2-price/

Li, M. (2013). Life Cycle Assessment of Residential Heating and Cooling Systems in Minnesota: A comprehensive analysis on life cycle greenhouse gas (GHG) emissions and cost-costeffectiveness of ground source heat pump (GSHP) systems compared to the conventional gas furnace and air conditioner system. Retrieved from http://conservancy.umn.edu/handle/11299/146449

Li, M., Smith, T. M., Yang, Y., & Wilson, E. J. (2017). Marginal Emission Factors Considering Renewables: A Case Study of the U.S. Midcontinent Independent System Operator (MISO) System. Environmental Science & Technology, 51(19), 11215–11223. https://doi.org/10.1021/acs.est.7b00034

Li, N., & Hedman, K. W. (2015). Economic Assessment of Energy Storage in Systems With High Levels of Renewable Resources. IEEE Transactions on Sustainable Energy, 6(3), 1103–1111. https://doi.org/10.1109/TSTE.2014.2329881

LIENAU, P. J. (1997). Geothermal Heat Pump Performance and Utility Programs in the United States. Energy Sources, 19(1), 1–8. https://doi.org/10.1080/00908319708908827

Liu, Z., Xu, W., Zhai, X., Qian, C., & Chen, X. (2017). Feasibility and performance study of the hybrid ground-source heat pump system for one office building in Chinese heating dominated areas. Renewable Energy, 101, 1131–1140. https://doi.org/10.1016/j.renene.2016.10.006

Lucia, U., Simonetti, M., Chiesa, G., & Grisolia, G. (2017). Ground-source pump system for heating and cooling: Review and thermodynamic approach. Renewable and Sustainable Energy Reviews, 70, 867–874. https://doi.org/10.1016/j.rser.2016.11.268

Lueken, R., & Apt, J. (2014). The effects of bulk electricity storage on the PJM market. Energy Systems, 5(4), 677–704. https://doi.org/10.1007/s12667-014-0123-7

Lujano-Rojas, J. M., Dufo-López, R., Bernal-Agustín, J. L., & Catalão, J. P. S. (2017). Optimizing Daily Operation of Battery Energy Storage Systems Under Real-Time Pricing Schemes. IEEE Transactions on Smart Grid, 8(1), 316–330. https://doi.org/10.1109/TSG.2016.2602268

Lund, H., & Kempton, W. (2008). Integration of renewable energy into the transport and electricity sectors through V2G. Energy Policy, 36(9), 3578–3587. https://doi.org/10.1016/j.enpol.2008.06.007

Lund, J. W. (1988). Geothermal Heat Pump Utilization in the United States. Retrieved from http://www.cres.gr/kape/pdf/geotherm/8.pdf

Lund, J. W., & Boyd, T. L. (2016). Direct utilization of geothermal energy 2015 worldwide review. Geothermics, 60, 66–93. https://doi.org/10.1016/j.geothermics.2015.11.004

Luo, J., Rohn, J., Bayer, M., Priess, A., Wilkmann, L., & Xiang, W. (2015). Heating and cooling performance analysis of a ground source heat pump system in Southern Germany. Geothermics, 53, 57–66. https://doi.org/10.1016/j.geothermics.2014.04.004

Lutsey, N., & Sperling, D. (2008). America's bottom-up climate change mitigation policy. Energy Policy, 36(2), 673–685. https://doi.org/10.1016/j.enpol.2007.10.018

Marnay, C., Fisher, D., Murtishaw, S., Phadke, A., Price, L., & Sathaye, J. (2002). Estimating carbon dioxide emissions factors for the California electric power sector. Lawrence Berkeley National Laboratory. Retrieved from https://escholarship.org/uc/item/3kc8r2n1.pdf

Marzband, M., Ghazimirsaeid, S. S., Uppal, H., & Fernando, T. (2017). A real-time evaluation of energy management systems for smart hybrid home Microgrids. Electric Power Systems Research, 143, 624–633. https://doi.org/10.1016/j.epsr.2016.10.054

Mattinen, M. K., Nissinen, A., Hyysalo, S., & Juntunen, J. K. (2015). Energy Use and Greenhouse Gas Emissions of Air-Source Heat Pump and Innovative Ground-Source Air Heat Pump in a Cold Climate. Journal of Industrial Ecology, 19(1), 61–70. https://doi.org/10.1111/jiec.12166

McCarthy, R., & Yang, C. (2010). Determining marginal electricity for near-term plug-in and fuel cell vehicle demands in California: Impacts on vehicle greenhouse gas emissions. Journal of Power Sources, 195(7), 2099–2109. https://doi.org/10.1016/j.jpowsour.2009.10.024

McConnell, B. W., Hadley, S. W., & Xu, Y. (2011). A Review of Barriers to and Opportunities for the Integration of Renewable Energy in the Southeast (No. ORNL/TM-2010/138). Oak Ridge, TN: Oak Ridge National Laboratory. Retrieved from http://info.ornl.gov/sites/publications/files/Pub24993.pdf

Meyer, J., Pride, D., O'Toole, J., Craven, C., & Spencer, V. (2011). Ground-Source Heat Pumps in Cold Climates - The Current State of the Alaska Industry, a Review of the Literature, a Preliminary Economic Assessment, and Recommendations for Research. Retrieved from http://www.uaf.edu/files/acep/Ground-Source-Heat-Pumps-in-Cold-Climates.pdf

MISO. (2011). MISO 2011 Wind Generation Update - With the focus on Dispatchable Intermittent Resources. Retrieved from https://www.misoenergy.org/Library/Repository/Meeting%20Material/Stakeholder/BOD/Markets%20Committee/2011/20110914/20110914%20BOD%20Markets%20Committee%20Item%2007%20Wind%20Generation%20Update.pdf

MISO. (2014a). MISO 2014 Real-Time Fuel on the Margin Report. Retrieved November 5, 2016, from https://www.misoenergy.org/Library/Repository/Market%20Reports/2014_rt_fuel_on_margin.zip

MISO. (2014b). MISO Fuel Mix Report Readers Guide.pdf. Retrieved from https://www.misoenergy.org/Library/Repository/Report/Readers%20Guide/MISO%20Fuel%20Mix%20Report%20Readers%20Guide.pdf

MISO. (2014c). MISO Historical Generation Fuel Mix for 2014. Retrieved November 5,

2016, from https://www.misoenergy.org/RTDisplays/MKTRPT/AllReportsList.html?rptName=Historical%20Generation%20Fuel%20Mix%20for%202014%20(xls)

MISO. (2014d). Monthly Market Report 2014. Retrieved November 1, 2016, from https://www.misoenergy.org/Library/Pages/ManagedFileSet.aspx?SetId=2070

MISO. (2015a). MISO 2015 Real-Time Fuel on the Margin Report. Retrieved November 5, 2016, from https://www.misoenergy.org/Library/Repository/Market%20Reports/2015_rt_fuel_on_margin.zip

MISO. (2015b). MTEP15 Chapter 9.1: MISO Overview. Retrieved from http://www.misomtep.org/miso-overview-mtep15/

MISO. (2015c). MTEP15 MISO Transmission Expansion Plan 2015. Retrieved from https://cdn.misoenergy.org/20151210%20BOD%20Item%2011a%20MTEP15%20Combined110771.pdf

MISO. (2015d, January). MISO Informational Forum. Retrieved from https://www.misoenergy.org/Library/Repository/Meeting%20Material/Stakeholder/Informational%20Forum/2015/20150120/20150120%20Informational%20Forum%20Presentation.pdf

MISO. (2015e, August). Wind Forecasting Review. Retrieved from https://www.misoenergy.org/Library/Repository/Meeting%20Material/Stakeholder/BOD/Markets%20Committee/2015/20150826/20150826%20Markets%20Committee%20of%20the%20BOD%20Item%2006%20Wind%20Forecasting.pdf

MISO. (2016a). MISO 2016 Real-Time Fuel on the Margin Report. Retrieved November 5, 2016, from https://www.misoenergy.org/Library/Repository/Market%20Reports/2016_rt_fuel_on_margin.zip

MISO. (2016b). MISO Market Data - Historical Generation Fuel Mix. Retrieved May 22, 2018, from https://www.misoenergy.org/markets-and-operations/market-reports/#nt=%2FMarketReportType%3ASummary%2FMarketReportName%3AHistorical%20Generation%20Fuel%20Mix%20(xls)&t=10&p=0&s=MarketReportPublished&sd=desc

MISO. (2018a). MISO Market Data: Weekly Real-Time 5-Min LMP. Retrieved May 14, 2018, from https://www.misoenergy.org/markets-and-operations/market-reports/#nt=%2FMarketReportType%3AHistorical%20LMP%2FMarketReportName%3AWeekly%20Real-Time%205-Min%20LMP%20(zip)&t=-1&p=0&s=MarketReportPublished&sd=desc

MISO. (2018b). MISO Real-Time LMP Contour Map. Retrieved May 14, 2018, from https://api.misoenergy.org/MISORTWD/lmpcontourmap.html

Moura, P. S., & de Almeida, A. T. (2010). The role of demand-side management in the grid integration of wind power. Applied Energy, 87(8), 2581–2588. https://doi.org/10.1016/j.apenergy.2010.03.019

Naili, N., Hazami, M., Attar, I., & Farhat, A. (2016). Assessment of surface geothermal energy for air conditioning in northern Tunisia: Direct test and deployment of ground source heat pump system. Energy and Buildings, 111, 207–217. https://doi.org/10.1016/j.enbuild.2015.11.024

Newcomer, A., & Apt, J. (2009). Near-Term Implications of a Ban on New Coal-Fired Power Plants in the United States. Environmental Science & Technology, 43(11), 3995–4001. https://doi.org/10.1021/es801729r

Newcomer, A., Blumsack, S. A., Apt, J., Lave, L. B., & Morgan, M. G. (2008). Short Run Effects of a Price on Carbon Dioxide Emissions from U.S. Electric Generators. Environmental Science & Technology, 42(9), 3139–3144. https://doi.org/10.1021/es071749d

NREL. (2018). Home | BEopt. Retrieved August 18, 2018, from https://beopt.nrel.gov/

Oregon. (2016). HB2193.pdf. Retrieved May 22, 2018, from https://olis.leg.state.or.us/liz/2015R1/Downloads/MeasureDocument/HB2193

Pachauri, R. K., Mayer, L., & IPCC (Eds.). (2015). Climate change 2014: synthesis report. Geneva, Switzerland: Intergovernmental Panel on Climate Change.

Paine, N., Homans, F. R., Pollak, M., Bielicki, J. M., & Wilson, E. J. (2014). Why market rules matter: Optimizing pumped hydroelectric storage when compensation rules differ. Energy Economics, 46, 10–19. https://doi.org/10.1016/j.eneco.2014.08.017

Peterson, S. B., Whitacre, J. F., & Apt, J. (2011). Net Air Emissions from Electric Vehicles: The Effect of Carbon Price and Charging Strategies. Environmental Science & Technology, 45(5), 1792–1797. https://doi.org/10.1021/es102464y

PJM. (2014). Marginal Fuel Type Data. Retrieved November 1, 2016, from http://www.pjm.com/markets-and-operations/energy/real-time/historical-bid-data/marg-fuel-type-data.aspx

Raichur, V., Callaway, D. S., & Skerlos, S. J. (2016). Estimating Emissions from Electricity Generation Using Electricity Dispatch Models: The Importance of System Operating Constraints. Journal of Industrial Ecology, 20(1), 42–53. https://doi.org/10.1111/jiec.12276

Ryan, N. A., Johnson, J. X., & Keoleian, G. A. (2016). Comparative Assessment of Models and Methods To Calculate Grid Electricity Emissions. Environmental Science & Technology, 50(17), 8937–8953. https://doi.org/10.1021/acs.est.5b05216

San Diego Gas & Electric. (2017, February 28). SDG&E Unveils World's Largest Lithium Ion Battery Storage Facility | San Diego Gas & Electric - NewsCenter. Retrieved May 22, 2018, from http://sdgenews.com/battery-storage/sdge-unveils-world%E2%80%99s-largest-lithium-ion-battery-storage-facility

Sarbu, I., & Sebarchievici, C. (2014). General review of ground-source heat pump systems for heating and cooling of buildings. Energy and Buildings, 70, 441–454. https://doi.org/10.1016/j.enbuild.2013.11.068

Self, S. J., Reddy, B. V., & Rosen, M. A. (2013). Geothermal heat pump systems: Status review and comparison with other heating options. Applied Energy, 101, 341–348. https://doi.org/10.1016/j.apenergy.2012.01.048

Shen, P., & Lukes, J. R. (2015). Impact of global warming on performance of ground source heat pumps in US climate zones. Energy Conversion and Management, 101, 632–643. https://doi.org/10.1016/j.enconman.2015.06.027

Siler-Evans, K., Azevedo, I. L., & Morgan, M. G. (2012). Marginal Emissions Factors for the U.S. Electricity System. Environmental Science & Technology, 46(9), 4742–4748. https://doi.org/10.1021/es300145v

Sivasakthivel, T., Murugesan, K., Kumar, S., Hu, P., & Kobiga, P. (2016). Experimental study of thermal performance of a ground source heat pump system installed in a Himalayan city of India for composite climatic conditions. Energy and Buildings, 131, 193–206. https://doi.org/10.1016/j.enbuild.2016.09.034

Smith, K. R., Jerrett, M., Anderson, H. R., Burnett, R. T., Stone, V., Derwent, R., … others. (2010). Public health benefits of strategies to reduce greenhouse-gas emissions: health implications of short-lived greenhouse pollutants. The Lancet, 374(9707), 2091–2103.

Southern California Edison. (2018). Energy Storage | Edison International. Retrieved May 22, 2018, from http://www.edison.com/home/innovation/energy-storage.html

Stadler, M., Siddiqui, A., Marnay, C., Aki, H., & Lai, J. (2011). Control of greenhouse gas emissions by optimal DER technology investment and energy management in zero-net-energy buildings. European Transactions on Electrical Power, 21(2), 1291–1309. https://doi.org/10.1002/etep.418

Staffell, I., & Rustomji, M. (2016). Maximising the value of electricity storage. Journal of Energy Storage, 8, 212–225. https://doi.org/10.1016/j.est.2016.08.010

Stafford, B. A., & Wilson, E. J. (2016). Winds of change in energy systems: Policy implementation, technology deployment, and regional transmission organizations. Energy Research & Social Science, 21, 222–236. https://doi.org/10.1016/j.erss.2016.08.001

State of Massachusetts. (2017, June). Energy Storage Target. Retrieved May 22, 2018, from https://www.mass.gov/service-details/energy-storage-target

State of New Jersey. (2018, March 22). Assembly No. 3723 State of New Jersey, 218th Legislature. Retrieved May 22, 2018, from http://www.njleg.state.nj.us/2018/Bills/A4000/3723_I1.PDF

State of New York. (2017, March 9). NY State Assembly Bill A6571. Retrieved May 22, 2018, from https://www.nysenate.gov/legislation/bills/2017/a6571/amendment/original

Statista. (2018). U.S. - projected inflation rate 2008-2023. Retrieved July 13, 2018, from https://www.statista.com/statistics/244983/projected-inflation-rate-in-the-united-states/

Stephan, C. H., & Sullivan, J. (2008). Environmental and Energy Implications of Plug-In Hybrid-Electric Vehicles. Environmental Science & Technology, 42(4), 1185–1190. https://doi.org/10.1021/es062314d

Swider, D. J. (2007). Compressed Air Energy Storage in an Electricity System With Significant Wind Power Generation. IEEE Transactions on Energy Conversion, 22(1), 95–102. https://doi.org/10.1109/TEC.2006.889547

Tamayao, M.-A. M., Michalek, J. J., Hendrickson, C., & Azevedo, I. M. L. (2015). Regional Variability and Uncertainty of Electric Vehicle Life Cycle CO 2 Emissions across the United States. Environmental Science & Technology, 49(14), 8844–8855. https://doi.org/10.1021/acs.est.5b00815

Tennessee Valley Authority. (2012). TVA - Wind Energy Contracts. Retrieved May 24, 2018, from https://www.tva.gov/Energy/Valley-Renewable-Energy/Wind-Energy-Contracts

Tesla. (2018). Tesla Powerpack Overall System Specifications. Retrieved May 16, 2018, from https://www.tesla.com/powerpack

Thind, M. P. S., Wilson, E. J., Azevedo, I. L., & Marshall, J. D. (2017). Marginal Emissions Factors for Electricity Generation in the Midcontinent ISO. Environmental Science & Technology, 51(24), 14445–14452. https://doi.org/10.1021/acs.est.7b03047

U.S. DOE. (2017). 2017 Grid Modernization Peer Review Report Foundational Projects and Technical Area Portfolio Review. Retrieved from https://www.energy.gov/sites/prod/files/2018/01/f46/GMI%20Peer%20Review%20Report%202017_1-22%20FINAL%20online.pdf

U.S. Energy Information Administration. (2018). Monthly Energy Review February 2018.

U.S. Energy Information Administration (EIA). (2009). Residential Energy Consumption Survey (RECS) - U.S. Energy Information Administration (EIA). Retrieved March 19, 2018, from https://www.eia.gov/consumption/residential/maps.php

U.S. Energy Information Administration (EIA). (2013, March 7). Heating and cooling no longer majority of U.S. home energy use - Today in Energy - U.S. Energy Information Administration (EIA). Retrieved February 17, 2018, from https://www.eia.gov/todayinenergy/detail.php?id=10271

U.S. Energy Information Administration (EIA). (2016, February 2). Carbon Dioxide Emissions Coefficients. Retrieved December 26, 2017, from https://www.eia.gov/environment/emissions/co2_vol_mass.php

U.S. EPA. (2012). Clean Power Plan: Description of 2012 Unit - level Data Using the eGRID Methodology. Retrieved November 1, 2016, from https://www.epa.gov/sites/production/files/2014-06/documents/20140602-description-egrid-methodology.pdf

U.S. EPA. (2018). Air Markets Program Data | Clean Air Markets | US EPA. Retrieved November 5, 2016, from https://ampd.epa.gov/ampd/

van Vliet, O., Brouwer, A. S., Kuramochi, T., van den Broek, M., & Faaij, A. (2011). Energy use, cost and CO2 emissions of electric cars. Journal of Power Sources, 196(4), 2298–2310. https://doi.org/10.1016/j.jpowsour.2010.09.119

Voorspools, K. R., & D D'haeseleer, W. (2000). The influence of the instantaneous fuel mix for electricity generation on the corresponding emissions. Energy, 25(11), 1119–1138.

Wang, K., & Wei, Y.-M. (2014). China's regional industrial energy efficiency and carbon emissions abatement costs. Applied Energy, 130, 617–631. https://doi.org/10.1016/j.apenergy.2014.03.010

Wang, P., Huang, J. Y., Ding, Y., Loh, P., & Goel, L. (2011). Demand side load management of smart grids using intelligent trading/metering/ billing system. In 2011 IEEE Trondheim PowerTech (pp. 1–6). https://doi.org/10.1109/PTC.2011.6019420

Wang, S., & Hao, J. (2012). Air quality management in China: Issues, challenges, and options. Journal of Environmental Sciences, 24(1), 2–13. https://doi.org/10.1016/S1001-0742(11)60724-9

White House. (2016). United States Mid-Century Strategy for Deep Decarbonization. Washington DC. Retrieved from https://unfccc.int/files/focus/long-term_strategies/application/pdf/us_mid_century_strategy.pdf

Williams, J. H., Haley, F., Moore, J., Jones, A. D., Torn, M. S., & McJeon, H. (2014). Pathways to Deep Decarbonization in the United States (The U.S. report of the Deep Decarbonization Pathways Project of the Sustainable Development Solutions Network and the Institute for Sustainable Development and International Relations.). Retrieved from http://unsdsn.org/wp-content/uploads/2014/09/US-Deep-Decarbonization-Report.pdf

Wilson, E., Engebrecht-Metzger, C., Horowitz, S., & Hendron, R. (2014). 2014 Building America house simulation protocols. National Renewable Energy Lab.(NREL), Golden, CO (United States).

Yuksel, T., & Michalek, J. J. (2015). Effects of Regional Temperature on Electric Vehicle Efficiency, Range, and Emissions in the United States. Environmental Science & Technology, 49(6), 3974–3980. https://doi.org/10.1021/es505621s

Yuksel, T., Tamayao, M.-A. M., Hendrickson, C., Azevedo, I. M. L., & Michalek, J. J. (2016). Effect of regional grid mix, driving patterns and climate on the comparative carbon footprint of gasoline and plug-in electric vehicles in the United States. Environmental Research Letters, 11(4), 044007. https://doi.org/10.1088/1748-9326/11/4/044007

Zhao, H., Wu, Q., Hu, S., Xu, H., & Rasmussen, C. N. (2015). Review of energy storage system for wind power integration support. Applied Energy, 137, 545–553. https://doi.org/10.1016/j.apenergy.2014.04.103

Zidar, M., Georgilakis, P. S., Hatziargyriou, N. D., Capuder, T., & Škrlec, D. (2016). Review of energy storage allocation in power distribution networks: applications, methods and future research. Transmission Distribution IET Generation, 10(3), 645–652. https://doi.org/10.1049/iet-gtd.2015.0447

Appendix A

Marginal Emission Factors Considering Renewables: A Case Study of the U.S. Midcontinent Independent System Operator (MISO) System

A1. MISO and its subregions

There are three subregions (North, Central and South) of the Midcontinent Independent System Operator (MISO) system. The North subregion includes Iowa, Minnesota, Montana, North Dakota, South Dakota, and Manitoba, Canada; the Central subregion includes Indiana, Illinois, Kentucky, Michigan, Missouri, and Wisconsin; and the South subregion includes Arkansas, Louisiana, Mississippi, and Texas. The map of MISO and its subregions is available here: http://www.misomtep.org/miso-overview-mtep15/.

Table A1 presents the total generation and the fuel mix for MISO and each subregion, based on 2014 MISO Hourly Fuel Mix data. The Central subregion has the largest total generation among all subregions, which is more than the sum of North's and South's total generation. Coal and gas are the dominant fossil-fuel sources; hydropower accounts for a very minor share; nuclear contributes between 12.77% and 26.05%; and wind power is significant in the North subregion (22.50%).

Table A 1. Total generation and fuel mix in 2014 by MISO and its subregions

	MISO	North	Central	South
Total Generation (TWh)	633	137	330	166
Coal	57.69%	57.73%	74.99%	23.82%
Natural Gas	15.47%	2.65%	7.49%	41.80%
Hydro	1.27%	1.14%	1.28%	1.36%
Nuclear	16.21%	12.77%	12.90%	26.05%
Other	3.02%	3.22%	0.96%	6.97%
Wind	6.34%	22.50%	2.39%	NA

A2. Linear regression details of the expanded MEFs

For MISO and its subregions, Figure A1 shows the change in emissions (CO_2, SO_2, and NO_X) as a function of change in system generation (emitting and non-emitting sources).

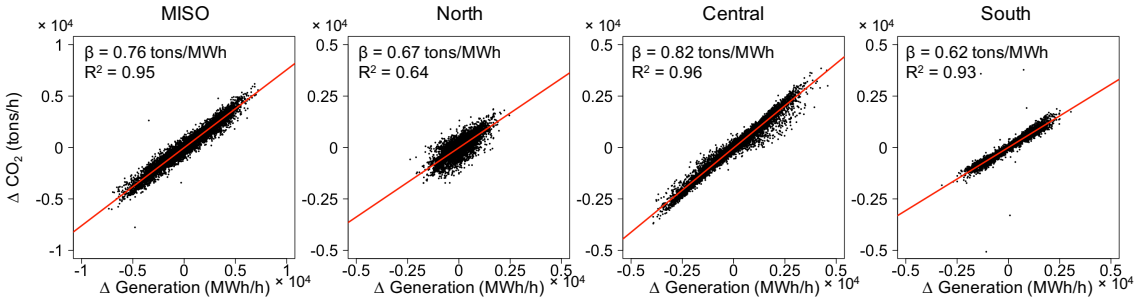

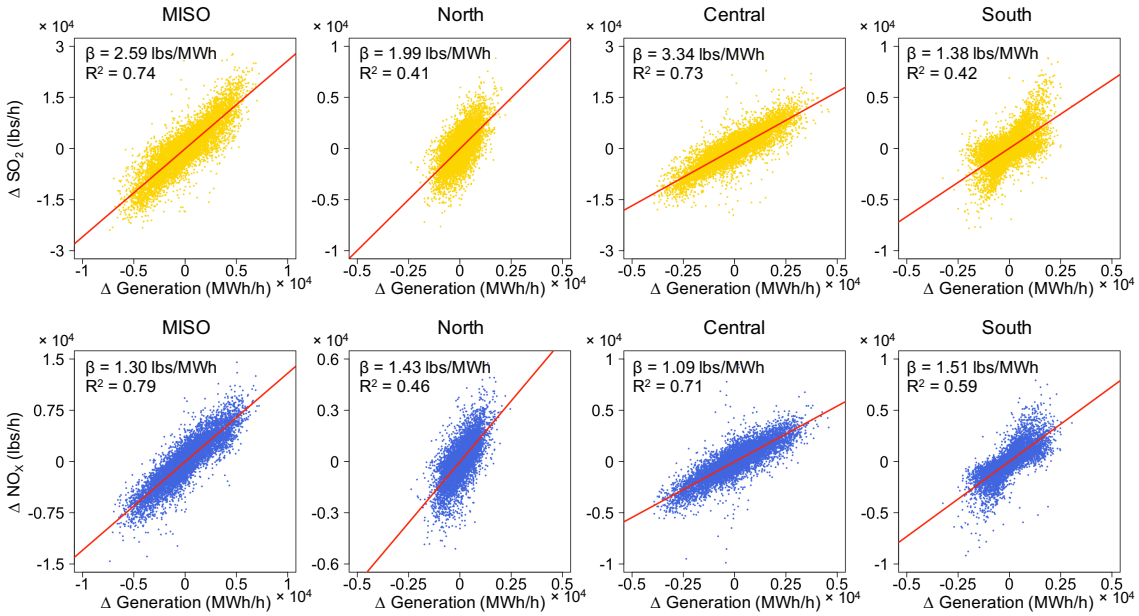

Figure A 1. Estimates of the expanded MEFs in 2014 for MISO and its subregions. Each point is the difference in emissions and generation between one hour and the next.

A3. Temporal trends of MEFs

Time of day trends by year and season of the expanded and the conventional MEFs are shown in Figure A2.

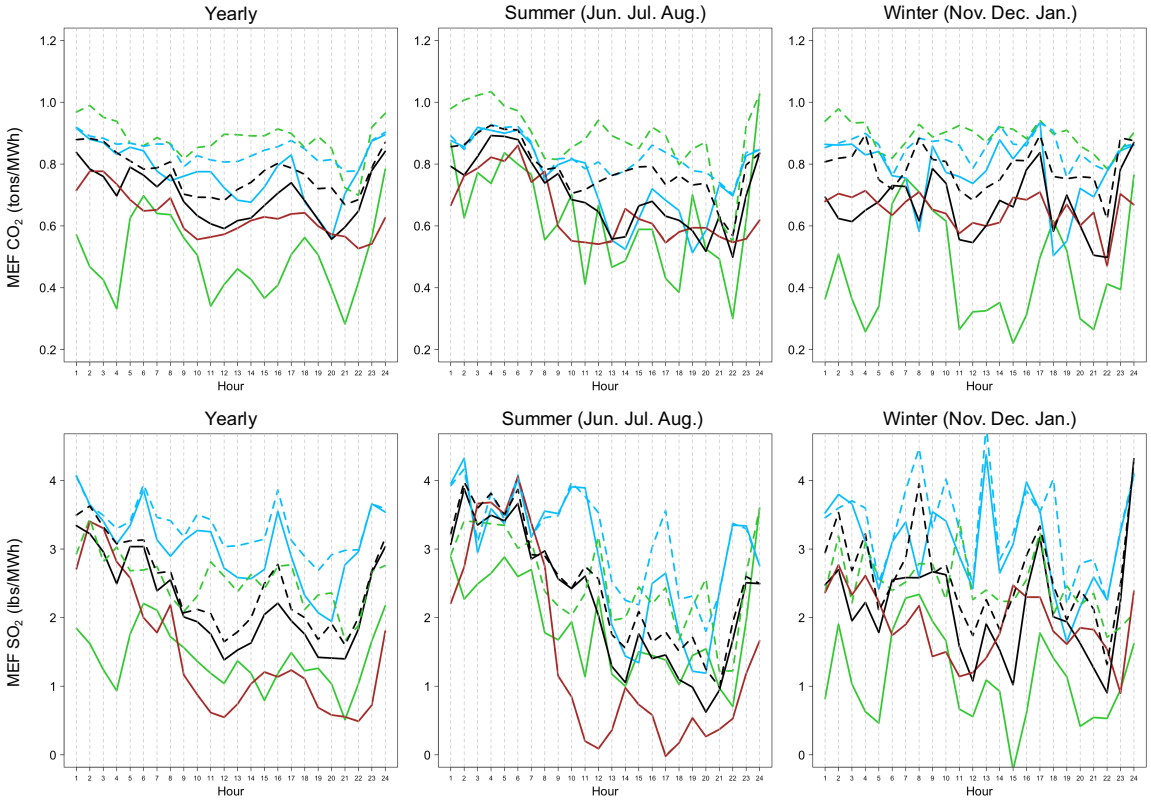

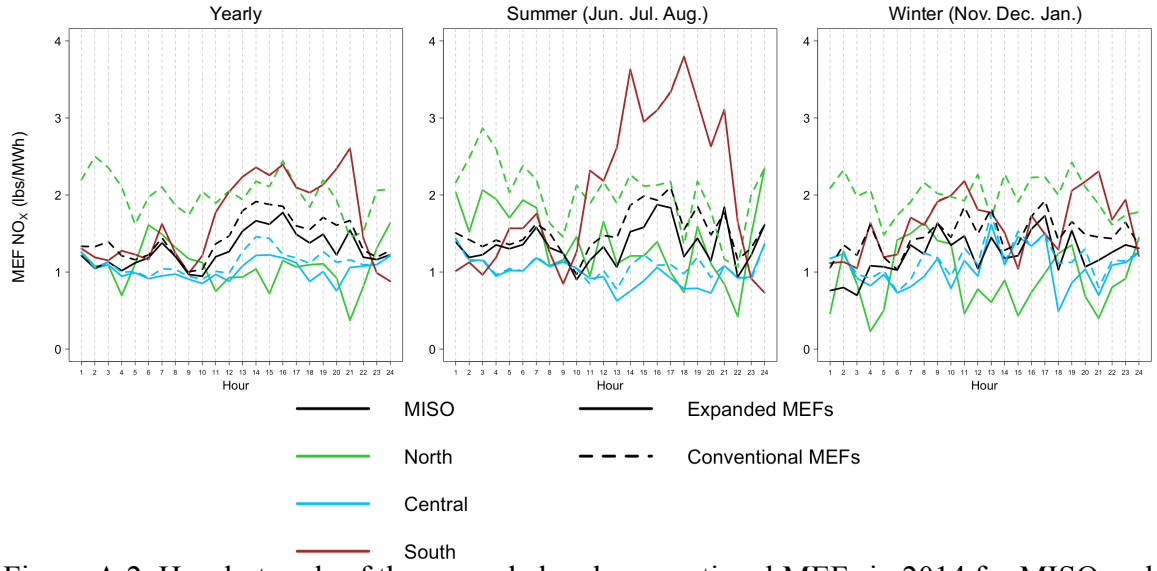

Figure A 2. Hourly trends of the expanded and conventional MEFs in 2014 for MISO and its subregions. Annual trend covers all twelve months. Summer trend covers June, July, and August. Winter trend covers November, December, and January.

A4. Sensitivity analysis on the MEFs based on simulated subregional electricity net interchange rates

We perform a sensitivity analysis on the expanded and conventional MEFs in response to simulated hourly electricity net interchange for the North, Central, and South subregions in MISO. We presumed six levels of the net interchange rate (5%, 10%, 15%, 20%, 25%, and 30%) and apply them to the linear regression equations on an hourly basis. The levels are set based on the rates found in existing research that characterizes the net interchange or import between MISO and neighboring ISO/RTOs, which range from 2% to 24% and indicate most of the electricity that is used within MISO is generated within MISO (according to the eGRID report by Diem and Quiroz, 2012). Thus, we only inspect effects of the subregional net interchange within MISO but not the regional net interchange between MISO and neighboring ISO/RTOs.

Due to transmission and efficiency constraints, there usually is very rare or no electricity interchange between the North and South subregion, therefore we assume the North and South subregion only imports from and exports to the Central subregion, while the Central subregion imports and exports to both North and South subregions. Detailed results of the sensitivity analysis are shown in Table A2.

Table A 2. Results of the sensitivity analysis on MEFs

Net interchange rate	MEFs	CO_2 (tons/MWh)	SO_2 (lbs/MWh)	NO_X (lbs/MWh)
0% net interchange rate	Expanded MEF MISO	0.76	2.59	1.30
	Expanded MEF North	0.67	1.99	1.43
	Expanded MEF Central	0.82	3.34	1.09

	Expanded MEF South	0.62	1.38	1.51
	Conventional MEF MISO	0.78	2.67	1.33
	Conventional MEF North	0.86	2.54	1.87
	Conventional MEF Central	0.85	3.47	1.12
	Conventional MEF South	0.62	1.38	1.51
	Expanded ~ Conventional MEFs diff.% MISO	2.78%	3.13%	2.60%
	Expanded ~ Conventional MEFs diff.% North	27.68%	27.78%	31.14%
	Expanded ~ Conventional MEFs diff.% Central	3.73%	3.87%	3.52%
	Expanded ~ Conventional MEFs diff.% South	0.01%	0.02%	0.01%
5% net interchange rate	Expanded MEF MISO	0.76	2.59	1.30
	Expanded MEF North	0.70	2.15	1.43
	Expanded MEF Central	0.82	3.29	1.10
	Expanded MEF South	0.63	1.50	1.48
	Conventional MEF MISO	0.78	2.67	1.33
	Conventional MEF North	0.86	2.62	1.79
	Conventional MEF Central	0.85	3.41	1.14
	Conventional MEF South	0.63	1.51	1.48
	Expanded ~ Conventional MEFs diff.% MISO	2.78%	3.13%	2.60%
	Expanded ~ Conventional MEFs diff.% North	22.12%	21.91%	25.46%
	Expanded ~ Conventional MEFs diff.% Central	3.48%	3.64%	3.25%
	Expanded ~ Conventional MEFs diff.% South	0.16%	0.24%	0.07%
10% net interchange rate	Expanded MEF MISO	0.76	2.59	1.30
	Expanded MEF North	0.73	2.29	1.42
	Expanded MEF Central	0.81	3.24	1.12
	Expanded MEF South	0.64	1.62	1.45
	Conventional MEF MISO	0.78	2.67	1.33
	Conventional MEF North	0.86	2.69	1.72
	Conventional MEF Central	0.84	3.35	1.15
	Conventional MEF South	0.65	1.63	1.46
	Expanded ~ Conventional MEFs diff.% MISO	2.78%	3.13%	2.60%
	Expanded ~ Conventional MEFs diff.% North	17.99%	17.61%	21.15%
	Expanded ~ Conventional MEFs diff.% Central	3.28%	3.44%	3.03%
	Expanded ~ Conventional MEFs diff.% South	0.32%	0.44%	0.15%
15% net interchange rate	Expanded MEF MISO	0.76	2.59	1.30
	Expanded MEF North	0.74	2.41	1.41
	Expanded MEF Central	0.81	3.18	1.14

	Expanded MEF South	0.66	1.73	1.43
	Conventional MEF MISO	0.78	2.67	1.33
	Conventional MEF North	0.86	2.76	1.66
	Conventional MEF Central	0.84	3.29	1.17
	Conventional MEF South	0.66	1.74	1.43
	Expanded ~ Conventional MEFs diff.% MISO	2.78%	3.13%	2.60%
	Expanded ~ Conventional MEFs diff.% North	14.90%	14.44%	17.85%
	Expanded ~ Conventional MEFs diff.% Central	3.10%	3.28%	2.85%
	Expanded ~ Conventional MEFs diff.% South	0.47%	0.62%	0.24%
20% net interchange rate	Expanded MEF MISO	0.76	2.59	1.30
	Expanded MEF North	0.76	2.52	1.39
	Expanded MEF Central	0.81	3.14	1.15
	Expanded MEF South	0.67	1.83	1.40
	Conventional MEF MISO	0.78	2.67	1.33
	Conventional MEF North	0.85	2.82	1.61
	Conventional MEF Central	0.83	3.23	1.18
	Conventional MEF South	0.67	1.84	1.41
	Expanded ~ Conventional MEFs diff.% MISO	2.78%	3.13%	2.60%
	Expanded ~ Conventional MEFs diff.% North	12.56%	12.08%	15.29%
	Expanded ~ Conventional MEFs diff.% Central	2.96%	3.14%	2.70%
	Expanded ~ Conventional MEFs diff.% South	0.61%	0.80%	0.34%
25% net interchange rate	Expanded MEF MISO	0.76	2.59	1.30
	Expanded MEF North	0.77	2.60	1.38
	Expanded MEF Central	0.80	3.09	1.17
	Expanded MEF South	0.68	1.92	1.38
	Conventional MEF MISO	0.78	2.67	1.33
	Conventional MEF North	0.85	2.87	1.56
	Conventional MEF Central	0.83	3.18	1.20
	Conventional MEF South	0.68	1.94	1.39
	Expanded ~ Conventional MEFs diff.% MISO	2.78%	3.13%	2.60%
	Expanded ~ Conventional MEFs diff.% North	10.77%	10.30%	13.29%
	Expanded ~ Conventional MEFs diff.% Central	2.83%	3.02%	2.58%
	Expanded ~ Conventional MEFs diff.% South	0.75%	0.96%	0.43%
30% net interchange rate	Expanded MEF MISO	0.76	2.59	1.30
	Expanded MEF North	0.78	2.68	1.36
	Expanded MEF Central	0.80	3.04	1.18

Expanded MEF South	0.68	2.00	1.37
Conventional MEF MISO	0.78	2.67	1.33
Conventional MEF North	0.85	2.92	1.52
Conventional MEF Central	0.82	3.13	1.21
Conventional MEF South	0.69	2.02	1.37
Expanded ~ Conventional MEFs diff.% MISO	2.78%	3.13%	2.60%
Expanded ~ Conventional MEFs diff.% North	9.38%	8.93%	11.70%
Expanded ~ Conventional MEFs diff.% Central	2.73%	2.92%	2.48%
Expanded ~ Conventional MEFs diff.% South	0.89%	1.11%	0.53%

Based on the results in Table A2, we create Figure A3 to compare the difference between the expanded and conventional MEFs at 0% and 30% subregional net interchange rates. As shown in Figure A3, even if the subregional net interchange rate reaches 30%, the difference between the expanded and conventional MEFs is still notable in the wind-rich North subregion.

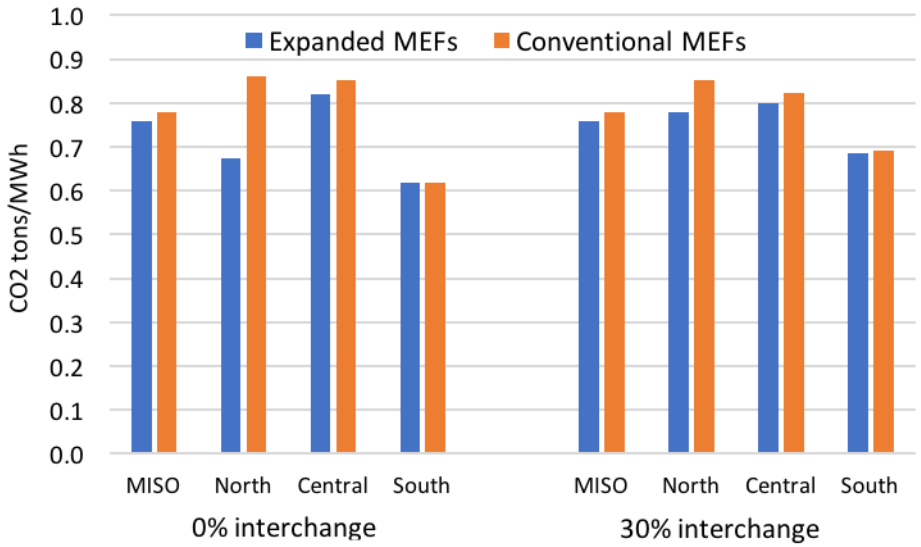

(A)

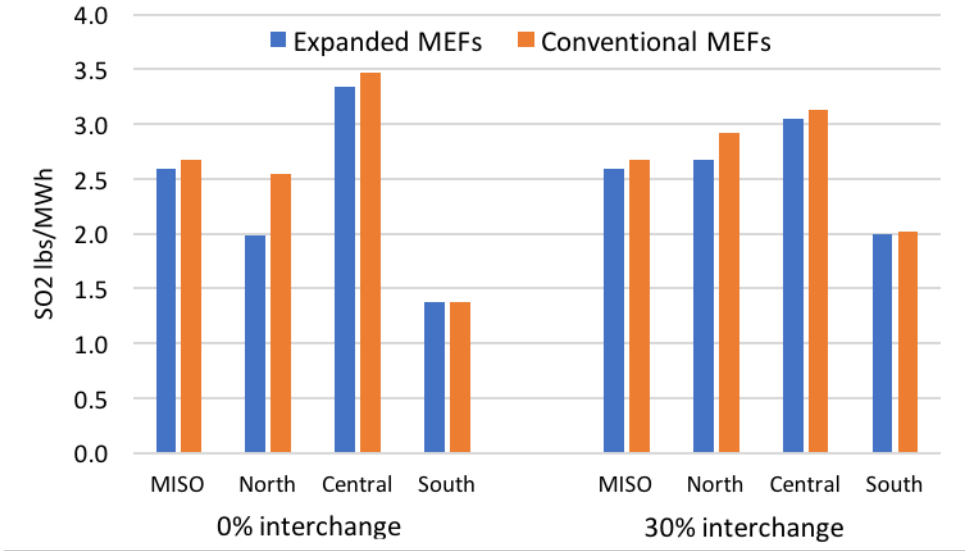

(B)

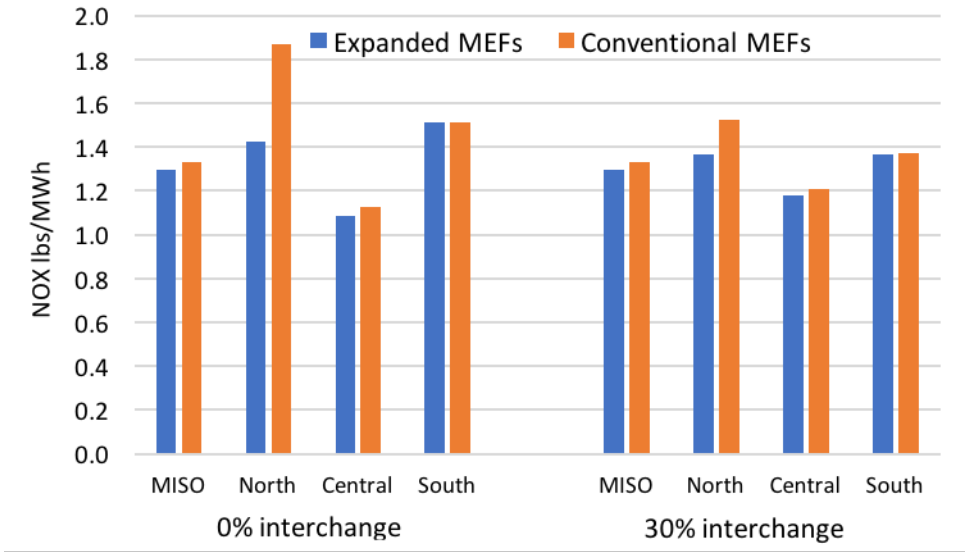

(C)

Figure A 3. Difference between the expanded and conventional MEFs for CO_2 (A), SO_2 (B), and NO_X (C) at 0% and 30% subregional net interchange rates.

We also examine and compare the spatiotemporal trends of the expanded MEFs at 0% and 30% subregional net interchange rates (Figure A4). In Figure A4 (A), we illustrate the *difference* (in tons/MWh) between the expanded MEFs at 0% and 30% subregional net interchange rates (MEFs at 30% minus MEFs at 0%), and it shows fairly small differences for the North, Central, and South subregions. In Figure A4 (B), we illustrate the *percentage difference* between the expanded MEFs at 0% and 30% subregional net interchange rates (MEFs at 30% minus MEFs at 0%), and it shows fairly small differences for the North, Central, and South subregions except for the 5am in January in North.

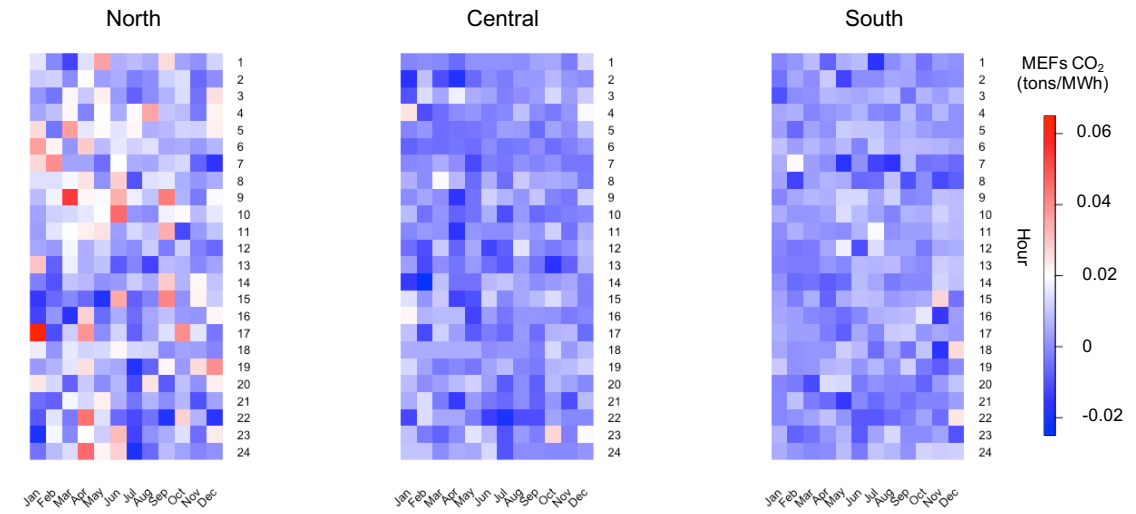

(A)

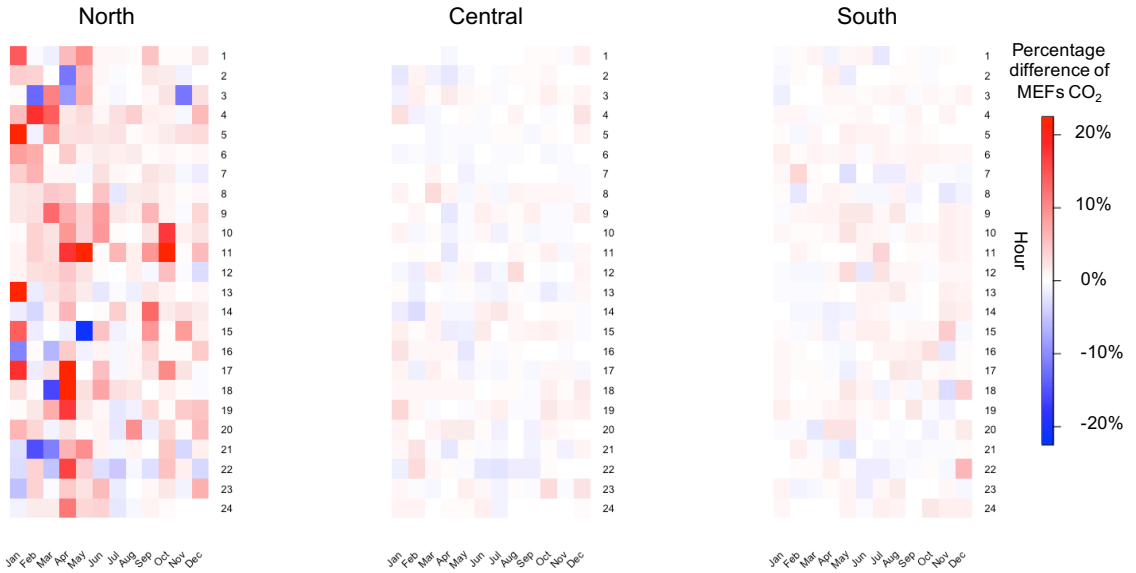

(B)

Figure A 4. Difference (in tons/MWh) (A) and percentage difference (B) between the expanded MEFs at 0% and 30% subregional net interchange rates

Appendix B

Multi-Regional Energy and Emissions Assessment on Electrification of Residential Energy Consumption for Space Conditioning

B1. Hourly Heating and Cooling Energy Use Simulation

Table B 1 Parameters in the BEopt model.
Highlighted selections indicate different parameters for low-, med-, and high-efficient houses.

Parameters	Low-Efficient House	Med-Efficient House	High-Efficient House
Building			
Orientation	North	North	North
Neighbors	None	None	None
Walls			
Wood Stud	R-11 Fiberglass Batt, 2x4, 16 in o.c.	R-19 Fiberglass Batt, 2x4, 16 in o.c.	R-21 Fiberglass Batt, 2x4, 16 in o.c.
Double Wood Stud	None	None	None
Steel Stud	None	None	None
CMU	None	None	None
SIP	None	None	None
ICF	None	None	None
Other	None	None	None
Wall Sheating	OSB	OSB	R-5 XPS
Exterior Finish	Vinyl, Light	Vinyl, Light	Vinyl, Light
Ceilings/Roofs			
Unfinished Attic	Ceiling R-13 Cellulose, Vented	Ceiling R-38 Cellulose, Vented	Ceiling R-49 Cellulose, Vented
Roof Material	Asphalt Shingles, Medium	Asphalt Shingles, Medium	Asphalt Shingles, Medium
Radiant Barrier	None	None	None
Foundation/Floors			
Slab	4ft R5 Exterior XPS	4ft R10 Exterior XPS	4ft R15 Exterior XPS
Carpet	80% Carpet	80% Carpet	80% Carpet
Thermal Mass			
Floor Mass	Wood Surface	Wood Surface	Wood Surface
Exterior Wall Mass	1/2 in. Drywall	1/2 in. Drywall	1/2 in. Drywall
Partition Wall Mass	1/2 in. Drywall	1/2 in. Drywall	1/2 in. Drywall
Ceiling Mass	1/2 in. Drywall	1/2 in. Drywall	1/2 in. Drywall
Windows & Doors			
Window Areas	F15 B15 L15 R15	F15 B15 L15 R15	F15 B15 L15 R15
Windows	Clear, Double, Non-metal, Air	Low-E, Double, Non-metal, Arg, M-Gain	Low-E, Double, Insulated, Arg, M-Gain
Interior Shading	Apr-Sep = 0.5, Oct-Mar = 0.95	Apr-Sep = 0.5, Oct-Mar = 0.95	Apr-Sep = 0.5, Oct-Mar = 0.95
Door Area	40 ft^2	40 ft^2	40 ft^2
Doors	Fiberglass	Fiberglass	Fiberglass
Eaves	2 ft	2 ft	2 ft
Overhangs	2ft, All Stories, All Windows	2ft, All Stories, All Windows	2ft, All Stories, All Windows
Airflow			

Air leakage	7 ACH50	5 ACH50	3 ACH50
Mechanical Ventilation	2010, Exhaust	2010, Exhaust	2010, Exhaust
Natural Ventilation	Cooling Months Only, 7 days/wk	Cooling Months Only, 7 days/wk	Cooling Months Only, 7 days/wk
Space Conditioning			
Central Air Conditioner	SEER 13	SEER 13	SEER 13
Room Air Conditioner	None	None	None
Furnace	Gas, 90% AFUE	Gas, 90% AFUE	Gas, 90% AFUE
Boiler	None	None	None
Electric Baseboard	None	None	None
Air Source Heat Pump	None	None	None
Mini-Split Heat Pump	None	None	None
Ground Source Heat Pump (low)	EER 16.6, COP 3.6, Low-k soil, Std grout	EER 16.6, COP 3.6, Low-k soil, Std grout	EER 16.6, COP 3.6, Low-k soil, Std grout
Ground Source Heat Pump (med)	EER 19.4, COP 3.8, Low-k soil, Std grout	EER 19.4, COP 3.8, Low-k soil, Std grout	EER 19.4, COP 3.8, Low-k soil, Std grout
Ground Source Heat Pump (high)	EER 20.2, COP 4.2, Low-k soil, Std grout	EER 20.2, COP 4.2, Low-k soil, Std grout	EER 20.2, COP 4.2, Low-k soil, Std grout
Ducts	In Finished Space	In Finished Space	In Finished Space
Ceiling Fan	National Average	National Average	National Average
Dehumidifier	None	None	None
Space Conditioning Schedules			
Cooling Set Point	76 F	76 F	76 F
Heating Set Point	71 F	71 F	71 F
Humidity Set Point	None	None	None
Water Heating			
Water Heater	Gas Standard	Gas Standard	Gas Standard
Distribution	Uninsulated, TrunkBranch, Copper	Uninsulated, TrunkBranch, Copper	Uninsulated, TrunkBranch, Copper
Solar Water Heating	None	None	None
Solar Water Heating Azimuth	Back Roof	Back Roof	Back Roof
Solar Water Heating Tilt	Roof Pitch	Roof Pitch	Roof Pitch
Lighting			
Lighting	34% CFL Hardwired, 34% CFL Plugin	34% CFL Hardwired, 34% CFL Plugin	34% CFL Hardwired, 34% CFL Plugin
Appliances & Fixtures			
Refrigerator	Top freezer, EF = 17.6	Top freezer, EF = 17.6	Top freezer, EF = 17.6
Cooking Range	Electric	Electric	Electric
Dishwasher	318 Rated kWh	318 Rated kWh	318 Rated kWh
Clothes Washer	Standard	Standard	Standard
Clothes Dryer	Electric	Electric	Electric
Hot Water Fixtures	1.00	1.00	1.00
Appliances & Fixtures Schedules			
Refrigerator Schedule	Standard	Standard	Standard
Cooking Range Schedule	Standard	Standard	Standard

Clothes Dryer Schedule	Standard	Standard	Standard
Miscellaneous			
Plug Loads	1.00	1.00	1.00
Extra Refrigerator	None	None	None
Freezer	None	None	None
Pool Heater	None	None	None
Pool Pump	None	None	None
Hot Tub/Spa Heater	None	None	None
Hot Tub/Spa Pump	None	None	None
Well Pump	None	None	None
Gas Fireplace	None	None	None
Gas Grill	None	None	None
Gas Lighting	None	None	None
Miscellaneous Schedules			
Plug Loads Schedule	Standard	Standard	Standard
Extra Refrigerator Schedule	Standard	Standard	Standard
Freezer Schedule	Standard	Standard	Standard
Pool Heater Schedule	Standard	Standard	Standard
Pool Pump Schedule	Standard	Standard	Standard
Hot Tub/Spa Heater Schedule	Standard	Standard	Standard
Hot Tub/Spa Pump Schedule	Standard	Standard	Standard
Well Pump Schedule	Standard	Standard	Standard
Gas Fireplace Schedule	Standard	Standard	Standard
Gas Grill Schedule	Standard	Standard	Standard
Gas Lighting Schedule	Standard	Standard	Standard
Power Generation			
PV System	None	None	None
PV Azimuth	Back Roof	Back Roof	Back Roof
PV Tilt	Roof, Pitch	Roof, Pitch	Roof, Pitch

B2 Annual CO_2 Emissions

Table B 2. Annual emissions calculated using the MISO AEF in Minneapolis, St. Louis, and New Orleans.

First number in brackets is heating CO_2 emissions; second number in brackets is cooling CO_2 emissions.

		Minneapolis	St. Louis	New Orleans
1984 sf low-eff house	GFAC	5790 (5410, 381)	3997 (3071, 926)	2620 (613, 2007)
	low-eff GSHP	6088 (5810, 277)	3831 (3037, 793)	2633 (542, 2091)
	med-eff GSHP	5792 (5546, 246)	3588 (2895, 693)	2360 (518, 1842)
	high-eff GSHP	5330 (5092, 237)	3320 (2653,666)	2260 (475, 1784)
1984 sf	GFAC	3889 (3617, 272)	2694 (1992, 702)	1975 (326, 1649)
	low-eff GSHP	4067 (3871, 196)	2504 (1915, 590)	2001 (280, 1721)

med-eff house	med-eff GSHP	3868 (3694, 174)	2337 (1823, 514)	1779 (267, 1512)
	high-eff GSHP	3560 (3392, 168)	2161 (1668, 493)	1709 (245, 1464)
1984 sf high-eff house	GFAC	2694 (2427, 267)	1940 (1279, 661)	1759 (160, 1598)
	low-eff GSHP	2716 (2527, 190)	1819 (1239, 580)	1839 (140, 1698)
	med-eff GSHP	2576 (2409, 167)	1683 (1179, 504)	1628 (134, 1494)
	high-eff GSHP	2368 (2207, 161)	1562 (1079, 484)	1569 (123, 1446)

Table B 3. Annual emissions calculated using the subregional AEFs in Minneapolis, St. Louis, and New Orleans.
First number in brackets is heating CO_2 emissions; second number in brackets is cooling CO_2 emissions.

		Minneapolis	St. Louis	New Orleans
1984 sf low-eff house	GFAC	5732 (5410, 323)	4173 (3071, 1102)	2164 (613, 1551)
	low-eff GSHP	5163 (4927, 235)	4558 (3614, 944)	2035 (419, 1616)
	med-eff GSHP	4912 (4703, 208)	4270 (3445, 825)	1824 (400, 1424)
	high-eff GSHP	4520 (4318, 201)	3950 (3157, 793)	1747 (367, 1379)
1984 sf med-eff house	GFAC	3848 (3617, 231)	2828 (1992, 835)	1600 (326, 1275)
	low-eff GSHP	3449 (3283, 167)	2980 (2278, 702)	1547 (217, 1330)
	med-eff GSHP	3280 (3133, 147)	2781 (2170, 611)	1375 (207, 1168)
	high-eff GSHP	3019 (2877, 142)	2571 (1985, 586)	1321 (189, 1131)
1984 sf high-eff house	GFAC	2653 (2427, 226)	2066 (1279, 787)	1396 (160, 1235)
	low-eff GSHP	2303 (2143, 161)	2164 (1474, 691)	1421 (108, 1313)
	med-eff GSHP	2184 (2043, 142)	2003 (1403, 600)	1258 (103, 1155)
	high-eff GSHP	2009 (1872, 137)	1859 (1284, 576)	1213 (95, 1118)

Table B 4. Annual emissions calculated using the spatiotemporal AEFs in Minneapolis, St. Louis, and New Orleans.
First number in brackets is heating CO2 emissions; second number in brackets is cooling CO_2 emissions.

		Minneapolis	St. Louis	New Orleans
1984 sf low-eff house	GFAC	5782 (5410, 373)	4215 (3701, 1144)	2214 (613, 1601)
	low-eff GSHP	4985 (4713, 272)	4503 (3522, 980)	2081 (413, 1668)
	med-eff GSHP	4740 (4499, 241)	4214 (3357, 857)	1864 (395, 1469)
	high-eff GSHP	4364 (4131, 232)	3900 (3077, 823)	1785 (362, 1423)
1984 sf med-eff house	GFAC	3884 (3617, 267)	2862 (1992, 869)	1636 (326, 1310)
	low-eff GSHP	3337 (3144, 193)	2952 (2221, 731)	1579 (213, 1366)
	med-eff GSHP	3171 (3001, 171)	2752 (2115, 637)	1403 (203, 1200)
	high-eff GSHP	2920 (2755, 165)	2456 (1935, 611)	1348 (186, 1162)
1984 sf high-eff house	GFAC	2688 (2427, 261)	2099 (1279, 820)	1426 (160, 1265)
	low-eff GSHP	2241 (2055, 186)	2158 (1438, 720)	1450 (106, 1344)
	med-eff GSHP	2123 (1960, 164)	1995 (1369, 626)	1284 (101, 1183)
	high-eff GSHP	1954 (1796, 158)	1852 (1252, 600)	1238 (93, 1145)

Table B 5. Annual emissions calculated using the spatiotemporal MEFs in Minneapolis, St. Louis, and New Orleans.
First number in brackets is heating CO_2 emissions; second number in brackets is cooling CO_2 emissions.

		Minneapolis	St. Louis	New Orleans
1984 sf low-eff house	GFAC	5699 (5410, 290)	3993 (3071, 922)	2637 (613, 2024)
	low-eff GSHP	4966 (4755, 211)	4324 (3532, 792)	2618 (514, 2105)
	med-eff GSHP	4726 (4539, 187)	4059 (3366, 692)	2345 (491, 1854)
	high-eff GSHP	4349 (4168, 181)	3751 (3085, 665)	2246 (450, 1796)
1984 sf med-eff house	GFAC	3827 (3617, 209)	2699 (1992, 707)	1977 (326, 1651)
	low-eff GSHP	3326 (3175, 151)	2826 (2231, 596)	1986 (267, 1719)
	med-eff GSHP	3164 (3030, 134)	2643 (2124, 519)	1765 (254, 1510)
	high-eff GSHP	2912 (2783, 129)	2441 (1943, 498)	1695 (233, 1462)
1984 sf high-eff house	GFAC	2632 (2427, 205)	1948 (1279, 669)	1756 (160, 1596)
	low-eff GSHP	2233 (2087, 146)	2034 (1445, 588)	1825 (133, 1692)
	med-eff GSHP	2118 (1989, 129)	1887 (1376, 512)	1616 (127, 1489)
	high-eff GSHP	1947 (1823, 124)	1749 (1259, 491)	1557 (117, 1441)

Appendix C

Locating Locational Marginal Prices in the Midcontinent Independent System Operator (MISO): Economic and Environmental Impacts of Emerging Grid-scale Electricity Storage across the Landscape

C1 Battery storage net operating revenue optimization results

Table C 1. Summary of battery storage net operating revenue optimization.

LMP name	LMP type	Hour	Annual net operating revenue ($)	Annual CO_2 (MT)	Annual SO_2 (kg)	Annual NO_x (kg)	Fuel type
ALTE.COLUMBAL1	GEN	8784	17207	190	356	91	Coal
ALTE.COLUMBAL2	GEN	8784	17202	190	356	91	Coal
ALTE.EDGG4G4	GEN	8784	15501	189	358	87	Coal
ALTE.EDGG5G5	GEN	8784	15485	189	358	87	Coal
ALTW.ALTW	LZN	8784	22636	79	147	50	N/A
ALTW.BRLGTN5	GEN	8784	33428	77	138	48	Coal
ALTW.DAEC	GEN	8784	23311	78	153	54	Nuclear
ALTW.FPL_DAEC	GEN	8784	23311	78	153	54	Nuclear
ALTW.JOUNEALS4	GEN	8784	16167	76	142	51	Coal
ALTW.LANSIN4	GEN	8784	24291	85	157	59	Coal
ALTW.OTTUMW1	GEN	8784	22486	80	137	59	Coal
AMIL.ALSEYCTG1	GEN	8784	30381	184	318	73	Gas (peaking)
AMIL.BALDWI51	GEN	8784	12312	190	362	80	Coal
AMIL.BALDWI52	GEN	8784	12312	190	362	80	Coal
AMIL.BALDWI53	GEN	8784	12312	190	362	80	Coal
AMIL.CLINTO51	GEN	8784	17674	188	350	83	Nuclear
AMIL.COFFEEN1	GEN	8784	13804	187	350	80	Coal
AMIL.COFFEEN2	GEN	8784	13967	188	350	80	Coal
AMIL.DUCKCRK1	GEN	8784	24163	188	350	87	Coal
AMIL.EDWARDS2	GEN	8784	18806	190	357	83	Coal
AMIL.EDWARDS3	GEN	8784	18798	190	358	82	Coal
AMIL.HAVANA86	GEN	8784	24580	187	341	87	Coal
AMIL.HENNEPN82	GEN	8784	21306	189	346	85	Coal
AMIL.NEWTON21	GEN	8784	13879	182	343	82	Coal
AMIL.NEWTON22	GEN	8040	12737	152	292	61	Coal
AMIL.PPI	GEN	8784	15460	187	360	81	N/A
AMIL.PSGC1.AMP	GEN	8784	12406	191	360	80	Coal

AMIL.PTWF	GEN	8784	21773	179	323	89	Wind
AMIL.STWF	GEN	8784	28071	178	325	84	Wind
AMIL.WOODRW85	GEN	5857	7996	109	225	47	Coal
AMMO.CALLAWAY1	GEN	8784	13340	190	355	77	Nuclear
AMMO.LABADIE1	GEN	8784	12558	190	355	80	Coal
AMMO.LABADIE2	GEN	8784	12529	190	355	80	Coal
AMMO.LABADIE3	GEN	8784	12528	190	355	80	Coal
AMMO.LABADIE4	GEN	8784	12554	190	355	80	Coal
AMMO.MERAMEC3	GEN	8784	12607	190	358	79	Coal
AMMO.MERAMEC4	GEN	8784	12611	190	358	80	Coal
AMMO.RUSHIS1	GEN	8784	12297	190	362	82	Coal
AMMO.RUSHIS2	GEN	8784	12314	191	363	82	Coal
AMMO.SIOUX1	GEN	8784	12753	192	360	79	Coal
AMMO.SIOUX2	GEN	8784	12677	191	361	80	Coal
AMMO.UE	LZN	8784	12775	192	360	78	N/A
AMMO.UE.AZ	LZN	8784	12772	192	359	79	N/A
AMMO.WVPA	LZN	8784	12510	191	362	81	N/A
AMMO.WVPA	LZN	8784	12510	191	362	81	N/A
ARKANSAS.HUB	HUB	8784	12473	-22	-51	-416	N/A
BREC.COLE1	GEN	8784	15520	188	363	88	Coal
BREC.COLE2	GEN	8784	15520	188	363	88	Coal
BREC.COLE3	GEN	8784	15520	188	363	88	Coal
BREC.GREEN1	GEN	8784	15202	187	358	86	Coal
BREC.GREEN2	GEN	8784	15202	187	358	86	Coal
BREC.HMP1	GEN	8784	15202	187	358	86	Coal
BREC.HMP2	GEN	8784	15202	187	358	86	Coal
BREC.WILSON1	GEN	8784	17597	190	367	91	Coal
CIN.CAYUGA.1	GEN	8784	39677	191	348	90	Coal
CIN.CAYUGA.2	GEN	8784	21021	188	341	91	Coal
CIN.CC.SUGRCK	GEN	8784	17604	185	344	94	Gas
CIN.CC.WR1	GEN	3651	7798	46	69	27	Coal
CIN.DEI.AZ	LZN	8784	20850	192	362	88	N/A
CIN.GIBSON.1	GEN	8784	14637	186	358	89	Coal
CIN.GIBSON.2	GEN	8784	14637	186	358	89	Coal
CIN.GIBSON.3	GEN	8784	15103	184	356	89	Coal

CIN.GIBSON.4	GEN	8784	14637	186	358	89	Coal
CIN.GIBSON.5	GEN	8784	14637	186	358	89	Coal
CIN.PSI	LZN	8784	20846	192	363	88	N/A
CIN.WABRIVR.6	GEN	8784	27450	190	353	88	Coal
CLEC.ACA11	GEN	8784	15596	-27	-61	-421	Gas
CLEC.ACA12	GEN	8784	15596	-27	-61	-421	Gas
CLEC.ACA13	GEN	8784	15596	-27	-61	-421	Gas
CLEC.CPS6	GEN	8784	14730	-26	-64	-417	Gas
CLEC.CPS6ST	GEN	8784	14867	-26	-64	-419	Gas
CLEC.CPS71	GEN	8784	14730	-26	-64	-417	Gas
CLEC.CPS72	GEN	8784	14730	-26	-64	-417	Gas
CLEC.CPS7ST	GEN	8784	14867	-26	-64	-419	Gas
CLEC.DPS	GEN	8784	14942	-14	-36	-405	Lignite
CLEC.HUNTER3	GEN	5857	8727	-52	-217	-314	Gas
CLEC.HUNTER5	GEN	730	993	11	43	-11	Gas
CLEC.MPS3	GEN	8784	13781	-23	-60	-413	Gas
CLEC.NPS1	GEN	8784	13778	-23	-61	-414	Gas
CLEC.RPS2	GEN	8784	13773	-23	-60	-414	Coal/Gas
CLEC.RPS2.LAFA	GEN	8784	13773	-23	-60	-414	Coal/Gas
CLEC.RPS2.LEPA	GEN	8784	13773	-23	-60	-414	Coal/Gas
CLEC.TPS1	GEN	8784	17855	-27	-64	-420	Gas
CLEC.TPS3	GEN	8784	17733	-27	-63	-419	Gas
CLEC.TPS4	GEN	8784	17750	-27	-63	-419	Gas
CONS.AZ	LZN	8784	18724	189	353	82	N/A
CONS.CAMPBELL1	GEN	8784	18088	184	342	80	Coal
CONS.CAMPBELL2	GEN	8784	18147	185	342	81	Coal
CONS.CAMPBELL3	GEN	8784	17039	185	343	80	Coal
CONS.CC.COVER3	GEN	3651	4150	45	69	26	Gas
CONS.CC.MICHP	GEN	8784	16667	182	338	77	Gas
CONS.CC.PLYM	GEN	8784	19562	191	349	86	Gas
CONS.CC.ZEELA2	GEN	8784	16975	185	343	81	Gas
CONS.CETR	LZN	8784	18750	190	355	83	N/A
CONS.FILERCITY	GEN	8784	16909	184	339	79	Coal
CONS.KARN1	GEN	8784	19769	185	344	79	Coal
CONS.KARN2	GEN	8784	19765	185	344	79	Coal
CONS.MCV.MCV	GEN	8784	17190	187	349	83	Gas

CONS.PALISA2A1	GEN	8784	17476	187	348	83	Nuclear
CONS.WPSC_2.AZ	LZN	8784	18936	190	355	83	N/A
CWLD.CWLD	GEN	8784	14150	194	362	77	Gas
CWLP.DALLMA84	GEN	8784	21127	186	345	79	Coal
DECO.AZ	LZN	8784	18324	190	355	82	N/A
DECO.BLR1.DEMO	GEN	8784	17556	188	354	81	Coal
DECO.BLR2.DEMO	GEN	8784	17545	188	355	82	Coal
DECO.CC.DIG2	GEN	8784	18556	189	354	82	Gas
DECO.CC.DIG3	GEN	8784	18556	189	354	82	Gas
DECO.FERMI2	GEN	8784	17506	189	356	84	Nuclear
DECO.MONROE1	GEN	8784	17273	190	357	83	Coal
DECO.MONROE2	GEN	8784	17240	190	357	83	Coal
DECO.MONROE3	GEN	8784	17704	189	355	82	Coal
DECO.MONROE4	GEN	8784	17721	190	355	82	Coal
DECO.NEC	LZN	8784	18303	190	355	82	N/A
DECO.RVRRGE2	GEN	8040	17206	160	303	61	Coal
DECO.RVRRGE3	GEN	8784	19170	189	357	82	Coal
DECO.STCLAIR6	GEN	8784	18877	189	354	81	Coal
DECO.STCLAIR7	GEN	8784	17570	188	353	81	Coal
DECO.TRNCNL9	GEN	8784	17858	189	356	82	Coal
DPC.DPC	GEN	8784	18719	193	365	92	Landfill Gas
DPC.DPC	GEN	8784	18719	193	365	92	Landfill Gas
DPC.GENOA3	GEN	8784	28102	191	348	96	Coal
DPC.JPM	GEN	8784	19973	188	348	94	Coal
EAI.AECCBAILEY	GEN	8784	16277	-22	-58	-400	Gas
EAI.AECCHYDRO2	GEN	8784	17287	-21	-53	-395	Hydro
EAI.AECCHYDRO9	GEN	8784	13078	-22	-56	-409	Hydro
EAI.AECCMCCLLN	GEN	8784	12405	-22	-65	-406	Gas
EAI.AECCMGVCT1	GEN	8784	12069	-19	-36	-413	Gas
EAI.AECCMGVCT2	GEN	8784	12069	-19	-36	-413	Gas
EAI.AECCMGVMST	GEN	8784	12069	-19	-36	-413	Gas
EAI.ANO1	GEN	8784	14417	-20	-48	-407	Nuclear
EAI.ANO2	GEN	8784	14425	-20	-48	-407	Nuclear

EAI.BLAKELY1	GEN	8784	13683	-20	-35	-415	Hydro
EAI.BLAKELY2	GEN	8784	13683	-20	-35	-415	Hydro
EAI.CARPEN1	GEN	8784	12796	-17	-23	-412	Hydro
EAI.CARPEN2	GEN	8784	12791	-17	-24	-410	Hydro
EAI.CWAYLD	GEN	8784	14339	-23	-55	-412	Waste
EAI.CWL_A	GEN	8784	14346	-21	-54	-412	Gas
EAI.CWL_B	GEN	8784	14346	-21	-54	-412	Gas
EAI.CWL_C	GEN	8784	14346	-21	-54	-412	Gas
EAI.CWL_D	GEN	8784	14346	-21	-54	-412	Gas
EAI.CWL_E	GEN	8784	14346	-21	-54	-412	Gas
EAI.DEGRAY1	GEN	8784	12339	-17	-33	-393	Hydro
EAI.DEGRAY2	GEN	8784	12339	-17	-33	-393	Hydro
EAI.H_SPR1_CT1	GEN	8784	11996	-20	-34	-414	Gas
EAI.H_SPR1_CT2	GEN	8784	11996	-20	-34	-414	Gas
EAI.H_SPR1_ST	GEN	8784	11996	-20	-34	-414	Gas
EAI.INDEPEND1	GEN	8784	11348	-26	-83	-387	Coal
EAI.INDEPEND2	GEN	8784	11370	-24	-61	-410	Coal
EAI.LK_CATH4	GEN	8784	12859	-19	-29	-410	Gas
EAI.MABELV1_CT	GEN	3651	2891	-37	-217	-117	Gas
EAI.MABELV3_CT	GEN	3651	2891	-37	-217	-117	Gas
EAI.PBENRGY_CT	GEN	8784	12610	-17	-43	-391	Gas
EAI.PBENRGY_ST	GEN	8784	12612	-17	-43	-391	Gas
EAI.PLUM_1C	GEN	8784	12435	-22	-55	-413	Coal
EAI.PLUM_PPEA	GEN	8784	12435	-22	-55	-413	Coal
EAI.PLUM1A_TEA	GEN	1440	660	-9	-53	-71	Coal
EAI.PUPP_2A	GEN	3651	2716	-35	-207	-119	Gas
EAI.PUPP_2B	GEN	3651	2716	-35	-207	-119	Gas
EAI.PUPP_2C	GEN	3651	2716	-35	-207	-119	Gas
EAI.PUPP_3A	GEN	3651	2716	-35	-207	-119	Gas
EAI.PUPP_3B	GEN	3651	2716	-35	-207	-119	Gas
EAI.PUPP_3C	GEN	3651	2716	-35	-207	-119	Gas
EAI.PUPP_4A	GEN	3651	2716	-35	-207	-119	Gas
EAI.PUPP_4B	GEN	3651	2716	-35	-207	-119	Gas
EAI.PUPP_4C	GEN	3651	2716	-35	-207	-119	Gas
EAI.PUPP1_CT1	GEN	3651	2716	-35	-207	-119	Gas
EAI.PUPP1_CT2	GEN	3651	2716	-35	-207	-119	Gas
EAI.PUPP1_ST	GEN	3651	2716	-35	-207	-119	Gas

EAI.REMMEL123	GEN	8784	12729	-18	-29	-408	Hydro
EAI.WH_BLUFF1	GEN	8784	11229	-20	-38	-409	Coal
EAI.WH_BLUFF2	GEN	8784	11126	-19	-33	-406	Coal
EES.ACAD2_CT1	GEN	8784	15994	-26	-60	-423	Gas
EES.ACAD2_CT2	GEN	8784	15994	-26	-60	-423	Gas
EES.ACAD2_ST	GEN	8784	15994	-26	-60	-423	Gas
EES.AXIALL	GEN	8784	16599	-24	-47	-418	Gas
EES.BURAS8_CT	GEN	8784	20604	-30	-75	-428	Gas
EES.CALCAS1_CT	GEN	8784	23233	-24	-51	-416	Gas
EES.CALCAS2_CT	GEN	8784	23233	-24	-51	-416	Gas
EES.CARV_A	GEN	8784	24279	-28	-76	-414	Gas
EES.CARV_BC	GEN	8784	24279	-28	-76	-414	Gas
EES.CONC	GEN	8784	15897	-14	-2	-408	Gas
EES.CYPRESS1CT	GEN	8784	17047	-22	-38	-414	N/A
EES.CYPRESS2CT	GEN	8784	17046	-22	-38	-414	N/A
EES.DOWCHEM	GEN	8784	19259	-17	-66	-328	Gas
EES.ENCO	GEN	8784	22059	-28	-72	-410	Gas
EES.ESSO	GEN	8784	22127	-28	-72	-412	Gas
EES.EVRGRN_LD	LZN	8784	23789	-28	-77	-415	N/A
EES.EWOM_RS	GEN	8784	16599	-24	-47	-418	Gas
EES.EXXOBMT	GEN	8784	17169	-18	-22	-414	Gas
EES.EXXON	GEN	8784	22102	-28	-72	-412	Gas
EES.FRONT_TX1	GEN	8784	24207	-10	-19	-387	Gas
EES.FRONT_TX2	GEN	8784	24207	-10	-19	-387	Gas
EES.L_CREEK1	GEN	8784	18936	-21	-42	-409	Gas
EES.L_CREEK2	GEN	8784	18921	-21	-40	-408	Gas
EES.L_GYPSY2	GEN	8784	21039	-27	-67	-422	Gas
EES.L_GYPSY3	GEN	8784	21529	-28	-68	-422	Gas
EES.LONSTR1	GEN	8784	16736	-23	-47	-417	N/A
EES.MICHOUD2	GEN	3651	4336	-42	-238	-123	Gas
EES.MICHOUD3	GEN	3651	4323	-42	-238	-123	Gas
EES.NELSON1	GEN	8784	16516	-24	-49	-417	Coal
EES.NELSON2	GEN	8784	16520	-24	-49	-418	Coal
EES.NELSON4	GEN	8784	16488	-24	-47	-418	Coal
EES.NELSON6	GEN	8784	16471	-23	-46	-418	Coal
EES.NINEMILE3	GEN	3651	4314	-42	-239	-122	Gas
EES.NINEMILE4	GEN	8784	20089	-30	-75	-428	Gas

EES.NINEMILE5	GEN	8784	20087	-30	-75	-428	Gas
EES.OUACHITA1	GEN	8784	14614	-17	-59	-379	Gas
EES.OUACHITA2	GEN	8784	14614	-17	-59	-379	Gas
EES.OUACHITA3	GEN	8784	14614	-17	-59	-379	Gas
EES.PERVL1	GEN	8784	14529	-17	-61	-380	Gas
EES.PERVL2_CT	GEN	8784	14529	-17	-61	-380	Gas
EES.RICE1	GEN	8784	19846	-26	-57	-423	Agricultural waste
EES.RVRBEND1	GEN	8784	21012	-27	-71	-410	Nuclear
EES.SABINE1	GEN	8784	15688	-14	-5	-408	Gas
EES.SABINE2	GEN	5857	10047	-44	-171	-306	Gas
EES.SABINE3	GEN	8784	15564	-15	-7	-409	Gas
EES.SABINE4	GEN	8784	17153	-19	-24	-408	Gas
EES.SABINE5	GEN	8784	17124	-19	-23	-406	Gas
EES.SABINECO	GEN	8784	15962	-14	-2	-409	Gas
EES.SAM_DAM_12	GEN	8784	18420	-19	-45	-409	Hydro
EES.SAN_JC1_CT	GEN	8784	18914	-19	-33	-409	Gas (peaking)
EES.SAN_JC2_CT	GEN	8784	18914	-19	-33	-409	Gas (peaking)
EES.STERL7	GEN	8784	14593	-20	-63	-390	Gas (peaking)
EES.TAFTCOGEN	GEN	8784	21294	-24	-54	-414	Gas
EES.TLD_CLECO1	GEN	8784	15304	-20	-57	-413	Hydro
EES.TLD_CLECO2	GEN	8784	15304	-20	-57	-413	Hydro
EES.TOL_BEND1	GEN	8784	15304	-20	-57	-413	Hydro
EES.TOL_BEND2	GEN	8784	15304	-20	-57	-413	Hydro
EES.UCB	GEN	8784	21308	-24	-55	-415	N/A
EES.VIDALIA	GEN	8784	31571	-22	-61	-399	Hydro
EES.W_GLEN2	GEN	3651	4466	-42	-235	-122	Gas
EES.W_GLEN4	GEN	3651	4569	-43	-239	-123	Gas
EES.WATRFD1	GEN	8784	21330	-25	-56	-415	Gas
EES.WATRFD2	GEN	8784	21330	-25	-56	-414	Gas
EES.WATRFD3	GEN	8784	21110	-24	-53	-415	Nuclear
EES.WATRFD4_CT	GEN	8784	21325	-24	-55	-415	Oil (peaking)
EMBA.ATTALA1	GEN	8784	16278	-19	-87	-357	Gas
EMBA.B_WILSON1	GEN	8784	20124	-23	-63	-400	Gas
EMBA.B_WILSON2	GEN	8784	18504	-23	-62	-403	Gas

EMBA.G_ANDRUS1	GEN	8784	15975	-25	-65	-406	Gas
EMBA.G_GULF_A	GEN	8784	18218	-23	-62	-401	Nuclear
EMBA.G_GULF_L	GEN	8784	18218	-23	-62	-401	Nuclear
EMBA.G_GULF_M	GEN	8784	18218	-23	-62	-401	Nuclear
EMBA.G_GULF_N	GEN	8784	18218	-23	-62	-401	Nuclear
EMBA.HEND1	GEN	8784	20986	-21	-70	-381	Gas
EMBA.HEND2	GEN	8784	20986	-21	-70	-381	Gas
EMBA.HINDS1_ST	GEN	8784	18733	-23	-64	-399	Gas
EMBA.RX_BRN3	GEN	8784	21263	-21	-54	-396	Gas
EMBA.RX_BRN4	GEN	8784	21238	-21	-54	-396	Gas
GRE.COALC1_AC	GEN	8784	16547	76	128	52	Coal
GRE.COALC2_AC	GEN	8784	16344	75	131	52	Coal
GRE.STANTO1	GEN	8784	16443	77	128	53	Coal
HE.MEROM1	GEN	8784	15977	185	348	93	Coal
HE.MEROM2	GEN	8784	15977	185	348	93	Coal
HE.RATTS1	GEN	3651	4615	46	77	30	Coal
HE.WORTH2	GEN	8784	16662	184	350	92	Gas
ILLINOIS.HUB	HUB	8784	17898	187	357	81	N/A
INDIANA.HUB	HUB	8784	19659	192	369	88	N/A
IPL.16PETEE1	GEN	8784	15206	187	359	89	Coal
IPL.16PETEE2	GEN	8784	15184	187	359	89	Coal
IPL.16PETEE3	GEN	8784	15217	187	359	89	Coal
IPL.16PETEE4	GEN	8784	15216	187	359	89	Coal
IPL.16STOU7O7	GEN	8784	21446	192	363	90	Coal
IPL.IPL	LZN	8784	21818	192	363	90	N/A
LAFA.BONIN2	GEN	8784	16310	-27	-61	-425	Gas
LAFA.BONIN3	GEN	8784	16282	-27	-60	-424	Gas
LAFA.HARGIS1	GEN	8784	16345	-27	-61	-425	Gas
LAFA.HARGIS2	GEN	8784	16345	-27	-61	-425	Gas
LAFA.LABBE1	GEN	8784	16109	-26	-59	-424	Gas
LAFA.LABBE2	GEN	8784	16109	-26	-59	-424	Gas
LAFA.LAFA	LZN	8784	16328	-27	-61	-424	N/A
LAGN.BC1T_3	GEN	8784	20550	-27	-74	-401	Gas
LAGN.BC1T_4	GEN	8784	20550	-27	-74	-401	Gas
LAGN.BC2_1	GEN	8784	15221	-27	-68	-411	Coal

LAGN.BC2_2	GEN	8784	15198	-27	-69	-411	Coal
LAGN.BC2_3	GEN	8784	15221	-27	-68	-411	Coal
LAGN.BCI_1	GEN	8784	20550	-27	-74	-401	Gas
LAGN.BCI_2	GEN	8784	20550	-27	-74	-401	Gas
LAGN.BYCT1	GEN	8784	16662	-25	-56	-421	Gas (peaking)
LAGN.BYCT2	GEN	8784	16655	-25	-56	-421	Gas (peaking)
LAGN.BYCT3	GEN	8784	16660	-25	-56	-421	Gas (peaking)
LAGN.BYCT4	GEN	8784	16659	-25	-56	-421	Gas (peaking)
LAGN.CTW1	GEN	8784	15918	-23	-39	-420	Gas
LAGN.CTW2	GEN	8784	16097	-23	-39	-420	Gas
LAGN.CTW3	GEN	8784	16098	-23	-39	-420	Gas
LAGN.CTW4	GEN	8784	16098	-23	-39	-420	Gas
LAGN.STET1	GEN	8784	16180	-13	-67	-350	Gas
LAGN.STET10	GEN	8784	16180	-13	-67	-350	Gas
LAGN.STET2	GEN	8784	16180	-13	-67	-350	Gas
LAGN.STET3	GEN	8784	16180	-13	-67	-350	Gas
LAGN.STET4	GEN	8784	16180	-13	-67	-350	Gas
LAGN.STET6	GEN	8784	16180	-13	-67	-350	Gas
LAGN.STET7	GEN	8784	16180	-13	-67	-350	Gas
LAGN.STET8	GEN	8784	16180	-13	-67	-350	Gas
LAGN.STET9	GEN	8784	16180	-13	-67	-350	Gas
LEPA.CC.MGC_01	GEN	2075	7303	-15	1	-186	Gas
LEPA.HOUMA_G14	GEN	8784	20884	-26	-60	-419	Gas
LEPA.HOUMA_G15	GEN	8784	20884	-26	-60	-419	Gas
LEPA.HOUMA_G16	GEN	8784	20884	-26	-60	-419	Gas
LEPA.LEPA	LZN	8784	19859	-25	-59	-408	N/A
LEPA.MGC_UNT01	GEN	2460	5483	23	120	-70	Gas
LEPA.MURRAY	GEN	8784	31571	-22	-61	-399	Hydro
LOUISIANA.HUB	HUB	8784	23215	-29	-72	-425	N/A
MDU.LEWIS1	GEN	8784	20224	85	129	56	Coal
MDU.TATANKA1	GEN	8784	15387	78	137	54	Wind
MEC.LOUISA_1	GEN	8784	19915	76	151	50	Coal
MEC.NEALN_2	GEN	3651	5169	3	8	-9	Coal
MEC.NEALN_3	GEN	8784	16180	75	141	50	Coal
MEC.NEALS_4	GEN	8784	16167	76	142	51	Coal

MEC.OTTUMWA 1	GEN	8784	22487	80	137	59	Coal
MEC.PPWIND	GEN	8784	18862	89	152	61	Wind
MEC.WSEC3	GEN	8784	16696	80	144	55	Coal
MEC.WSEC4	GEN	8784	16709	80	143	54	Coal
MHEB	GEN	8784	14782	76	143	49	Hydro
MICHIGAN.HUB	HUB	8784	18045	190	354	82	N/A
MINN.HUB	HUB	8784	16083	82	153	53	N/A
MP.BOS233	GEN	8784	14718	78	142	51	Coal
MP.MP_BOS4	GEN	8784	14691	78	142	51	Coal
MPW.UNIT_9	GEN	8784	24964	77	143	48	Coal
NIPS.BAILLP8	GEN	8784	25679	190	344	86	Coal
NIPS.CC.WHITN	GEN	8784	20635	192	355	90	Gas
NIPS.MICHCP12	GEN	8784	16878	189	356	87	Coal
NIPS.NIPS	LZN	8784	21345	191	353	84	N/A
NIPS.SCHAHP14	GEN	8784	17875	188	343	84	Coal
NIPS.SCHAHP15	GEN	8784	17875	188	343	84	Coal
NIPS.SCHAHP17	GEN	8784	17875	188	343	84	Coal
NIPS.SCHAHP18	GEN	8784	17875	188	343	84	Coal
NSP.AZ	LZN	8784	16048	82	152	54	N/A
NSP.CC.HIBRDG 1	GEN	8784	16158	81	150	55	Coal
NSP.KING1	GEN	8784	16616	81	152	54	Coal
NSP.MNTCEL1	GEN	8784	15843	76	147	49	Nuclear
NSP.NSP	LZN	8784	16029	82	152	54	N/A
NSP.PRISL1	GEN	8784	16759	88	154	59	Nuclear
NSP.PRISL2	GEN	8784	16754	88	154	59	Nuclear
NSP.SHERCO1	GEN	8784	13717	76	151	49	Coal
NSP.SHERCO2	GEN	8784	13738	75	151	48	Coal
OTP.BIGSTON1	GEN	8784	14517	79	142	55	Coal
OTP.CENTER1	GEN	8784	16731	76	131	54	Coal
OTP.MPC	GEN	8784	15358	77	140	52	Wind
OTP.MPC.LANG DN	GEN	8784	16007	79	127	55	Wind
SIGE.10ABBGN1	GEN	8784	14824	182	351	85	Coal
SIGE.10ABBGN2	GEN	8784	14823	182	351	85	Coal
SIGE.10CULGN3	GEN	8784	14423	181	345	85	Coal
SIGE.WAR4ALC OA	GEN	8784	14426	181	344	85	Coal
SIGE.WAR5SIGE	GEN	8784	14427	181	344	85	Coal
SIGE.WARR4SIG E	GEN	8784	14426	181	344	85	Coal

SIPC.5MRN_PN14	GEN	8784	13677	187	354	79	Coal
SME.BATESV_1	GEN	8784	13940	-15	-36	-383	Gas
SME.BATESV_2	GEN	8784	13940	-15	-36	-383	Gas
SME.BATESV_3	GEN	8784	13940	-15	-36	-383	Gas
SME.BENN_GT	GEN	8784	14901	-27	-65	-426	Gas
SME.GRANDGULF	GEN	8784	18233	-23	-62	-402	Nuclear
SME.MORROW_1	GEN	8784	15628	-27	-64	-424	Coal
SME.MORROW_2	GEN	8784	15628	-27	-64	-424	Coal
SME.MOS_3	GEN	8784	15180	-25	-63	-419	Gas
SME.MOS_4	GEN	8784	15278	-25	-65	-420	Gas
SME.MOS_5	GEN	8784	15278	-25	-65	-420	Gas
SME.MOS_CTG_1	GEN	8784	15278	-25	-65	-420	Gas
SME.MOS_CTG_2	GEN	8784	15278	-25	-65	-420	Gas
SME.MOS_STG_1	GEN	8784	15180	-25	-63	-419	Gas
SME.MOS_STG_2	GEN	8784	15180	-25	-63	-419	Gas
SME.PAULDING	GEN	8784	14957	-26	-65	-427	Oil
SME.PLUMPOINT	GEN	8784	12434	-22	-55	-413	Coal
SME.SLVRCRK_1	GEN	8784	17014	-27	-69	-423	Gas
SME.SLVRCRK_2	GEN	8784	17014	-27	-69	-423	Gas
SME.SLVRCRK_3	GEN	8784	17014	-27	-69	-423	Gas
SME.SYLV_1	GEN	8784	14672	-24	-63	-417	Gas
SME.SYLV_2	GEN	8784	14672	-24	-63	-417	Gas
SME.SYLV_3	GEN	8784	14672	-24	-63	-417	Gas
SMP.OWEF	GEN	8784	19463	79	144	54	N/A
TEXAS.HUB	HUB	8784	17228	-19	-25	-414	N/A
TVA.CALRIDGE	GEN	8784	25708	182	327	89	Wind
TVA.WHITEOAK	GEN	8784	19712	187	349	82	Wind
UPPC.ESC	GEN	280	514	10	18	7	Coal
UPPC.ESCCT	GEN	3651	5905	49	79	30	Coal
UPPC.INTEGRATD	GEN	280	513	10	18	7	Hydro
UPPC.WARDEN	GEN	8784	22911	194	371	92	Biomass
WEC.CC.PORTW1	GEN	8784	15056	187	351	86	Gas
WEC.CC.PORTW2	GEN	8784	15056	187	351	86	Gas

WEC.ERG2	GEN	8784	15083	186	362	85	Coal
WEC.OAKCREKC5	GEN	8784	15145	186	361	86	Coal
WEC.OKCGC6	GEN	8784	15108	186	360	86	Coal
WEC.OKCGC7	GEN	8784	15110	186	360	86	Coal
WEC.OKCGC8	GEN	8784	15109	186	360	86	Coal
WEC.PLEASA142	GEN	8784	15386	186	357	86	Coal
WEC.PLPRG41	GEN	8784	15386	186	357	86	Coal
WEC.PTBHGB1	GEN	8784	16240	190	355	87	Nuclear
WEC.PTBHGB2	GEN	8784	16241	190	355	87	Nuclear
WEC.S	LZN	8784	15425	190	368	87	N/A
WPS.COLUMBIA1	GEN	8784	17207	190	356	91	Coal
WPS.COLUMBIA2	GEN	8784	17202	190	356	91	Coal
WPS.DPC.WESTN4	GEN	8784	17459	192	366	89	Coal
WPS.WESTON3	GEN	8784	17987	192	365	91	Coal
WPS.WESTON4	GEN	8784	17459	192	366	89	Coal
WPS.WPSM	LZN	8784	20117	194	372	92	N/A